Greenhouse Gas Production and Nutrient Reductions in Denitrifying Bioreactors

Emily MacLauren Bock

Thesis submitted to the faculty of the Virginia Polytechnic Institute and State University in partial fulfillment of the requirements for the degree of

Master of Science
In
Biological Systems Engineering

Zachary M. Easton, Chair

Matthew J. Eick

William C. Hession

May 7, 2014

Blacksburg, VA

Keywords: denitrifying bioreactor, nitrous oxide, biochar, static headspace analysis, gaseous standard addition method

Greenhouse Gas Production and Nutrient Reductions in Denitrifying Bioreactors

Emily MacLauren Bock

Abstract

The global nitrogen cycle has been disrupted by large anthropogenic inputs of reactive nitrogen to the environment. Excess nitrogen underlies environmental problems such as eutrophication, and can negatively affect human health. Managing the natural microbial process of denitrification is advocated as a promising avenue to reduce excess nitrogen, and denitrifying bioreactors (DNBRs) are an emerging technology harnessing this biochemical process. Previous DNBR research has established successful nitrate removal, whereas this study examines the potential to expand DNBR functionality to address excess phosphorus and mitigate the production of nitrous oxide, a potent greenhouse gas.

Results from a laboratory experiment supported the hypothesis that the addition of biochar, a charcoal-like soil amendment and novel organic carbon source in DNBR research, would increase nitrate and phosphorus removal as well as decrease the accumulation of nitrous oxide, an intermediate product of microbial denitrification.

In order more closely examine the ratio of the products nitrous oxide and inert dinitrogen, development of a novel analytical method to quantify dissolved gases in environmental water samples using gas chromatography mass spectrometry was undertaken. Although static headspace analysis is a common technique for quantifying dissolved volatiles, the variation in sample preparation has recently been revealed to affect the determination of dissolved concentrations of permanent gases and convolute comparison between studies. This work demonstrates the viability of internal calibration with gaseous standard addition to make dissolved gas analysis more robust to variable sample processing and to correct for matrix effects on gas partitioning that may occur in environmental samples.

Acknowledgements

Thank you to my husband, **James W. Bock Jr**., for his unwavering support of my academic endeavors and for all the joy he brings to our life together. I am so thankful that you have been on this journey with me.

My parents, **Jane Corson** and **David Lassiter**, have instilled the drive for achievement and confidence in my ability to succeed. **Daniel Lassiter**, my brother who is currently pursuing his undergraduate degree in engineering, constantly inspires me to set goals for myself both personally and educationally. My entire family has always upheld the value of education as paramount, and left me with no doubt in my course on an engaging, challenging, and rewarding career path. Thank you to my in-laws, **Trish** and **Jim Bock** and their daughter **Erika**, for always believing in me.

Zachary Easton, my mentor and committee chair, continues to encourage my professional growth and inspire me to succeed. His admirable work ethic and record of achievement motivate me as does his confidence in me. I sincerely thank him for his guidance and friendship.

Cully Hession and **Matthew Eick** have served as enduring committee members during my ambitious endeavors.

A special thank you to **Mary Leigh Wolfe**, our department head, who invited me to continue on with my PhD, an undertaking in which I now have confidence bolstered by the encouragement and confidence in my abilities she and Zach supplied.

Thank you to **Paul Macek**, analytical chemist from the Shimadzu Corporation, for his assistance in developing analytical methods for gas analysis with GC/MS and our continuing collaboration. Thank you to **Nick Smith** for conducting the DNBR column experiment and **Brady Coleman** for his assistance in the lab.

Finally, many friends and colleagues have helped me thrive in my academic and equally important personal life, thank you to **Kate Levy, Cathy Flemming, Adam Weimer, Katie Keyes, The Ya-Yas, and all the folks at Chair Place**. Special thanks to **Laura Holt**.

Funding for this research was provided by the Virginia Tech Institute for Critical Technology and Applied Science (Fund 119115) with additional support from Virginia Water Resources Research Center Student Research Competitive Grant (Fund 119659).

Table of Contents

Abstract ii
Acknowledgements iii
List of Figures vi
List of Tables viii
Attribution ix
1.0 Background 1
1.1 Introduction and Problem Statement 1
1.2 Research Objectives 3
1.3 Organization of Thesis 4
1.4 Literature Review 5
1.4.1 Introduction 5
1.4.2 Global Nitrogen Cycle 5
1.4.3 Transformation and Transportation of Nitrogen 7
1.4.4 Denitrification Management 10
1.4.5 Denitrifying Bioreactor Case Studies 11
1.4.6 Properties of Biochar 14
1.4.7 Quantifying Denitrification 17
1.4.8 Dissolved Gas Analysis 23
1.4.9 Context and Motivation: Anthropogenic Impacts on the Chesapeake Bay 24
1.5 References 27
2.0 Enhanced Nitrate and Phosphate Removal within a Denitrifying Bioreactor with Biochar ..35
2.1 Abstract 36
2.2 Introduction 36
2.3 Materials and Methods 39
2.3.1 DNBR Column Construction 39
2.3.2 Properties of Organic Carbon Media 40
2.3.3 Nutrient Addition, Sampling and Analysis 40
2.3.4 Statistical Analysis 41
2.3.5 ANOVA: nutrient concentration by treatment and time 41
2.3.6 ANOVA: nutrient concentration by presence of biochar and time 42

2.3.7 ANOVA: nutrient concentration by feedstock, particle size, application rate and time 42
2.3.8 Gas Sampling and Analysis 42
2.4 Results and Discussion 43
2.4.1 Phosphorus 43
2.4.2 Nitrate 45
2.4.3 Nitrous Oxide 46
2.4.4 Relevance in Application 47
2.4.5 Conclusions 48
2.5 Acknowledgements 49
2.6 Tables and Figures 49
2.7 References 49
3.0 Examining Denitrification with Dissolved Gas Analysis 61
3.1 Abstract 62
3.2 Introduction 62
3.3 Materials and Methods 65
3.3.1 Isotopic Analysis—Proof of Concept Data 65
3.3.2 Determination of Dissolved Gas Component in Environmental Samples: Gaseous Standard Addition Method Static Headspace Analysis 66
3.3.2.1 GCMS Configuration and Programs 68
3.3.2.2 Isolation of Error 70
3.4 Results and Discussion 82
3.4.1 Analysis of Isotope Data 82
3.4.2 Gaseous Standard Addition Method 84
3.5 Conclusions and Future Work 86
3.6 References 89
4.0 Conclusions 92
4.1 Summary and Future Work 92
4.2 References 94
Appendix A. Comparison of selected laboratory and field DNBR studies 95

List of Figures

Figure 2.1 Changes in mean phosphorus concentrations and standard errors over time and the difference between the biochar amended treatments and the woodchip control (A) and the levels of biochar characteristics feedstock (B), particle size (C), and volumetric application rate (D) 54

Figure 2.2 Changes in mean nitrate concentrations and standard errors over time and the difference between the biochar amended treatments and the woodchip control (A) and the levels of biochar characteristics feedstock (B), particle size (C), and volumetric application rate (D) 54

Figure 2.3 Loess fit of mean N_2O concentrations in the column headspace (solid lines) and 95% confidence interval (dashed lines). Points represent the means of measured concentrations. Confidence intervals that do not overlap indicate significant differences 55

Figure 3.1 Sample vial prepared for static headspace analysis showing equilibrium of the analyte between the gaseous headspace and liquid sample 65

Figure 3.2 Idealized standard addition curve 68

Figure 3.3 Chromatogram showing peaks for O_2 and Ar (overlaid), N_2, CO_2, and N_2O present in a custom gas mixture consisting of 5.02% O_2, 1.00% Ar, 40.0% CO_2, 5.09% N_2O, and 48.9 N_2 69

Figure 3.4 Seven 100 µL injections of air analyzed with the NOA method. %RSD of N_2, O_2, and Ar of 5.06, 4.31, and 4.01, respectively 71

Figure 3.5 Total ion chromatogram (top) with coelution of Ar and O_2 from poor chromatographic separation due to similar solubilities revealed by the mass chromatogram output of the MS which distinguishes the Ar and O_2 peaks by their mass to charge ratio, demonstrating the necessity of the MS as detector for this application 71

Figure 3.6 Seven 100 µL injections of air analyzed with the GHG method with %RSD of 4.48 72

Figure 3.7 Demonstration of the carryover of N_2O present in air injections following an injection of 10 ppm standard at approximately 40 times more N_2O than air 73

Figure 3.8 N_2O peaks for injections of air before and after injection of 10 ppm standard, showing no carry over effect because the syringe was purged with He prior to each injection 74

Figure 3.9 Purge technique developed to prevent air contamination within the helium introduced

as headspace consisted of pumping the syringe in a stream of He 74
Figure 3.10 Water guard constructed from Falcon tube to prevent contact between sample vial septum and air to minimize air intrusion during septum puncture and reduce vial leakage 76
Figure 3.11 Shows the large variability in 200 uL injections of He with the 5 mL syringe used to introduce the He headspace. The %RSD for N_2, O_2, and Ar were 69.3, 58.6, and 65.5, respectively 77
Figure 3.12 Seven repeated 10 µL injections of headspace from a vial with a 4.2626 mL headspace (B = 0.3558) 78
Figure 3.13 Seven repeated 10 µL injections of headspace from a vial with a 8.1700 mL headspace (B = 1.0126) to which 30 µL of air has been added 79
Figure 3.14 A leak test of a prepared sample vial consisting of five injections of headspace made every hour beginning at time zero after the headspace had been created and the vial equilibrated, until hour 4 80
Figure 3.15 Reproducibility from seven injections of a standard mixture consisting of consisting of 5.02% O_2, 1.00% Ar, 40.0% CO_2, 5.09% N_2O, and 48.9 N_2 are extracted from gas cylinder and transferred to GC/MS by gas tight syringe 81
Figure 3.16 Reproducibility from seven injections of a 10 ppm N_2O extracted from gas cylinder and transferred to GC/MS by gas tight syringe. The %RSD for N_2O was 5.88 81
Figure 3.17 (a-c) A) Linear relationship between $\delta^{15}N$ and the natural logarithm of the dissolved concentration of N_2. B) Non-significant correlation between $\delta^{15}N$ and $\delta^{18}O$ in N_2O. C) Moderate correlation between $\delta^{15}N$ and the natural logarithm of the dissolved concentration of N_2O 83

List of Tables

Table 2.1 Nine experimental treatments and description of the characteristics of the biochar amendment 49

Table 2.2 (a-c) Results from repeated measures ANOVA testing the effect of column, time, and their interaction on the concentration of dissolved phosphorus, nitrate, and ammonium 50

Table 2.3 Mean and (SE) of nutrient concentrations, dissolved phosphorus, nitrate, and ammonium, observed in aqueous samples from the DNBR columns 18, 48, and 72 hours after introduction of a nutrient solution 51

Table 2.4 (a-c) Results from a repeated measures ANOVAs testing the effect of biochar, time and their interaction on phosphorus, nitrate, and ammonium concentrations 52

Table 2.5 (a-c) Results from a repeated measures ANOVA testing the effect of biochar feedstock, size, application rate, time, as well as their interaction on dissolved phosphorus, nitrate, and ammonium 53

Table 3.1 Shows the goodness of fit of six standard additions for each of the three analytes N_2, O_2, and Ar as well as the values of the original dissolved concentration present in the sample calculated from the respective standard addition curves as the x intercept divided by the volume of liquid sample in the vial 87

Table 3.2 Summarizes the goodness of fit and p-values from four linear regressions of the headspace to liquid sample ratio (B) as the independent variable and the dependent variables 1) original dissolved gas concentration calculated as the x intercept of the standard addition curve divided by the volume of liquid sample in the vial 2) the total dissolved mass taken to be the x intercept of the standard addition curve 3) the initial headspace response form the GCMS, which is proportional to the mass detected and also the headspace concentration of analyte, and 4) the slope of the standard addition curves 88

Attribution

Chapter 2 is a manuscript by the same title is in press in the Journal of Environmental Quality. The coauthors are: Emily Bock[1], Nick Smith[1], Mark Rogers[1], Brady Coleman[2], Mark Reiter[3], Brian Benham[1], and Zachary M. Easton[1*]

This work was supported by a grant from the Institute of Critical Science and Technology at Virginia Tech, funds from the Virginia Department of Environmental Quality and funds from USDA.

*Corresponding Author: zeaston@vt.edu

- Emily Bock, MS student, Department of Biological Systems Engineering, Virginia Tech, Blacksburg VA, wrote the manuscript, conducted statistical analysis, and contributed to experimental design and sample analysis.
- Nick Smith, MS student, Department of Biological Systems Engineering, Virginia Tech, Blacksburg VA conducted the majority of the experimental data collection and analysis.
- Mark Rogers, PhD student, Department of Biological Systems Engineering, Virginia Tech, Blacksburg VA assisted in analysis of N_2O data.
- Brady Coleman, undergraduate student, Department of Biological Science, William and Mary, Williamsburg VA, assisted in sample collection and analysis as well as provided supporting work in the laboratory.
- Mark Reiter, Assistant Professor, Department of Crop, Soil, and Environmental, Science, Virginia Tech Eastern Shore Agricultural Research and Extension Center, Painter VA, provided the instrumentation for nutrient analysis.
- Brian Benham, Associate Professor, Department of Biological Systems Engineering, Virginia Tech, Blacksburg VA, reviewed and edited the manuscript.
- Zachary Easton, Assistant Professor, Department of Biological Systems Engineering, Virginia Tech, Blacksburg VA, reviewed and edited the manuscript, as well as provided input on experimental design, methods of statistical analysis, and manuscript structure.

1.0 Background

1.1 Introduction and Problem Statement

Management of the global nitrogen (N) cycle has been identified as a central environmental issue and engineering challenge in the 21st century (Galloway et al. 2008; Seitzinger et al. 2006). This priority is reflected internationally by pollution control goals focused on reactive nitrogen (N_r), the form of N that is biochemically available, in both the United States and Europe, as well as regionally in the nutrient load reductions called for the Chesapeake Bay Total Maximum Daily Load (Melillo and Cowling 2002). Human activities including fossil fuel combustion and manufacture of artificial fertilizer have doubled the input of N_r to the environment as compared with preindustrial loadings (Erisman et al. 2004; Galloway et al. 1995). Historically, reservoirs of N_r did not exist in the biosphere because denitrification, the process converting N_r back to atmospheric nitrogen (N_2), was approximately in balance with natural fixation (Aryes 1997). Coastal ecosystems and estuaries, like the Chesapeake Bay, have been particularly severely impacted by excess N_r because they are dependent on riverine nutrient sources that have doubled N loading (Galloway et al. 1995). The consequences of an oversupply of nutrients, both N and phosphorus (P), include the eutrophication and associated anoxic or dead zone impacting the Bay damaging valuable fisheries and other ecosystem services.

Reduction of excess nutrients on a watershed scale to global scale must rely on multiple strategies employed in concert. Galloway et al. (2008) suggested four major management categories to control N pollution: minimize nitric (NO) and nitrous oxide (N_2O) emissions from fossil fuel combustion, improve N uptake efficiency in crops, increase nutrient management of livestock operations, and expand access to sewage treatment globally. Yet even these load reductions will not reduce N_r inputs sufficiently to restore the balance in the global N cycle (Schipper et al. 2010a). Not only the quantity of excess N_r, but also its persistence determines its impact, because as N is transported through the environment and undergoes transformation, a single molecule may have multiple negative impacts. This concept was introduced by Galloway (2003) as the nitrogen cascade, and emphasizes the importance of balancing anthropogenic nitrogen inputs with denitrification as well as the potential negative consequences of removing ecosystems with naturally high denitrification potential such as wetlands and riparian buffers.

Denitrification management, promoting this natural microbial process of N_r removal within the landscape (throughout the N cascade) is receiving growing attention as a mechanism to mitigate the impacts of anthropogenic nitrogen, especially with respect diffuse pollution (Rivett et al. 2008; Schipper et al. 2010a; Seitzinger et al. 2006). Denitrifying bioreactors (DNBRs) are an emerging and promising technology for N_r attenuation that function by supporting ubiquitous soil denitrifiers in a favorable habitat, organic carbon medium that is saturated sufficiently to allow anoxic conditions to develop. Successful N removal, averaging over 50% and reaching upwards of 90% periodically, has been observed in these field scale systems for up to 15 years even with fluctuating influent concentrations and flow rates (Robertson et al. 2008). DNBR implementation in strategic locations, for example receiving shallow groundwater or tile drainage impacted by excess nitrogen in agricultural ecosystems within the Chesapeake Bay watershed, has the potential to provide measurable nitrogen removal levels on site that translate into downstream water quality improvement.

DNBRs have particular potential in agricultural systems due to their low cost, low maintenance, long lifespan, and ability to handle the variability in the nutrient concentration and flow rate of the influent. Additionally, agriculture demonstrates a need for innovative nutrient management practices given that globally 75% of anthropogenic N_r is utilized in agro-ecosystems, of which approximately half is lost to the atmosphere (as ammonia (NH_3), NO, N_2O, and N_2) or to water (as nitrate (NO_3^-)), complete denitrification to N_2 only accounting for a minor portion (Seitzinger et al. 2006). However, P export in agricultural systems is also a major contributor of nutrient pollution resulting in buildup in soils during cultivation with fertilizer or grazing (Sharpley et al. 1996) and exported in runoff and subsurface pathways, including tile drainage (Kleinman et al. 2011). The next logical step in DNBR engineering and design is expanding the functionality beyond N removal to also mitigate P fluxes, the other major nutrient comprising agricultural nonpoint source pollution and contributing to eutrophication and environmental degradation. This research explores the potential to incorporate a novel substrate into the traditional woodchip organic carbon media in DNBRs to promote P adsorption and/or precipitation.

Simultaneously, revisiting the underlying assumption that denitrification is the primary nitrogen removal pathway in both field and laboratory DNBR experiments (Gibert et al. 2008; Warneke et al. 2011) is warranted. The majority of these studies do not measure the rates of denitrification directly because the biochemically produced N_2 is difficult to resolve against the

background N_2 (Blowes et al. 1994; Groffman et al. 2006; Long et al. 2011; Robertson and Cherry 1995). With the assumption that denitrification is the main nitrate removal mechanism, incomplete denitrification resulting in N_2O emission has been recognized as a potential drawback to DNBR implementation (Shipper et al. 2010b). Although four DNBR studies, namely Elgood et al. (2010), Mooreman et al. (2010) Warneke et al. (2011), and Woli et al. (2010) have quantified N_2O emission from these systems, the opportunity to engineer these systems to minimize N_2O emissions remains. Although N_2O emissions have not been established as problematic in DNBRs, more deliberately promoting complete denitrification presents an opportunity for N_2O mitigation. Agricultural systems result in a significant amount of N_2O emissions directly from their soils and indirectly from aquatic systems where exported dissolved N undergoes subsequent transformations (Mosier et al. 1998). Indirect emissions from agriculture refer to the applied NO_3^- that is converted to gaseous forms such as N_2O. The International Panel on Climate Change (IPCC) has assigned an indirect N_2O emissions factor of 0.0025 from groundwater, which represents the percentage of NO_3^- that is converted to N_2O (Weymann et al. 2008). Engineering DNBRs to promote complete denitrification over accumulation of greenhouse gas intermediates to minimize the percentage of NO_3^- converted to N_2O may result in a lower fraction than the IPCC indirect emissions factor, thus enabling DNBRs to contribute to GHG mitigation. Biochar shows potential here as well because it is associated with lower N_2O emissions in soils under conditions favorable for denitrification.

Biochar, a charcoal-like pyrolysis product of biomass, was selected as a novel organic carbon substrate in DNBRs based on its previously studied ability to reduce N and P leaching as well as GHG emissions in agricultural soils. This research investigates the effect of biochar addition to the traditional woodchip media in DNBRs, hypothesizing that biochar will enhance P removal as well as complete denitrification, resulting in both greater N removal and lower N_2O production. The sustained high nitrate removal rates recorded in DNBRs point to their potential application as cost-effective N attenuation tools in watersheds dominated by agricultural land use. However, as outlined above, opportunities remain to optimize the performance of these systems.

1.2 Research Objectives

This research focuses on engineering DNBRs to maximize complete denitrification while minimizing greenhouse gas (GHG) emission, and in addition, remove dissolved reactive phosphorus. A laboratory scale experiment was used to evaluate the ability of biochar to enhance

DNBR performance. To quantify both denitrification and the ratio of denitrification products, direct measurement of dissolved gases uses the ratio of dissolved N_2/Ar to quantify excess N_2 attributable to denitrification while simultaneously measuring N_2O. In response to recent work revealing the confounding effects of sample processing on dissolved gas quantification in environmental samples, development of an analytical solution to the lack of comparability was undertaken. The explicit objectives of this study were to:

1. To determine the effect of biochar addition to traditional woodchip media on NO_3^- and P removal as well as N_2O production;
2. To develop a more robust method of quantifying dissolved gases in environmental water samples that can be employed to directly measure denitrification by the N_2/Ar method as well as measure the ratio of N_2:N_2O production.

1.3 Organization of Thesis

This document consists of a comprehensive literature review (Section 1), a journal article in press in the Journal of Environmental Quality (Section 2), a chapter describing the motivation and method development of the gaseous standard addition method applied to static headspace analysis of dissolved gases (Section 3), followed by a summary of the project and description of ongoing and future research (Section 4). The comprehensive literature review provides the context and motivation for this research. Section 2 serves as a portion of the thesis describing a laboratory experiment testing the effect of biochar on NO_3^- and P removal, but constitutes an individual document with a full abstract, introduction, methods, results and discussion, acknowledgements, and references. The coauthors are listed in the attribution. Section 3 provides isotopic evidence for the accumulation of N_2O during denitrification and demonstrates the effect of biochar on reducing N_2O production in laboratory scale DNBRs which motivate further examination of N_2O:N_2 dynamics during denitrification. Section 3 continues by detailing the initial stages of method development to improve dissolved gas analysis by static headspace technique by employing a gaseous standard addition for the purpose of quantifying denitrification and the ratio of its products. Section 4 concludes by reiterating impacts of this work and describes horizons of future work. Section 5 provides supporting tables not included in the main text.

1.4 Literature Review

1.4.1 Introduction

The overarching goal of the proposed work is to improve the health of water resources, with a particular focus on opportunities in the Chesapeake Bay watershed, by contributing to the development of denitrifying bioreactors that can be implemented strategically within the watershed as part of a broader management scheme to mitigate excess reactive nitrogen, as well as phosphorus and GHG emissions. The main objective of this research is to engineer DNBRs to maximize nitrogen removal via complete denitrification while exploring the potential of biochar addition, a novel organic carbon substrate in DNBR research, to simultaneously foster mitigating of GHG emissions and phosphorus export. To place these efforts in context, the following literature review includes a description of the nitrogen cycle, transformation and transportation of N, case studies of DNBRs and how they emerged from the larger strategy of denitrification management, the properties of biochar that make it a desirable DNBR amendment, and outlines dissolved gas analysis and how it can be employed to measure denitrification and the ratio of its products.

1.4.2 Global Nitrogen Cycle

The global nitrogen cycle consists of biochemical and physiochemical processes that transform as well as the hydrologic and atmospheric mechanisms that transport nitrogen species. Historically, most ecosystems have been nitrogen limited because the largest reservoir of nitrogen is inert dinitrogen gas (N_2), comprising 78% of the atmosphere (Galloway et al. 1995); few organisms are capable of fixing nitrogen, converting N_2 to biologically available, reactive forms (N_r) (Ayres 1997; Galloway et al. 1995). Drastic increases in anthropogenic reactive nitrogen inputs to the environment have resulted from the doubling of the conversion of atmospheric nitrogen to reactive nitrogen through the combustion of fossil fuels, intense cultivation of legumes and other crops that depend on nitrogen fixation in the rhizosphere (e.g. rice), and the use of industrial fertilizer produced by the Haber-Bosch process (Gruber and Galloway 2008; Seitzinger et al. 2006). Indeed, much of the increase in agricultural productivity over the last century is attributable to the increased usage of nitrogen fertilizers (Erisman 2004). Smil (2001) estimated that 40% of the world's population would not have survived if the anthropogenic alteration of the carbon cycle by industrial fertilizer production.

Denitrification is the link completing the nitrogen cycle by converting reactive nitrogen back to dinitrogen, the only able to remove nitrogen from the reactive pool other than the recently discovered anaerobic oxidation of ammonium (Anammox) (Burgin and Hamilton 2007). Delwiche (1970) concluded that the transformation between the reactive and nonreactive pools of nitrogen was balanced prior human activities, but today we face a different reality. Denitrification has not kept pace with increased inputs of reactive nitrogen, and has often been spatially separated from reactive nitrogen sources through the destruction of ecosystems in which denitrification naturally occurs, such as riparian buffers and wetlands (Schipper et al. 2010a). As a result, net accumulation of reactive nitrogen is occurring and projected to increase with the human population (Ayres 1997; Galloway et al. 2003). Galloway (2003) introduced the term "nitrogen cascade" to describe the accumulating effects that result from temporary storage of reactive nitrogen in its various chemical forms as it is transported through the environment by water and air, each atom resulting in multiple, and potentially deleterious, consequences.

Excess reactive nitrogen underlies a suite of environmental and health problems. Environmental degradation resulting from elevated nitrogen levels includes eutrophication of receiving water bodies, global acidification, stratospheric ozone depletion, and tropospheric accumulation of ozone and aerosols, which can lead to respiratory illness, cardiac disease, and cancer in humans (Dinnes et al. 2002; Driscoll et al. 2003; Galloway et al. 2003). Nitrogen can contaminate potable water, high concentrations of nitrate being toxic to infants, resulting in methemoglobinemia, as well as livestock, while nitrite reacting with secondary amines forms carcinogenic nitrosamines (Averill and Tiedje 1982; Ayres 1997; Gruber and Galloway 2008; Trudell et al. 1986). Disruption of the global nitrogen cycle also has a multitude of potential impacts on the other major chemical cycles of carbon, phosphorus, and sulfur, which have become a topic of increasing study, particularly with respect to global climate change (Ayres 1997; Gruber and Galloway 2008; Rabalais et al. 2009). Mitigating the effects of anthropogenic nitrogen inputs is vital to protection of our health and natural resources while continuing to produce food and energy for a growing population. Appropriately, the National Academy of Engineering has cited management of the global nitrogen cycle as one of the 14 Grand Challenges for Engineering in the 21st century (http://www.engineeringchallenges.org). This priority is echoed by the nitrogen pollution control goals set by both the United States and Europe (Melillo and Cowling 2002). The importance of denitrification management is

paramount since the human population is sustained by anthropogenic increase in reactive nitrogen (Galloway et al. 2008; Schipper et al. 2010a).

1.4.3 Transformation and Transportation of Nitrogen

Efforts to mitigate the effects of anthropogenic nitrogen on a global, regional, or watershed scale require a comprehensive understanding of reactions that transform nitrogen species as well as how these species are transported through the environment. Transformations of nitrogen species are both abiotic and biologically mediated, but biological processes dominate nitrogen cycling (Galloway et al. 2008). These processes include nitrogen fixation, nitrification, denitrification, ammonification, immobilization, mineralization, and the more recently discovered anammox (Burgin and Hamilton 2007; Mulder et al. 1995; Novotny 2002). These reactions have been widely studied (Kumar and Lin 2010; Seitzinger et al. 2006; Zumft 1997), as defined and described by Novotny (2002). Brandy and Weil (2008) and Easton and Lassiter (2013) are summarized below. Chemical equations are credited to Brady and Weil (2008).

Nitrogen fixation

Nitrogen fixation is the process by which atmospheric nitrogen (N_2) is converted to organic nitrogen via microbial nitrogen fixation and lightening by breaking the triple bond between the two N atoms. Nitrogen fixation is conducted by certain prokaryotes, in symbiosis with plants as well as independently (Son 2001). The most typical example of nitrogen fixation occurs in legumes (e.g. soybeans, beans, peas) due to the well-known symbiosis with *Rhizobia* and *Bradyrhizobia* bacteria in root nodules (Brady and Weil 2008). All biological nitrogen fixation requires the enzyme Nitrogenase (Zumft 1997). Anthropogenic nitrogen fixation has also been developed; the Haber-Bosch process used in the manufacture of artificial nitrogen fertilizer uses large amounts of energy to fix nitrogen (Seitzinger et al. 2006). Note that the process is unidirectional.

$$N_2 + 8H + 6e^- + \text{energy} \Rightarrow 2NH_3 + H_2 \quad (1)$$

Immobilization

Abiotic reactions that sequester mineral nitrogen (e.g. ammonium fixation (sorption) by clay minerals) and biotic uptake and conversion of nitrogen to proteins and cell tissue by plants and microbes, mainly in its mineral forms nitrate (NO_3^-) and ammonium (NH_4^+), constitutes

immobilization, but this transformation may also include uptake of soluble organic nitrogen. Biotic immobilization is also referred to as accumulation.

Mineralization

Mineralization is the microbial decomposition of organic nitrogen to mineral forms (reverse of immobilization). Ammonification is a subset of mineralization that results in the formation of NH_4^+.

$$\Rightarrow \text{Mineralization} \Rightarrow$$

$$+H_2O \qquad +O_2 \qquad +{}^1/_2O_2$$

$$R\text{—}NH_2 \Leftrightarrow OH^- + NH_4^+ \Leftrightarrow 4H^+ + \text{energy} + NO_2^- \Leftrightarrow \text{energy} + NO_3^- \quad (2)$$

$$-H_2O \qquad -O_2 \qquad -{}^1/_2O_2$$

$$\Leftarrow \text{Immobilization} \Leftarrow$$

Ammonia Volatilization

Production of ammonia gas (NH_3) from NH_4^+ (as a dissolved ion) in soils with high concentrations of NH_4^+ and a pH greater than 7.5.

$$NH_4^+ + OH^- \Leftrightarrow H_2O + NH_3 \quad (3)$$

Nitrification

Nitrification is the stepwise microbial oxidation of ammonium to nitrite to nitrate by the autotrophic bacteria *Nitrosomonas* and *Nitrobacter* respectively. Nitrifiers under anaerobic conditions can also produce the GHGs NO and N_2O. Note that the reactions are unidirectional.

Nitrosomonas $NH_{4+} + {}^1/_2O_2 \Rightarrow NO_2 + 2H^+ + H_2O + 275$ kJ energy (4)

Nitrobacter $NO_2^- + {}^1/_2O_2 \Rightarrow NO_3^- + 76$ kJ energy (5)

Denitrification

Denitrification is the microbially mediated stepwise reduction of nitrate to dinitrogen gas. Organic carbon serves as an energy source and the electron donor for this reduction-oxidation reaction, and a nitrogen oxyanion (NO_3, NO_2) or oxide (NO, N_2O) serves as the terminal electron

acceptor in the absence of oxygen: $NO_3 \Rightarrow NO_2 \Rightarrow NO \Rightarrow N_2O \Rightarrow N_2$, utilizing an organic source and producing CO_2 and H_2O at each step (Istock et al. 1997). Excluding anammox, denitrification is the only transformation that removes reactive nitrogen from an ecosystem by transforming reactive nitrogen to its inert form. Denitrification is conducted mainly by heterotrophic bacteria, but also by some chemolithic and autotrophic bacteria, Archaea, and fungi (Mateju et al. 1992; Zumft 1997). The heterotrophic denitrifying bacteria are taxonomically diverse and ubiquitous in surface water and the subsurface, both soil and groundwater (Rivett et al. 2008). Denitrification serves as the basis for N removal in traditional municipal wastewater treatment, coupled nitrification-denitrification being the single most common method to reduce N in wastewater (Mulder et al. 1995).

Anammox

Anaerobic oxidation of ammonium (Anammox) utilizing carbon dioxide (that is, bicarbonate in aqueous environment) as an electron donor and nitrite as an electron acceptor (Kumar and Lin 2010). Anammox converts 90% of the reactant nitrogen to N_2 while converting 10% to NO_3. This process was discovered in a denitrifying wastewater treatment reactor in 1994 (Mulder et al. 1995). Modified (unbalanced) chemical equation borrowed from Kumar and Lin (2010):

$$NH_4 + NO_2 + HCO_3 + H^+ \Rightarrow N_2 + NO_3^- + CH_2O_{0.5}N_{0.15} \quad (6)$$

In sum, the main forms of nitrogen present in the environment are nitrogen gas, organic N, ammonium/ammonia, and nitrate (Novotny 2003). The various N species are transported by surface flow, groundwater, ocean currents, the atmosphere, and to a lesser extent, erosion.

Nitrate is primarily transported by water; due to the net negative charge of soils this anion NO_3 is not adsorbed to soil colloids like ammonium (Mitsch et al. 2001). Nitrate-nitrogen is the form most often associated with water quality problems (Brady and Weil 2008; Novotny 2003). However, soluble organic nitrogen also deserves attention with respect to water quality, as it is also susceptible to leaching (Jickells 2005; Schipper et al. 2010b). In fact, 25% of the nitrogen carried by the Mississippi River that reaches the Gulf of Mexico is in the form of soluble organic nitrogen (CAST 1999). Soluble nitrogen is transported in both surface and groundwater, with a much longer residence time in the latter; in long subsurface flow paths with low velocities, the ground water and its solutes can have highly variable residence times on the order of weeks to

centuries (Winter et al. 1998). Surface water and groundwater transport are not distinct because groundwater often makes up a substantial portion of stream base flow (Lindsey et al. 2003). Coastal ecosystems have historically been dependent on rivers as nutrient sources, and eutrophication has become a major issue as these riverine N_r inputs have doubled (Galloway et al. 1995). Subsequently, ocean currents redistribute reactive nitrogen in the marine environment (Galloway et al. 1995).

Atmospheric transport is responsible for the largest-scale redistribution of nitrogen, in both particulate and gaseous forms. In pre-industrial times only 10-20% of reactive nitrogen ever reached the atmosphere, but Galloway et al. (1995) estimated that 55% of anthropogenic fixed N is redistributed by the atmosphere today. Evidence of the significance of this transport mechanism is observed in the increased ammonium and nitrate levels in Antarctica ice cores (Galloway 1995). The residence time in the atmosphere for NH_3 and NO is hours to days before deposition, whereas N_2O can be stored longer, with residence time estimates up to 150 years (Galloway et al. 2003, Zumft 1997). In contrast, the smallest-scale transport of nitrogen is via wind erosion of soil particles carrying adsorbed N_r (mainly ammonium) until it enters larger atmospheric or hydrologic pathways.

Not only do these transport mechanisms redistribute substantial quantities of reactive nitrogen, but they also provide an opportunity for each nitrogen atom to undergo a series of reactions and encounter temporary storage. The propagation of the effects of these multiple reactions, amplifying the effect of a single nitrogen molecule, is the underlying concept of the nitrogen cascade (Galloway et al. 2003).

1.4.4 Denitrification Management

Reduction of excess reactive nitrogen on a watershed scale to global scale must rely on multiple strategies employed in concert (Galloway et al. 2008; Mitsch et al. 2001; Seitzinger et al. 2006). Galloway et al. (2008) suggested four major management categories: minimize nitric (NO) and nitrous oxide (N_2O) emissions from fossil fuel combustion, improve nitrogen uptake efficiency in crops, increase nutrient management of livestock operations, and expand access to sewage treatment globally. Yet even these load reductions will not reduce reactive nitrogen inputs sufficiently to restore the balance in the global nitrogen cycle and innovative management practices are necessary (Galloway et al. 2008; Shipper et al. 2010b). Denitrification management, promoting reactive nitrogen removal throughout the cascade, is increasingly

recognized as an essential component of managing the global nitrogen cycle, especially with respect to diffuse pollution (Kumar and Lin 2010; Seitzinger et al. 2006). Restoration and construction of wetlands and riparian buffers for nitrogen removal are examples of denitrification management applicable to a wide range of landscapes (Mitsch et al. 2001; Seitzinger et al. 2006). Denitrifying bioreactors are emerging as effective treatment systems as well (Schipper et al. 2010b, Warneke et al. 2010). However, studies that address watershed scale benefits from denitrification management, namely water quality improvement, have yet to be conducted (Seitzinger et al. 2006).

Denitrification management is thought to have some of the highest potential in agro-ecosystems (Seitzinger et al. 2006, Schipper et al. 2010a). Globally, 75% of anthropogenic N_r is utilized in agro-ecosystems, of which approximately half is lost to the atmosphere (NH_3, NO, N_2O, N_2) or to water (NO_3), complete denitrification to N_2 only accounting for a minor portion (Galloway et al. 2003). Thus, agriculture is the single largest source of reactive nitrogen entry into the cascade. Even with the extensive implementation of agricultural best management practices (BMPs) such as nutrient management plans dictating the appropriate rates and timing of fertilizer applications for a given crop, fertilizer use efficiency will never reach 100%, so additional management is required. Most of the nitrogen that is lost from agro-ecosystems is leached to the groundwater and eventually discharged into surface water, contributing to eutrophication downstream (Mitch et al. 2001). Denitrifying bioreactors have been successfully implemented in agricultural settings both to intercept shallow groundwater flow and to treat tile drained runoff (Schipper et al. 2010b).

1.4.5 Denitrifying Bioreactor Case Studies

Denitrifying bioreactors promote anaerobic heterotrophic denitrification by maintaining an anaerobic environment with an available organic carbon source. Fundamentally, a DNBR is an organic carbon substrate that is at least periodically saturated with sufficient duration and frequency for denitrification to occur. DNBRs have been used to treat a range of nitrate-laden waters including greenhouse effluent, contaminated groundwater, septic system plumes, domestic wastewater, and most commonly agricultural runoff; see Appendix A for a comparison of DNBR field studies. DNBRs are designed to sustain nitrogen removal levels over the long term (up to 15 years) with minimal maintenance while handling fluctuating influent flow rates and nitrogen concentrations (Robertson et al. 2008). Schipper et al. (2010b) describes common

hydraulic designs, which include walls receiving shallow groundwater and/or tile drained agricultural runoff, beds where the influent and effluent are piped, streambed bioreactors, upflow bioreactors, and layers that receive effluent from above.

A large variety of carbon substrates for use in DNBRs have also been tested in the laboratory setting, including maize cobs, green waste, wheat straw, and a variety of cellulose based media (Cameron and Schipper 2010; Gibert et al. 2008; Greenan et al. 2006; Saliling et al. 2007). However, wood-based media is by far the most common carbon media that has been utilized in the field (Blowes et al. 1994; Elgood et al. 2010; Long et al. 2011; Moorman et al. 2010; Robertson and Cherry 1995; Schipper and Vojvodić-Vuković 2000). Refer to Shipper et al. (2010b) for a review of DNBR studies with wood-based media as a carbon source. Factors controlling the rate of denitrification in DNBRs identified at the field scale include nitrate concentration, available carbon source, substrate particle size, temperature, and dissolved oxygen concentration (Cornwell et al. 1999).

Denitrification has been shown to be the main mechanism of nitrate removal in DNBRs in both column (Gibert et al. 2008; Warneke et al. 2011) and laboratory studies (Greenan et al. 2006; Robertson 2010; Warneke et al. 2011). However, as pointed out by Burgin and Hamilton (2007), alternative pathways for nitrate include accumulation in biomass (immobilization), dissimilatory nitrate reduction to ammonium (DNRA), and anaerobic respiration of ammonium (Anammox). Although these all of these pathways can be perceived as nitrate removal when comparing influent and effluent concentrations of nitrate, only denitrification and anammox permanently remove reactive nitrogen by complete reduction to dinitrogen gas. DNRA and immobilization are at best long-term nitrogen sinks because their end products, organic N and ammonium respectively, are reactive. Herein lies one disadvantage of assuming that nitrate removal is attributable to denitrification without substantial evidence, potentially overestimating the mitigation of 'downstream' impact by delaying instead of reducing export. However, Seitzinger et al. (2006) identified that most DNBR studies have failed to distinguish denitrification from other nitrate removal processes, citing Blowes et al. 1994 and Robertson et al. 1995.

Determination of the fate of nitrogen in a DNBR is limited by the measurement techniques available to distinguish the different pathways. Immobilization is difficult to quantify because the changes in total N in the reactor may be imperceptible even over the course of years,

as was the case after 14 years in a DNBR study by Long et al. (2011). The contribution of DNRA is often dismissed based on low effluent ammonium concentrations, but this reasoning ignores the possibility that the ammonium itself is immobilized. However, measurement of immobilization and DNRA is possible under laboratory conditions, as demonstrated by Greenan et al. (2006) in a 180-day column study using ^{15}N isotope, who found that immobilization accounted for approximately 2.4% and DNRA 1% of nitrate removal in woodchips. Schipper and Vojvodić-Vuković (2000) also provided evidence from a laboratory study that denitrification was sufficiently high to account for nitrate removal in the field, indirectly evidencing low rates of DNRA and immobilization.

Denitrification itself is a challenge to quantify, and a detailed discussion of these obstacles is provided in the following section. If denitrification is accepted as the main nitrate removal mechanism in DNBRs, quantification not only of the total rate of denitrification, but also the rates at which the intermediates NO_2, NO, and N_2O are produced within the DNBR becomes the critical. The accumulation of any of these intermediates, although generally thought to occur only in low levels (Kuenen 2008), is worth serious consideration because of their severe consequences, NO_2 reacting to form a carcinogen and NO and N_2O being potent GHG, among the issues previously described. No DNBR field study to the author's knowledge has attempted to quantify the production of all of the denitrification intermediates. Significant GHG production has been observed in other nitrogen removal systems utilizing denitrification including constructed wetlands, which have been shown to act as both sources and sinks of nitrogen gases, occasionally producing high emissions of N_2O (Søvik and Mørkved 2007). Although the production of GHGs has been cited as a potential drawback to DNBR implementation (Robertson 2010; Schipper et al. 2010b), only four studies to the author's knowledge have attempted to quantify N_2O emissions in situ: (Elgood et al. 2010; Mooreman et al. 2010; Warneke et al. 2011; Woli et al. 2010)

Assuming complete reduction of nitrate to dinitrogen gas is not yet justified by experimental findings because the controlling factors on the accumulation of denitrification intermediate products have yet to be fully identified. Initial evidence from laboratory testing does suggest that DNBR GHG emissions are low under the appropriate conditions. Mooreman et al. (2010) presented encouraging findings that nitrous oxide emissions from DNBRs are lower than those from agricultural land or nitrogen polluted streams. However, a soil core study by

Warneke (2011) showed that factors such as increased temperature and certain substrate types, likely due to the higher labile carbon content (e.g. maize cobs), can increase nitrous oxide production via denitrification (Warneke et al. 2011), although significant nitrous oxide production was not observed in the woodchip treatment. Although these emissions were low in the relatively stable laboratory environment, in the field where influent nitrate concentrations and saturation conditions fluctuate with precipitation events and seasonality of the water table, emissions cannot be predicted and warrant investigation in situ (Moorman et al. 2010). Consequently, further DNBR research must not focus promoting nitrate optimization design and management for removal via ambiguous pathways, or even promote the highest rates of denitrification, but should instead identify the factors that promote the complete reduction of NO_3 to N_2 while avoiding accumulation of the denitrification intermediates. Investigation of novel organic carbon substrates in DNBRs may provide an opportunity to mitigate N_2O emissions. The application of biochar has been found to reduce N_2O production, as well as reducing leaching of N and P in agricultural soils.

1.4.6 Properties of Biochar

Biochar, as defined by the International Biochar Institute (IBI), is "a solid material obtained from thermochemical conversion of biomass in an oxygen limited environment" which is distinguished from charcoal by its intended application as a soil amendment (IBI 2014, McLaughlin et al 2009, Verheijhen et al. 2010). Biochar is also associated with energy production during low temperature pyrolysis (burning at less than 700 C with little to no oxygen present) of biomass, in which the gasses given off are used to produce heat, electricity or biofuel (Lehmann et al. 2011). Long-term carbon sequestration is cited as a driving application of biochar and excites interest in its ability to mitigate climate change (Clough and Condron 2010; IBI 2014; Lehmann et al. 2011, Singh et al. 2010). Biochar is termed carbon net-negative because more CO_2 is removed from the atmosphere during biomass growth and then is released during pyrolysis, transforming the biomass into more stable biochar, which can remain in the soil for hundreds to thousands of years (Fruth and Ponzi 2010; Renner 2007).

Biochar application is also associated with improvement of soil function via increased cation exchange capacity (CEC), soil water retention, and enhanced microbial growth (Christianson et al. 2011; Lehmann et al. 2011; McLaughlin et al. 2009), as well as increased crop yields in some cases (Beck et al. 2011). General characteristics of biochars underlying

induced soil properties include high specific surface area and high micropore volume, which cause biochar to be an effective sorbent (Kookana et al. 2011). Logically, biochar amendment also impacts nitrogen and phosphorus cycling by changing the physiochemical soil environment and consequently altering the structure and activity of the microbial community (Anderson et al. 2011), although the effects on nutrient transformations and interrelated mechanisms are incompletely understood (Clough and Condron 2010; Nelson et al. 2011). However, biochar application to soil has been shown to reduce leaching of nitrogen, phosphorus, and organic carbon (Beck et al. 2011).

In a review "Biochar and the Nitrogen Cycle: Introduction" Clough and Condron (2010) summarize the findings of studies on biochar and nitrogen:

> "studies have suggested or shown that biochar has the ability (i) to retain N within soils by enhancing ammonia (NH_3) and ammonium (NH_4) retention, (ii) to reduce nitrous oxide (N_2O) and nitrate leaching (NO_3-) fluxes, and (iii) to enhance biological N fixation and beneficially influence soil microbial communities."

For example, Singh et al. (2010) demonstrated that biochar reduces emissions of N_2O emissions and ammonium leaching after four months. Independently, oxidation of biochar has been shown to increase cation exchange capacity, which could account for the retention of ammonium (Clough and Condron 2010). Raising the soil pH with the addition of alkaline biochar may also contribute to reduced N_2O emissions (Clough and Condron 2010), as increasing pH has been shown to favor the production of N_2 over the accumulation of N_2O during denitrification (Firestone et al. 1980). Other studies have shown that biochar amendment has increased N_2O emissions (Yanai et al. 2007), which is likely due to the resultant increase in water holding capacity that allows anaerobic microsites supporting denitrification to persist longer. Factors identified in the literature impacting N_2O:N_2 during denitrification include soil water content as a function of soil type, pH, microbial respiration rates, available carbon, and soil NO_3- content (Clough and Condron 2010; Firestone et al. 1980; Parton et al. 1996).

Consequently, biochar amendment can reduce runoff quantity while improving the water quality and potentially reduce greenhouse gas emissions. However, due to the variety of feedstocks (biomass) and pyrolysis conditions utilized, biochars are in practice a heterogeneous

group of materials (Kookana et al. 2011). Many researchers point out the futility of reporting responses to biochar addition without sufficient characterization of the material (McLaughlin et al 2009). The IBI (2014) has developed both a biochar certification program for biochars which meed the IBI Biochar Standards, which "provide[s] common reporting requirements for biochar that will aid researchers in their ongoing efforst to link specific funcitons of biochar to its beneficial soil and crop impacts."

Biochar is of particular in interest for application in denitrifying bioreactors not only for its capacity to reduce nutrient leaching, but also because its organic matter is more resistant to degradation than the original biomass and can provide a long term carbon source for the heterotrophic denitrifying microbes. However, its half-life is the subject of debate and likely varies with feedstock and pyrolysis conditions (Lehmann et al. 2011). The utility of DNBRs relies on supplying sufficient labile (easily degraded) organic carbon so that the rate of denitrification is not reduced due to carbon limitation, but also maintaining a stock of organic carbon over the long-term (on the order of decades) for the system to remain self-reliant and maintenance free. Therefore, biochar may hold promise for both reducing nutrient export from DNBRs and increasing their lifespans.

Currently, only one study has been published that addresses the use of biochar in a DNBR. Christianson et al. (2011) examined the effect of fresh biochar addition to a seven-year-old woodchips (*Pinus radiata*) in a laboratory-scale column experiment, hypothesizing that amendment would increase nitrate removal while decreasing the ammonium loss. Two application rates, 7% and 14% by dry weight, of *P. radiata* biochar prepared at three pyrolysis temperatures were compared. No significant differences between the biochar treatments and the control (woodchips only) were observed during this trial. However, greater depth of saturation and residence time of the 20 mg/L nitrate influent were found to increase nitrate removal (Christianson et al. 2011); saturation and residence time have been previously documented to affect nitrate removal in laboratory (e.g. Cameron and Schipper 2010) and field scale (e.g. Moorman et al. 2010) DNBR studies. However, the effect of biochar amendment in a DNBR at the field scale should not be extrapolated from the results of this incubation experiment due to the short duration of the study (3 days), the freshness of the biochar, and differences in environmental conditions between a controlled laboratory and fluctuating field conditions. Christianson et al. (2011) acknowledge that the aging effect of biochar may increase adsorbtion

capacity that would be expected to result in increased retention of NH_4^+ and other cations. Biochar incorporation into DNBRs merits further investigation.

1.4.7 Quantifying Denitrification

Quantification of complete and partial denitrification is essential because these intermediate products have the potential to be more harmful than the initial reactant, nitrate. Although, nitrate is toxic to human infants and livestock in high concentrations (EPA Maximum Contaminant Level for drinking water <10 mg/L), nitrite (NO_{2-}) reacts with secondary amines to form carcinogenic nitrosamines, nitric oxide (NO) contributes to tropospheric ozone and produces, acid rain, and nitrous oxide (N_2O) which destroy the stratospheric ozone layer and is a potent GHG (Conrad 1996). Nitrous oxide emissions account for approximately 7-8% of the 'anthropogenic warming effect,' and have a radiative forcing over three hundred times that of CO_2 and an atmospheric lifespan of 120 years (EPA 2006; Singh et al. 2010). The sustained high nitrate removal rates recorded in DNBRs point to their potential application as cost-effective nitrogen attenuation tools, but it remains unclear what controls the proportion of the nitrate is completely reduced to N_2 and how much is lost to the environment, largely through emissions, as N_r. Optimization of DNBR performance necessitates engineering these systems to favor complete denitrification over the accumulation of N_2O.

Direct measurement of denitrification must surmount the central obstacle of resolving small fluxes of N_2 in the presence of high atmospheric and dissolved aqueous N_2 (Cornwell et al. 1999; Eyre et al. 2002; Groffman et al. 2006; Warneke et al. 2011). A range of methodologies has been developed to meet this challenge since the 1960s (Greene 2005). The following comparison of measurement techniques will focus on those that are appropriately applied in situ, and have been used in a variety of natural and constructed terrestrial and aquatic ecosystems. Given the primary objective of determining the ratio of denitrification products, methods that may be adapted to quantify complete denitrification to N_2 as well as denitrification halted an intermediate step, allowing accumulation of NO_2, NO, and N_2O, will be discussed in more detail. Method that provide a comparative index of denitrification, but do not constitute rate measurements, such as stoichiometric and molecular approaches (Groffman et al. 2006), will not be discussed. This summary draws largely on two published reviews of denitrification quantification methods, one out of the University of Maryland Center for Environmental Studies Chesapeake Biological Laboratory (Greene 2005) and a paper as a result of a workshop on

denitrification methodology held by the U.S. National Science Foundation in conjunction with the Denitrification Research Coordination Network (www.denitrification.org) in May 2004 (Groffman et al. 2006) to which the reader is referred for a more complete comparison of methods and their applicability.

The majority of denitrification measurements in both terrestrial and aquatic environments have relied on the acetylene block technique (Groffman et al. 2006). Acetylene (C_2H_2) inhibits the reduction of N_2O to N_2, thereby allowing indirect measurement of complete reduction to N_2 with N_2O flux as a proxy (Greene 2005). The advantage of this technique is that N2O flux can be more easily be resolved due low background concentrations (Greene 2005). Drawbacks of the acetylene block technique include the inhibition of nitrification, which lead to underestimation of denitrification in situ particularly in N-limited environments (Groffman et al. 2006). There is also evidence to support that incomplete blockage of reduction of N_2O to N_2 often occurs (Cornwell et al. 1999). Additionally, C_2H_2 is easily decomposed and increases microbial respiration, altering carbon availability, one of the controlling environmental factors on denitrification (Groffman et al. 2006). The acetylene block technique can be applied both in the field and to soil cores in vitro, but laboratory studies provide variable removal rates and may not be representative of field conditions due to the comparatively steady conditions and the likelihood that such small volumes are representative samples (Groffman et al. 2006; Warneke et al. 2011). However, this technique does have the advantage easily replicating measurements, allowing for the examination of the environmental controls as well as the spatial and temporal variability of denitrification (Groffman et al. 2006). Yet Warneke et al. (2011) concluded that the acetylene block technique cannot provide robust estimates of denitrification rates in situ, due to high variation and the unwanted side effects of acetylene, in a comparative study of four denitrification measurement techniques in a DNBR: acetylene block, direct measurement of N_2O and N_2, natural isotope abundance, and the push-pull method.

Direct quantification of N_2 and N_2O fluxes with high precision gas chromatography or gas chromatography mass spectrometry was recommended by Warneke et al. (2011) as the preferred measurement in DNBRs due to its accuracy and low expense. Effluent samples were collected from multiple locations along the bed with a pump and stopcock apparatus connected to a pure helium tank to prevent atmospheric contamination with nitrogen or oxygen; the headspace of the effluent was also sampled to be analyzed for N_2 and N_2O (Warneke et al. 2011).

Warneke et al. (2011) calculated the denitrification rate relying on the assumption that the denitrification rate was the slope of the linear regression of N_2 and N_2O concentrations down-gradient in the bed, assuming that the rate was constant over the length of the bed. Although this measurement may provide a reasonable estimate of the denitrification rate across an entire bioreactor bed, it cannot be used to examine the spatial and temporal variability of denitrification. Notably, this method quantifies N_2O flux from the DNBR, an essential requisite to the implementation of DNBRs as best management practices, and provides a more accurate rate of denitrification than measuring N_2 evolution alone. In contrast to the acetylene block technique, there is no inhibitor and higher analytical precision can be attained when samples are collected with airtight equipment, 0.1-0.3% precision with gas chromatography mass spectrometry (GCMS) (Groffman et al. 2006). Direct measurement of denitrification products is best suited to deep ground water where little gas exchange occurs and background N_2 concentrations in soil water are low compared to atmospheric concentrations, and thus may be inappropriate in near-surface environments where degassing occurs (Groffman et al. 2006). The magnitude of degassing can only be ascertained by comparison with a conservative tracer susceptible to degassing.

The ratio of dissolved N_2 to argon (Ar) ratio in water samples can also be used to determine the rate of denitrification by separating the amount of N_2 present due to contact with the atmosphere and the excess N_2 attributable to denitrification. (Eyre et al. 2002; Kana et al. 1994). Since both biological and physical processes affect N, while the Ar is only subject to physical processes, the biologically driven transformations on N to be distinguished by using Ar as an inert tracer of atmospheric incorporation (Kana et al. 1994). The calculation of excess N_2 attributable to denitrification is described by Weymann et al. (2008) with the following equations:

$$X_{excess}\ N_2 = XN_2\ T - X\ N_{2\ EA} - X\ N_2 \qquad (7)$$

"where X denotes molar concentration of the parameters. $X\ N_2\ T$ represents the molar concentration of the total dissolved N_2 in the [water] sample. $X\ N_2$ EQ is the molar concentration of dissolved N_2 in equilibrium with the atmospheric conditions." The contribution of excess air (EA) can be calculated in two ways depending on whether it is assumed that the air was

incorporated as air bubbles with the composition of the atmosphere that were not dissolved (Equation 8) or can be calculated as if the excess air resulted from bubbles that *were* completely dissolved (Equation 9).

$$X\ N_{2\ EA} = (X\ Ar_{\ T} - X\ Ar_{\ EQ}) * (X\ N_{2\ atm} / X\ Ar_{\ atm}) \quad (8)$$

$$X\ N_2\ EA = (X\ Ar_{\ T} - X\ Ar_{\ EQ}) * (X\ N_{2\ EQ} / X\ Ar_{\ EQ}) \quad (9)$$

The uncertainty due to two ways of calculating excess air is expressed as $U\ N_{2\ EA}$ in equation 10.

$$U\ N_{2\ EA} = (X\ Ar_{\ T} - X\ Ar_{\ EQ}) * (X\ N_{2\ atm} / X\ Ar_{\ atm} - X\ N_{2\ EQ} / X\ Ar_{\ EQ}) \quad (10)$$

It should be acknowledged that, alternatively, Blicher-Mathiesen et al. (1998) also used dissolved N_2 and Ar to simultaneously measure denitrification and degassing in an aquifer. However, the equations presented above by Weymann et al. (2008) assume that dissolved gases are conserved.

Nitrogen isotope methods rely the natural process of isotope fractionation, the partitioning of isotopes in products and reactants due to the differences in thermodynamic characteristics of the isotopes that dictate a difference in the probability that a given reaction will occur with that isotope (Germon et al. 1981). In addition to quantifying denitrification, isotope methods have the advantage of also being able to examine the fate and transport of NO_3 (Chen and MacQuarrie 2005). Denitrification measurements that utilize nitrogen isotopes include analysis of natural abundance, isotope pairing, and direct measurement of ^{15}N-labled denitrification products, e.g. the push-pull technique. Analysis of natural isotope abundance depends upon the isotope fractionation of the stable ^{15}N isotope and the most abundant ^{14}N as a result of physical, chemical and biochemical processes, including denitrification (Germon et al. 1981); ^{14}N, light nitrogen, is preferentially used as an electron acceptor by denitrifying bacteria, enriching the ^{15}N-NO_3^- in comparison to the ^{15}N incorporated into reduction products as described by a Rayleigh distribution, although other processes resulting in fractionation are occurring simultaneously (Germon et al. 1981; Groffman et al. 2006). Laboratory cultures have found enrichment factors of 0 to -30 $^0/_{00}$ of heavy nitrogen in the unreacted NO_3^- pool, and there

is evidence to suggest that the magnitude of enrichment does not directly reflect the denitrification rate as abiotic factors also result in isotope fractionation, e.g. slower diffusion of ^{15}N or source of NO_3^- that varies in natural isotope abundance (Chen and MacQuarrie 2005; Groffman et al. 2006). Therefore analysis of natural isotope abundance provides an unreliable measurement of denitrification due to the lack of correlation between ^{15}N enrichment factors and denitrification rates.

The isotope pairing technique, pioneered by Nielsen (1992), examines N fractionation as a result of the addition of ^{15}N-NO_3, and the fluxes of the three different N_2 molecules ($^{14}N^{14}N$, $^{14}N^{15}N$, and $^{15}N^{15}N$) are compared (Greene 2005). This method is often applied in contained soil cores (Eyre et al. 2002; Risgaard-Petersen et al. 1998), but can also be applied to buried chambers in situ (e.g. Sanders and Trimmer 2006). Abundance of the N_2 isotopes is used to determine the rate of denitrification that would occur without the $^{15}NO_3$ addition using the Nielsen IPT equation (1992):

$$^{28}N_2 = \frac{p^{29}N_2 * (2*p^{30}N_2 + p2^{9}N_2)}{2*p^{30}N_2} \quad (11)$$

Here p refers to the production rate, calculated from the concentrations present in samples extracted over time. This methodology has the advantage of being able to distinguish between coupled nitrification-denitrification and denitrification alone (Cornwell et al. 1999). Simultaneous analysis of oxygen isotope partitioning (^{16}O and ^{18}O) has been shown to make this method more robust (Chen and MacQuarrie 2005). Experimentally, it has been found that enrichment of heavy nitrogen and heavy oxygen in the unreacted nitrate correlate during denitrification, and thus a constant ratio of N to O fractionation is evidence for the occurrence of denitrification thought to be more convincing that ^{15}N enrichment alone (Nielsen 1992). Underlying assumptions of the isotope pairing technique include homogeneous isotope mixing and a linear relationship between denitrification rates and NO_3^- concentration (Risgaard-Petersen et al. 1998; Sanders and Trimmer 2006), which are unlikely to be met in systems that are carbon rather than N-limited, where the denitrification becomes independent of NO_3^- concentration (zero order) (Groffman et al. 2006). Application of this technique to DNBRs treating effluent or tile

drainage with low nitrate levels is inappropriate because these assumptions are unlikely to be met.

The push-pull method of denitrification measurement consists of the injection ("push") of reactant(s) and conservative tracer(s) into a saturated substrate via a piezometer, followed by an immediate extraction ("pull") or extraction after an incubation period during which samples are collected at prescribed intervals (Addy et al. 2002; Istok et al. 1997; Trudell et al. 1986). This method, originally developed by Trudell et al. (1986), quantifies denitrification in situ via breakthrough curve analysis of NO_3 and at least one conservative tracer, e.g. bromide (Br^-). The breakthrough curve of Br^-, plot of relative concentration over time, is used to correct the NO_3 curve for the processes outside of denitrification that lower NO_3 concentration over time, namely the physical processes of advection, dispersion, and diffusion to which Br^- is similarly susceptible (Trudell et al. 1986). The "dilution factor" is calculated as the bromide concentration at a given time divided by the injected bromide concentration. The corrected nitrate concentration is the concentration at a given time multiplied by the dilution factor for that time. The denitrification rate is taken to the slope of the corrected NO_3 concentration versus time (Trudell et al. 1986). Istock et al. (1997) expanded the use of this method to quantify aerobic respiration, sulfate reduction, methanogenesis in an alluvial aquifer by injecting a cocktail of multiple reactants and Br^-.

Addy et al. (2002) substantially modified the push-pull method to optimize recovery of the nitrate plume and account for degassing with the use of an additional conservative tracer and the use of ^{15}N to improve resolution of nitrogen gas fluxes. Sulfur hexaflouide (SF_6), was added to the injectate to correct for the magnitude of degassing of denitrification products, SF_6 being susceptible to degassing at a comparable rate to nitrogen gases (Addy et al. 2002). A conservative tracer pretest was also included to determine the length of incubation period that would optimize recovery of the NO_3 plume, losses of Br^- and SF_6 being attributable to physical processes. Incubation time can exhibit substantial variability under hydrologic different conditions based on the 5 and 72-hour incubation periods used in the Addy et al. (2002) study. Previously extracted groundwater was used as the injectate solution to minimize disturbance of geochemical conditions, amended with ^{15}N-NO_3 and Br^-, and bubbled with SF_6 to lower dissolved oxygen to ambient levels within the aquifer after the solution had been exposed to the atmosphere (Addy et al. 2002). Pumping rates during injection and extraction were low (10-12

L/h) to minimize changes in the hydraulic gradient (Addy et al. 2002). All water samples were collected in a manner to avoid atmospheric contact.

The push-pull technique allows for the examination of the spatial and temporal variability of denitrification rates (Addy et al. 2002, Warneke et al. 2011); the volume in substrate affected by the injection, in which denitrification is being measured, can be calculated based on the porosity and injectate volume as:

$$V_I = \frac{V_i - V_w}{O} - \frac{V_s}{O_s} \quad (12)$$

where V_I is the volume of aquifer examined, V_i is the volume injected, V_w is the volume of water remaining in the well, V_s is volume of the sand pack (if present), O is the effective porosity of the aquifer, and O_s is the effective porosity of the sand pack (Istock et al 1997). The shape of this volume will depend upon substrate heterogeneity, piezometer screen length, thickness of initial saturated zone, injection rate, well development method (Istock et al. 1997), and presumably the groundwater velocity and hydrologic gradient. Given a relatively short incubation period and return to background concentrations of tracers, the push-pull method can be employed at a site with sufficient frequency to examine seasonal if not precipitation event-based variation.

In sum, direct measurement of dissolved gases and quantification of denitrification with the N_2/Ar method is one of the most appropriate for application in DNBR research because it allows for the variability of denitrification rates to be examined over space and time as well as the accumulation of denitrification intermediates to be measured. In contrast, although the acetylene block technique can be used to examine variability in the denitrification rate, it cannot be used to determine the ratio of intermediate products to N_2. Methods relying on isotope fractionation alone do not address intermediate formation either.

1.4.8 Dissolved Gas Analysis

Analysis of the dissolved gas component of natural waters is critical to the study of biogeochemical cycles, groundwater origination, and hydrocarbon contamination. Dissolved gas analysis has the potential to be important tool for studying indirect emissions of N_2O associated

with contamination of groundwater with hydrocarbons or excess nitrate in agricultural setting. As discussed in the previous section, denitrification itself is a difficult process to quantify, and measurement of the N_2 to Ar ratio is one of the most straightforward quantification techniques. Liotta and Martelli (2012) provide a summary of the four main methods used to analyze dissolved gas and cite reviews of the application of these methods: gas stripping (also known as purge and trap), passive diffusion sampling, "release of gas into the headspace of a previously evacuated container into which water is aspirated", and static headspace analysis. Static headspace analysis is the most widely used methodology for analysis of permanent and biogenic dissolved gases in environmental water samples, mainly because it is relatively simple, as it does not require special purge and trap apparatus, evacuated containers, or passive diffusion gas samplers.

Dissolved gas analysis is particularly well suited to application in DNBRs for quantifying denitrification and the ratio of denitrification products due to its simplicity, low expense, ability to examine spatial and temporal variability of denitrification rates, and rapidity with which samples can be collected in the field. Additionally atmospheric contamination of a water sample can easily be minimized by collection in a serum vial with a crimp seal with zero headspace. It is essential to have no atmospheric exchange subsequent to sample collection to accurately quantify excess N with the Ar tracer method as well as other processes that involve atmospheric gases such as methanogenesis or using excess carbon dioxide as a proxy for microbial metabolism. Simultaneous evaluation of all major dissolved gas constituents is useful to understand the in situ dynamics of any single analyte due to the interaction through their partial pressures (Gardner and Solomon 2009).

1.4.9 Context and Motivation: Anthropogenic Impacts on the Chesapeake Bay

Coastal ecosystems and estuaries have been particularly severely impacted by excess Nr because they are dependent on riverine nutrient sources that have doubled nitrogen loading (Galloway et al. 1995), and they are the sites of some of the most intense nutrient recycling because coastal environments are N-limited in temperate regions (Mitsch et al. 2001; Nedwell et al. 1999; Purvaja et al. 2008). The consequences of an oversupply of nutrients can be observed on the large scale in the eutrophication of the Gulf of Mexico and the Chesapeake Bay (Brady and Weil 2008).

The Chesapeake Bay is listed as impaired under the Clean Water Act due to an overabundance of nitrogen, phosphorus, and sediment (EPA 2010). In May 2009, executive order 13508 called for a renewed effort to improve water quality in the Bay, acknowledging the plethora of ecosystem services and values provided by the largest estuary in the US, from its highly productive fisheries to its attractiveness as a tourist destination. The most extensive and complex Total Maximum Daily Load (TMDL) ever developed, encompassing a 64,000 mi^2 watershed, was introduced in December 2010 dictating loading reductions of 25% for nitrogen, 24% phosphorus, and 20% sediment to be achieved over the six states and D.C. contained within the watershed by 2025 (EPA 2010). The Chesapeake Bay Commission summarized six of the most cost-effective strategies reduce nutrient and sediment loading at the "local or tributary" scale: wastewater treatment plant upgrades, diet and feed adjustments, nutrient management plans (NMPs), enhanced nutrient management (15% reduction in applied nutrients beyond traditional NMP), conservation tillage, and cover crops. However, implementation of all of these measures could achieve a maximum 75% of the necessary nitrogen (Chesapeake Bay Commission 2004), so additional innovative solutions remain necessary.

The Chesapeake Bay, the largest and one of the most productive estuaries in the United States, is a grand example of eutrophication, and the site of some of the most intense study of the phenomenon (Boesch et al. 2000). As defined by Nixon (2009), eutrophication refers to "an increase in the rate of supply of organic matter", but the term is often associated with nutrient pollution, the most common but not the only cause of eutrophication. Estuaries and coastal marine environments in the temperate zone are particularly susceptible eutrophication due to excess nitrogen loading because their primary production nitrogen limited (Galloway et al. 2003; Nedwell et al. 1999). In the Bay, increased loadings of both nitrogen and phosphorus have been indicated as contributing factors to the eutrophication (Jickells 2005, Kemp et al. 2005). The resultant algal blooms increased turbidity, blocking light penetration and leading to a decline in submerged aquatic vegetation and overall biodiversity (Boesch et al. 2000, EPA 2010). A positive feedback loop results because aquatic vegetation induces sedimentation by slowing the water (Purvaja et al. 2008). As heterotrophic microorganisms decompose the algae, oxygen is consumed and hypoxia develops, a condition in which dissolved oxygen levels are below those to which native organisms are adapted (Purvaja et al. 2008; Rabalais et al. 2009). Although the Bay is naturally susceptible to seasonal hypoxia, its extent and duration increased between the

1950s and 1980s and has impaired benthic communities during which time inorganic fertilizer application within the watershed tripled (Boesch et al. 2000, EPA 2010).

A Total Maximum Daily Load (TMDL) was established for the Chesapeake Bay on December 29, 2010 because it does not meet the water quality standards set forth by the Clean Water Act due to impairment by excess nitrogen, phosphorus, and sediment (EPA 2010). Target load reductions to be achieved by 2025 were set as 185.9 million pounds of nitrogen per year (25% load reduction), 12.5 million pounds of phosphorus per year, and 6.45 billion pounds of sediment per year (EPA 2010). Management of both nitrogen and phosphorus is necessary to reduce the effects of eutrophication in the Bay, because the limiting macronutrient (N or P) varies seasonally (Cornwell et al. 1999, Kemp et al. 2005). Total nutrient and sediment loadings from agricultural land use has decreased since 1985, but the reductions are lower than those corresponding to point sources, likely due to the voluntary and incentive-based nature of agricultural BMPs as opposed to regulated point source discharges (Novotny 2002).

Excess nitrogen in the Chesapeake Bay watersheds emanates from point source discharges from treated municipal and industrial wastewater, as well as from nonpoint sources including agriculture, residential land use, and private septic systems (EPA 2010, Novotny 2002). Municipal wastewater treatment plants are the largest point source of nitrogen in the US (Mitsch et al. 2001), and modernization of these systems within the Chesapeake Bay watershed achieved substantial point source nutrient loading reductions by 2003 (Novotny 2002). Traditional wastewater treatment is effective for treating effluent from municipal or industrial sources with high nutrient concentrations, it is expensive and labor intensive requiring continuous maintenance and monitoring (Kumar and Lin 2010). Attenuating nutrients from diffuse pollution requires a different approach, and treatment systems must be able to handle fluctuating flow rates and nutrient concentrations as well as be relatively inexpensive and self-sustaining to be deployed in a range of landscape positions. The development of ecological engineering approaches to denitrification management, such as denitrifying bioreactors, has high potential to assist in meeting the nitrogen reduction goals set by the Bay TMDL.

References

Addy, K., D.Q. Kellogg, A.J. Gold, P.M. Groffman, G. Ferendo and C. Sawyer. 2002. In situ push–pull method to determine ground water denitrification in riparian zones. J. Environ. Qual. 31:1017–1024.

Anderson, C.R., L.M. Condron, T.J. Clough, M. Fiers, A. Stewart,. R.A. Hill and R.R. Sherlock. 2011. Biochar induced soil microbial community change: Implications for biogeochemical cycling of carbon, nitrogen and phosphorus. Pedobiologia 54:309–320.

Averill, B.A., and J.M. Tiedje. 1982. The chemical mechanism of microbial denitrification. FEBS Lett. 138:8–12.

Ayres, R. 1997. Integrated assessment of the grand nutrient cycles. Environ. Model Assess. 2:107–128.

Beck, D.A., G.R. Johnson and G.A. Spolek. 2011. Amending greenroof soil with biochar to affect runoff water quantity and quality. Environ. Poll. 159:2111–2118.

Blicher-Mathiesen, G., G.W. McCarty and L.P. Nielsen. 1999. Denitrification and degassing in groundwater estimated from dissolved dinitrogen and argon. J. Hydrol. 208:16–24.

Blowes, D.W., W.D. Robertson, C.J. Ptacek and C. Merkley. 1994. Removal of agricultural nitrate from tile-drainage effluent water using in-line bioreactors. J. Contam. Hydrol. 15:207–221.

Boesch, D.F., R.B. Brinsfield and R.E Magnien. 2001. Chesapeake Bay eutrophication: scientific understanding, ecosystem restoration, and challenges for agriculture. J. Environ. Qual. 30:303–320.

Brady, N.C., and R.R. Weil. 2008. The Nature and Properties of Soils. Fourteenth Edition. Pearson Educaiton, Ltd.

Burgin, A.J., and S.K. Hamilton. 2007. Have we overemphasized the role of denitrification in aquatic ecosystems? A review of nitrate removal pathways. Front. Ecol. Environ. 5:89–96.

Cameron, S.G., and L.A. Schipper. 2010. Nitrate removal and hydraulic performance of organic carbon for use in denitrification beds. Ecol. Eng. 36:1588–1595.

CAST. 1999. Gulf of Mexico hypoxia: land and sea interactions. Task Force Report 134. (Ames, Iowa: Council for Agricultural Science and Technology.)

Chen, D.J.Z., and K.T.B. MacQuarrie. 2005. Correlation of δ15N and δ18O in NO_3^-

during denitrification in groundwater. J. Environ. Eng. Sci. 4:221–226.

Chesapeake Bay Commission. 2004. Cost-effective strategies for the Bay: six smart investments for nutrient and sediment reduction. < http://www.chesbay.us/Publications/cost%20 effective.pdf >

Christianson, L., M. Hedley, M. Camps, H. Free and S. Saggar. 2011. Influence of biochar amendments on denitrification bioreactor performance. IBI <http://www.biochar international.org/node/2699>

Clough, T.J., and L.M. Condron. 2010. Biochar and the nitrogen cycle: introduction. J. Environ. Qual. 39:1218–1223.

Conrad, R. 1996. Soil microorganisms as controllers of atmospheric trace gases. Microb. Rev. 60:609-615.

Cornwell, J.C., W.M. Kemp and T.M. Kana. 1999. Denitrification in coastal ecosystems: methods, environmental controls, and ecosystem level controls, a review. Aqua. Ecol. 33:41–54.

Delwiche, C.C. 1970. The nitrogen cycle. Sci. Am. 223:136–147.

Dinnes, D.L. Assessments of practices to reduce nitrogen and phosphorus nonpoint source pollution of Iowa's surface waters. Review Article. USDA Agricultural Research Services.

Driscoll, C.T., D. Whitall, J. Aber, E. Boyer, M. Castro, C. Cronan, C., Goodale, P. Groffman, C. Hopkinson, K. Lambert, G. Lawrence and S. Ollinger. 2003. Nitrogen pollution in the Northeastern United States: Sources, effects, and management options. BioScience. 53:357–374.

Easton, Z.M., and E.M. Lassiter. 2013. Denitrification Management. VCE Extension Publication BSE-54P.

Elgood, Z., W.D. Robertson, S.L. Schiff and R. Elgood. 2010. Nitrate removal and greenhouse gas production in a stream-bed denitrifying bioreactor. Ecol. Eng. 36:1575–1580.

EPA. 2006. Global Mitigation of non-CO_2 Greenhouse Gases. < http://www.epa.gov/ climatechange/EPAactivities/economics/nonco2projections.html >

EPA. 2010. Chesapeake Bay TMDL Executive Summary. <http://www.epa.gov/reg3wapd/tmdl/ ChesapeakeBay/tmdlexec.html>

Erisman, J.W. 2004. The Nanjing Declaration on Management of Reactive Nitogen. BioScience 54:286–287.

Eyre, B.D., S. Rysgaard, T. Dalsgaard and P.B. Christensen. 2002. Comparison of isotope pairing and N_2:Ar methods for measuring sediment denitrification assumptions, modifications, and implications. Estuaries. 25:1077–1087.

Firestone, M.K., R.B. Firestone and J.M. Tiedje. 1980. Nitrous oxide from soil denitrification: factors controlling its biological production. Science. 208:749–751.

Furth, D.A., and J.A. Ponzi. 2010. Adjusting carbon management policies to encourage renewable, net-negative projects such as biochar sequestration. William Mitchell Law Rev. 36:992.

Galloway, J., W. Schlesinger, H. Levy, A. Michaels and J. Schnoor. 1995. Nitrogen fixation–anthropogenic enhancement–environmental response. Global Biogeochem. Cycles. 9:235–252.

Galloway, J., J. Aber, J. Erisman. S. Seitzinger, R. Howarth, E. Cowling and B. Cosby. 2003. The nitrogen cascade. BioScience 5:341–356.

Galloway, J.N., A.R. Townsend, J.W. Erisman, J. W., M. Bekunda, Z. Cai, Z., J.R. Freney, L.A. Martinelli, S.P. Seitzinger and M.A. Sutton. 2008. Transformation of the nitrogen cycle: recent trends, questions, and potential solutions. Science 320:889–892.

Gardner, P. and D.K. Solomon. 2009. An advanced passive diffusion sampler for the determination of dissolved gas concentrations. Water Resour. Res. 54:W06423.

Germon, J.C., P. Kaiser, A. Mariotti, P. Hubert, P. Tardieux, A. Tardieux and R. Letolle. 1981. Experimental determination of nitrogen kinetic isotope fractionation: some principles; illustration for the denitrification and nitrification processes. Plant Soil. 62:413.

Gibert, O., S. Pomierny, I. Rowe and R.M. Kalin. 2008. Selection of organic substrates as potential reactive materials for use in a denitrification permeable reactive barrier (PRB). Bioresour. Technol. 99:7587–7596.

Greenan, C.M., T.B. Moorman, T.C. Kaspar, T.B. Parkin and D.B. Jaynes, D. B. 2006. Comparing carbon substrates for denitrification of subsurface drainage water. J. Environ. Qual. 35:824–829.

Greene, S. 2005. Measurements of Denitrification in Aquatic Ecosystems; literature review and data report. University of Maryland Center for Environmental Science Technical Report Series. Ref. No. [UMCES]CBL 05-094.

Groffman, P.M., M.A. Altabet, J.K. Böhlke, K. Butterbach-Bahl, M.B. David, M. Firestone, A.E. Giblin, T.M. Kana, L.P. Nielsen, and M.A. Voytek. 2006. Methods for measuring denitrification: diverse approaches to a difficult problem. Ecol. App. 16:2091–2122.

Gruber, N., and J.N. Galloway. 2008. An Earth-system perspective of the global nitrogen cycle. Nature. 451:293-296.

International Biochar Initiative. 2014. What is Biochar? <www.biochar-international.org/biochar>

Istok, J.D., M.D. Humphrey, M.H. Schroth, M.R. Hyman and K.T. O'Reilly, K. T. 1997. Single well, 'push-pull' test for in situ determination of microbial activities. Ground Water 35:619–631.

Jickells, T. 2005. External inputs as a contributor to eutrophication problems. J. Sea Res. 54:58–69.

Kana, T., C. Darkangelo, M. Hunt, J. Oldham, G. Bennett and J. Cornwell. 1994. Membrane inlet mass spectrometer for rapid high-precision determination. Anal. Chem. 66:4166–4170.

Kemp, W.M., W.R. Boynton, J.E. Adolf, D.F. Boesh, W.C. Biocourt, G. Brush, J.C. Cornwell, T.R. Fisher, P.M. Gilbert, J.D. Hagy, L.W. Harding, E.D. Houde, D.G. Kimmel, W.D. Miller, R.I.E. Newell, M.R. Roman, E.M. Smith and J.C. Stevenson. 2005. Eutrophication of the Chesapeake Bay: historical trends and ecological interactions. Mar. Ecol. Prog. Ser. 303:1–29.

Kleinmann, P.J.A., A.N. Sharpley, R.W. McDowell, D.N. Flaten, A.R. Buda, T. Liang, L. Bergstrom and Z. Quing. 2011. Managing agricultural phosphorus for water quality protection: Principles and progress. Plant Soil. 349:169–182.

Kookana, R.S., A.K. Sarmah, L. Van Zwieten, E. Krull and B. Singh. 2011. Biochar application to soil: agronomic and environmental benefits and unintended consequences. Adv. Agron. 112:103–143.

Kuenen, J.G. 2008. Anammox bacteria: from discovery to application. Nat Rev Micro. 6:320–326.

Kumar, M., and J.G. Lin. 2010. Co-existence of anammox and denitrification for simultaneous nitrogen and carbon removal—strategies and issues. J. Hazard. Mat. 178:1–9.

Lehmann, J., M.C. Rilig, J. Thies, C.A. Masiello, W.C. Hockaday and D. Crowley. 2011. Biochar effects on soil biota: a review. Soil Bio. Biochem. 43:1812–1836.

Liotta, M., and M. Martelli. 2012. Dissolved gases in brackish thermal waters: an improved analytical method. Geofluids 12:236–244.

Long, L.M., L.A. Schipper and D.A. Bruesewitz. 2011. Long-term nitrate removal in a denitrification wall. Argic. Ecosyst. Environ. 140:514–520.

Mateju, V., S. Cizinska, J. Krejci, and T. Janoch, T. 1992. Biological water denitrification -a review. Enzyme and Micro. Technol. 14:170–183.

McLaughlin, H., P.S. Anderson, F.E. Shields and T.B. Reed. 2009. All biochars are not created equal and how to tell them apart. Proceedings N. Amer. Biochar Conf. Boulder, Co.

Melillo, J.M. and E.B. Cowling. 2002. Reactive nitrogen and public policies for environmental protection. AMBIO 31:150–158.

Mitsch, W.J., J. Day, J.W. Gilliam, P.M. Groffman, D.L. Hey, G.W. Randall and N. Wang. 2001. Reducing nitrogen loading to the Gulf of Mexico from the Mississippi River basin: strategies to counter a persistent ecological problem. BioScience 51:373.

Moorman, T.B., T.B. Parkin, T.C. Kaspar and D.B. Jaynes. 2010. Denitrification activity, wood loss, and N_2O emissions over 9 years from a wood chip bioreactor. Ecol. Eng. 36:1567–1574.

Mosier, A., C. Kroeze, C. Nevison, O. Oenema, S. Seitzinger and O. van Cleemput. 1998. Closing the global N_2O budget: Nitrous oxide emissions through the agricultural nitrogen cycle.OECD/IPCC/IEA Phase II: development of IPCC guidelines for national greenhouse gas inventory methodology. Nutr. Cycl. Agroecosys. 52:225–248.

Mulder, A., A.A. van de Graaf, L.A. Robertson and J.G. Kuenen. 1995. Anaerobic ammonium oxidation discovered in a denitrifying fluidized bed reactor. FEMS Micro. Ecol. 16:177–183.

Nedwell, D.B., T.D. Jickells, M. Trimmer and R. Sanders. 1999. Nutrients in Estuaries. Estuaries. 29:43–92.

Nelson, N.O., S.C. Agudelo, Y. Wenqia and G. Jing. 2011. Nitrogen and phosphorus availability in biochar-amended soils. Soil Sci. 176:218–226.

Nielsen, L.P. 1992. Denitrification in sediment determined from nitrogen isotope pairing. FEMS microb. ecol. 86:357–362.

Nixon, S.W. 2009. Eutrophication and the macroscope. Hydrobiologia. 629:5-19.

Novotny, V. 2002. Water quality: diffuse pollution and watershed management. John Wiley & Sons.

Parton, W., A. Mosier, D. Ojima, D. Valentine, D. Schimel, K. Weier and A. Kulmala. 1996. Generalized model for N_2 and N_2O production from nitrification and denitrification. Global Biogeochem. Cyc. 10:401–412.

Purvaja, R., R. Ramesh, A.K. Ray and T. Rixen. 2008. Nitrogen cycling: A review of the processes, transformations and fluxes in coastal ecosystems. Curr. Sci. 94:1419–1438.

Rabalais, N.N., R.E. Turner, R.J. Díaz and D. Justić. 2009. Global change and eutrophication of coastal waters. ICES J. Marine Sci. 66:1528–1537.

Rennar, R. 2007. Rethinking biochar. Environ. Sci. Technol. 41:5932–5933.

Risgaard-Petersen, N., L.P. Nielsen and T.H. Blackburn. 1998. Simultaneous measurement of benthic denitrification, with the isotope pairing technique and the N_2 flux method in a continuous flow-through system. Water Res. 32:3371–3377.

Rivett, M.O., S.R. Buss, P. Morgan, J.W.N. Smith and C.D. Bemment. 2008. Nitrate attenuation in groundwater: A review of biogeochemical controlling processes. Water Res. 42:4215–4232.

Robertson, W.D. 2010. Nitrate removal rates in woodchip media of varying age. Ecol. Eng. 36:1581–1587.

Robertson, W.D., and J.A. Cherry. 1995. In situ denitrification of septic-system nitrate using reactive porous media barriers: field trials. Ground Water 33:99–111.

Robertson, W.D., J.L. Vogan and P.S. Lombardo. 2008. Nitrate removal rates in a 15-year-old permeable reactive barrier treating septic system nitrate. Ground Water Monit. Rem. 28:65–72.

Saliling, W.J.B., P.W. Westerman and T.M. Losordo. 2007. Wood chips and wheat straw as alternative biofilter media for denitrification reactors treating aquaculture and other wastewaters with high nitrate concentrations. Aquacul. Eng. 37:222–233.

Sanders, I.A., and M. Trimmer. 2006. In situ application of the $^{15}NO_3^-$ isotope pairing technique to measure denitrification in sediments at the surface-water interface. Limn. Ocean. 4:142–152.

Schipper, L.A., and M. Vojvodić-Vuković. 2000. Nitrate removal from groundwater and

denitrification rates in a porous treatment wall amended with sawdust. Ecol. Eng. 14:269–278.

Schipper, L.A., A.J. Gold and E.A. Davidson. 2010a. Managing denitrification in human dominated landscapes. Ecol. Eng. 36:1503–1506.

Schipper, L.A., W.D. Robertson, A.J. Gold, D.B. Jaynes and S.C. Cameron. 2010b. Denitrifying bioreactors—An approach for reducing nitrate loads to receiving waters. Ecol. Eng. 14:269–278.

Seitzinger, S., J.A. Harrison, J.K. Böhlke, A.F. Bouwman, R. Lowrance, B. Peterson, C. Tobias and G.V. Drecht. 2006. Denitrification across landscapes and waterscapes: A synthesis. Ecol. App. 6:2064–2090.

Sharpley, A., T.C. Daniel, J.T. Sims and D.H. Pote. 1996. Determining environmentally sound soil phosphorus levels. J. Soil Water Conserv. 51:160–166.

Singh, B.P., B.J. Hattion, B. Singh, A.L. Cowie and A. Kathuria. 2010. Influence of biochars on nitrous oxide emission and nitrogen leaching in two contrasting soils. J. Environ. Qual. 39:1224–1235.

Smil, V. 2001. Enriching the earth. Cambridge, MA, MIT Press.

Son, Y. 2001. Non-symbiotic nitrogen fixation in forest ecosystems. Ecol. Res. 16:183–196.

Søvik, A.K., and P.T. Mørkved. 2007. Nitrogen isotope fractionation as a tool for determining denitrification in constructed wetlands. Water Sci.Technol. 56:167–173.

Trudell, M.R., R.W. Gillham and J.A. Cherry. 1986. An in-situ study of the occurrence and rate of denitrification in a shallow unconfined sand aquifer. J. Hydro. 83:251–268.

Verheijen, F., S. Jeffery, A.C. Bastos, M. van der Velde and I. Diafas. 2010. Biochar application to soils: a critical scientific review of effects on soil properties, processes and functions. European Commission Joint Research Centre, Institute for Environment and Sustainability.

Warneke, S., L.A. Schipper, D.A. Bruesewitz and W.T. Baisden. 2011a. A comparison of different approaches for measuring denitrification rates in a nitrate removing bioreactor. Water Res. 45:4141–4151.

Warneke, S., L.A. Schipper, D.A. Bruesewitz, I. McDonald and S. Cameron. 2011b. Rates, controls and potential adverse effects of nitrate removal in a denitrification bed. Ecol. Eng. 37:511–522.

Warneke, S., L.A. Schipper, M.G. Matiasek, K.M. Scow, S. Cameron, D.A. Bruesewitz and I.R. McDonald. 2011c. Nitrate removal, communities of denitrifiers and adverse effects in different carbon substrates for use in denitrification beds. Water Res. 45:5463–5475.

Weymann, D., R. Well, H. Fless, C. von der Heide, M. Deurer, K. Meyer, C. Konrad and W. Walther. 2008. Groundwater N_2O emission factors of nitrate-contaminated aquifers as derived from denitrification progress and N_2O accumulation. Biogeosciences 5:1215–1226.

Winter, T.C., J.W. LaBaugh and D.O. Rosenberry. 1998. The design and use of a hydraulic potentiomanometer for direct measurement of differences in hydraulic head between groundwater and surface water. Limn. Ocean. 33:1209–1214.

Woli, K.P., M.B. David, R.A. Cooke, G.F. McIsaac and C.A. Mitchell. 2010. Nitrogen balance in and export from agricultural fields associated with controlled drainage systems and denitrifying bioreactors. Ecol. Eng. 36:1558–1566.

Yanai, Y., K. Toyota and M. Okazaki. 2007. Effects of charcoal addition on N2O emissions from soil resulting from rewetting air-dried soil in short-term laboratory experiments. Soil Sci. Plant Nutr. 53:181–188.

Zumft, W.G. 1997. Cell biology and molecular basis of denitrification. Microbio. Molec. Bio. Rev. 61:533–556.

2.0 Enhanced Nitrate and Phosphate Removal within a Denitrifying Bioreactor with Biochar

Emily Bock[1], Nick Smith[1], Mark Rogers[1], Brady Coleman[2], Mark Reiter[3], Brian Benham[1], and Zachary M. Easton[1*]

This work was supported by a grant from the Institute of Critical Science and Technology at Virginia Tech, funds from the Virginia Department of Environmental Quality and funds from USDA.

[1] Department of Biological Systems Engineering, Virginia Tech, Blacksburg VA 24061
[2] Department of Geology, College of William and Mary, Williamsburg VA
[3] Department of Crop and Soil Environmental Science, Virginia Tech, Blacksburg VA 24061
*Corresponding Author: zeaston@vt.edu

Full citation:
Enhanced Nitrate and Phosphate Removal in a Denitrifying Bioreactor with Biochar. Bock, E.M. N. Smith, M. Rogers, B. Coleman, M. Reiter, B. Benham, and Z. M. Easton
doi:10.2134/jeq2014.03.0111; posted 5 May 2014

Used with verbal permission from Scott Bradford, technical editor of the Journal of Environmental Quality.

2.1 Abstract

Denitrifying bioreactors (DNBRs) are an emerging technology used to remove nitrate-nitrogen (NO_3^-) from enriched waters by supporting denitrifying microorganisms with organic carbon in an anaerobic environment. Field-scale investigations establish successful removal of NO_3^- from agricultural drainage, but the potential for DNBRs to remediate excess phosphorus (P) exported from agricultural systems has not been addressed. We hypothesized that biochar addition to traditional woodchip DNBRs would enhance NO_3^- and P removal as well as reduce nitrous oxide (N_2O) emissions based upon previous research demonstrating reduced leaching of NO_3^- and P and lower greenhouse gas production associated with biochar amendment of agricultural soils. Nine laboratory-scale DNBRs, a woodchip control, and eight different woodchip-biochar treatments were used to test the effect of biochar on nutrient removal. The biochar treatments constituted a full factorial design of three factors, each with two levels: biochar source material (feedstock), particle size, and application rate. Statistical analysis by repeated measures ANOVA showed a significant effect of biochar, time, and their interaction on NO_3^- and dissolved P removal. Average P removal of 65% was observed in the biochar treatments by 18 hours, after which the concentrations remained stable, compared to an 8% increase in the control after 72 hours. Biochar addition resulted in average NO_3^- removal of 86% after 18 hours and 97% after 72 hours compared to only 13% at 18 hours and 75% at 72 hours in the control. Biochar addition also resulted in significantly lower N_2O production. These results suggest that biochar can reduce the design residence time by enhancing nutrient removal rates.

2.2 Introduction

The link between nutrient loss from agricultural systems and environmental degradation is well established and has prompted approaches ranging from incentive-based programs designed to encourage nutrient management planning to best management practices including cover crops, conservation tillage, and drainage water management (Melillo and Cowling 2002; Kleinman et al. 2011). Innovative strategies are critical given that excess nitrogen (N) and phosphorus (P) underlie a suite of environmental problems such as eutrophication (Duarte 2009; Jickells 2005) and negative impacts on human health (Ayres 1997; Galloway et al. 2003), and that current practices remain inadequate to reach target nutrient load reductions such as those set for the Chesapeake Bay (Chesapeake Bay Commission 2004), particularly in response to the demands of an increasing

population on agricultural production (Erisman 2004; Jaynes et al. 2001; USEPA 2009). Denitrification management is increasingly recognized as a means to mitigate diffuse sources of pollution such as nitrate (NO_3^-) export from agricultural ecosystems. Permanent removal of N from an ecosystem is achieved via microbial denitrification, the stepwise reduction of nitrate to nonreactive dinitrogen gas (N_2) via anaerobic heterotrophic bacteria: $NO_3^- \Rightarrow NO_2 \Rightarrow NO \Rightarrow N_2O \Rightarrow N_2$ (Averill and Tiedje 1982).

Denitrifying bioreactors (DNBRs) attenuate N by promoting the activity of naturally occurring anaerobic, heterotrophic denitrifying bacteria in an organic carbon medium that is saturated sufficiently to allow anoxic conditions to develop. The most common DNBR configurations include denitrification walls intercepting shallow groundwater flow and denitrification beds that receive convergent flow such as agricultural tile drainage. A study conducted by Woli et al. (2010) demonstrated that N removal varied widely in DNBRs receiving agricultural tile drainage, averaging 33% removal while up to nearly 100% removal was achieved with sufficient residence time. Schipper et al. (2010) presented a broad review of N removal rates in DNBR beds and showed a removal range of 2 - 22 g of N m^3 d^{-1}. While it is clear from past studies that DNBRs provide an effective means of NO_3^- removal, in many agricultural systems P is also an important constituent of concern in drainage water, as it can likewise promote eutrophication in freshwater systems (Dils and Heathwaite 1999; Macrae et al. 2007). Unfortunately, P removal has not been a focus of previous DNBR studies. Thus there remain significant opportunities to engineer DNBR systems to treat P as well as NO_3^-.

Woodchips are by far the most common carbon substrate utilized in the field-scale DNBRs due to their availability and low cost, in conjunction with the balance between the lability and long-term stability of this organic carbon energy source (Blowes et al. 1994; Elgood et al. 2010; Long et al. 2011; Moorman et al. 2010; Robertson and Cherry 1995; Schipper and Vojvodić-Vuković 2000). Successful N removal has been observed in these woodchip-based, field-scale systems for up to 15 years without substrate replenishment or other maintenance, even with fluctuating influent NO_3^- concentrations and flow rates (Robertson et al. 2008; Schipper et al. 2010). However, emission of N_2O, an intermediate product of denitrification, has been identified as a concern of widespread DNBR implementation (Moorman et al. 2010; Warneke et al. 2011). Researchers are beginning to explore the potential to expand the application of DNBRs to mitigating other pollutants present in agricultural drainage, including pesticides (Ilhan et al. 2011)

and P. We elected to examine the effect of biochar, a newly emerging soil amendment that has the potential to increase N and P removal in DNBRs and mitigate N_2O emissions.

Biochar has been proven successful in reducing the mobility of N and P in agricultural soils as demonstrated in previous studies (Agudelo et al. 2011; Beck et al 2011; Clough and Condron 2010; Coumaravel et al. 2011). Reduced N_2O emission from soil has also been observed in response to biochar addition (Anderson et al. 2011; Cayuela et al. 2013; Saarnio et al. 2013). Biochar, as defined by the International Biochar Institute (IBI), is "a solid material obtained from thermochemical conversion of biomass in an oxygen limited environment" which is distinguished from charcoal by its intended application as a soil amendment (IBI, McLaughlin et al 2009; Verheijhen et al. 2010). Biochar constitutes a diverse group of materials, and although guidelines are provided by IBI for its categorization, thorough description of its chemical properties and application is critical to the assessing the effect of the amendment on soil properties, nutrient retention, and induced changes to the microbial community.

Biochar application is sometimes associated with improvement of soil function via increased cation exchange capacity (CEC), soil water retention, and enhanced microbial growth (Anderson et al. 2011; Lehmann et al. 2011) as well as increased crop yields in some cases (Beck et al. 2011). Biochar amendment to soil has been shown to reduce leaching of N, P, and organic carbon (Beck et al. 2011; Laird et al. 2010). General characteristics of biochars underlying induced soil properties include high surface charge density, relatively low bulk density, as well as high specific surface area and high micropore volume, which cause biochar to be an effective sorbent (Kookana et al. 2011; Laird et al. 2010). Biochar generally has both polar and non-polar surface sites which allows it to adsorb both organic molecules and nutrients (Laird et al. 2010). Logically, biochar amendment also impacts N and P cycling by changing the physiochemical soil environment and consequently altering the structure and activity of the microbial community (Anderson et al. 2011; Coumaravel et al. 2011). However, the effects of biochar on nutrient transformations and interrelated mechanisms are incompletely understood (Clough and Condron 2010; Nelson et al. 2011).

Current work suggests that the enhancement of microbial activity subsequent to biochar amendment increases nutrient recycling and retention, consequently increasing the probability that the available nutrients will be taken up by plants as opposed to being leached from the soil (Coumaravel et al. 2011; Laird et al. 2010). The increase in soil surface area with the addition of

biochar increases both the soil's water holding capacity and aeration, and is thought to contribute to enhancement of microbial activity by providing greater area for colonization and a higher density of favorable microsites (Coumaravel et al. 2011). A study by Kolb et al. (2009) revealed that biochar boosted microbial efficiency, defined as CO_2 evolved per unit microbial biomass, and specifically increased microbial N fixation.

Soil P availability is increased with biochar amendment due to the increase in pH and CEC and the concurrent decrease in exchangeable Al^{3+} (Nelson et al. 2011). A study by Yao et al. (2011) revealed that the main mechanism of P adsorption to biochar is via colloidal and nano-sized metal oxides, specifically MgO. However, due to the variety of feedstocks and pyrolysis conditions utilized, biochars are in practice a heterogeneous group of materials (Kookana et al. 2011). Many researchers point out the futility of reporting responses to biochar addition without sufficient characterization of the material (McLaughlin et al 2009).

The objective of this study is to determine if biochar addition can enhance N and P removal while simultaneously reducing N_2O production in DNBRs. Although research has established the ability of biochar to reduce P leaching from agricultural soils, particularly in the context of increasing fertilizer use efficiency and P availability to crops (Beck et al. 2011; Laird et al. 2010), fewer studies examine the capacity of biochar to remove P from water (Yao et al. 2011). The composition of the original biomass, the particle size of the biochar, and the volume of biochar added relative to the volume of woodchips are hypothesized to reduce the concentrations of and removal rates for NO_3^- and dissolved P in the DNBR both on a total mass and rate basis.

2.3 Materials and Methods

2.3.1 DNBR Column Construction

Nine experimental columns were constructed from PVC tubing (61 cm L X 10 cm D) fitted with an end cap on one end and a threaded plug with adaptor and coupling on the other. Total inner volume of each column was 5660 +/- 30 mL. Columns were fitted with 15 cm of 1.9 cm ID vinyl tubing protruding from a hole drilled in the end cap and attached to a stopcock for collecting aqueous samples. A butyl rubber septum was affixed to the treaded plug on the top end of each column for gas sampling. The end cap and the threaded plug were attached with PVC-primer and cement and columns were tested for gas and water tightness prior to use. Wire mesh followed by 50 µm filter paper (VWR Filter Paper) was placed at the bottom end cap to prevent solids from

leaching into the sampling tube. 5000 mL of mixed hardwood woodchips were added to nine columns. Eight of the columns received a biochar amendment, either 10% (500 mL) or 30% (1500 mL) by volume addition of one of four different types of biochar. Biochar type was defined by the source feedstock and particle size, Table 1. The biochar was mixed into the woodchips to achieve a near uniform distribution, and since the biochar filled the interstitial spaces between the woodchips, the total volume occupied by substrate in each column was not increased. Columns were stored vertically at approximately 22^0C. Prior to running any experimental trials, the columns were flushed with deionized water (> 10 mOhms) twice to minimize the initial effects such as the first flush of dissolved organic carbon (Schipper et al. 2010), that are not representative of established DNBR performance.

2.3.2 Properties of Organic Carbon Media

Woodchips consisting of mixed hardwood species were obtained from Eastern Shore Forest Products (Salisbury, MD). Four types of biochar were selected from Biochar Now (Berthoud, CO) with differing feedstocks and particle sizes: 3 mm pine feedstock, 26 mesh (~0.6 mm maximum diameter) pine, 3 mm mixed hardwood, and 26 mesh mixed hardwood, Table 1. The hardwood biochar had 71% (dry weight) organic carbon with a hydrogen/carbon ratio of 0.68. The pine biochar had 87% (dry weight) organic carbon with a hydrogen/carbon ratio of 0.30. In addition to the woodchip control treatment, the 8 combinations of the biochar characteristics constituted a full factorial design of three factors each with two levels. Columns were not inoculated with bacteria as those naturally occurring with the woodchips have been found to be sufficient for NO_3^- removal via denitrification to occur (Rogers et al., 2014).

2.3.3 Nutrient Addition, Sampling and Analysis

To begin each trial a solution of deionized water with 35 mg L^{-1} NO_3^--N and 6.8 mg L^{-1} PO_4^{3-}-P was added to each column until the substrate was completely saturated, approximately 3500 mL for the woodchip treatment and 3000 mL for the biochar treatments. Initial nutrient concentrations were selected to represent the maximum concentrations observed in shallow groundwater at the site of a field-scale DNBR located on the Delmarva portion of Virginia (Bock, unpublished data). The experiment was conducted in batches, allowing the solution to remain in the column for the duration rather than using a flow-through system. By examining the change in nutrient concentration over time as opposed to calculating the difference between an average

influent and effluent concentration in a flow-though system, sample time was used to approximate the effect of variable residence time with fewer trials. Aqueous samples were collected in 10 mL aliquots at 18, 48, and 72 hours after the introduction of the nutrient solution. The monitoring period was established based on the time until nearly complete NO_3^- removal. Samples were immediately filtered through a 0.45 µm nylon filters and stored at -4°C until analysis. Water samples were analyzed for NO_3^--N, NH_4^+-N, and PO_4^{3-}-P (often referred to as dissolved reactive P, DRP) using flow injection analysis (Lachat QuikChem 8500 series 2, the method numbers were 10-107-04-1-A for NO_3^-, 10-107-06-2-L for NH_4^+, and 10-115-01-1-A for PO_4^{3-}). Three replicate trials were conducted on each of the nine columns. Columns were drained of initial solution, filled with fresh nutrient solution, recapped, and the sampling procedure replicated. Note that the mixture of woodchips and biochar was not replaced. This procedure represents how a DNBR might be cycled in field applications.

2.3.4 Statistical Analysis

Three separate repeated measures ANOVAs conducted using the ezANOVA package in R (RCD 2012) were used to determine if the treatments, biochar addition, and specific characteristics of biochar had a significant effect of NO_3^- and P removal. The concentrations at three time points (18, 48, and 72 hours) with data from each of the three trials were the response variables in the ANOVAs. Trials were treated as independent because the nutrient solution was considered to be the experimental unit and the individual columns to be separate treatments. The measured N and P concentrations were natural log transformed to correct for non-normal distribution of the residuals. Additionally, the Greenhouse-Geisser correction (Park et al. 2009) was applied to the results of the repeated measures ANOVA since Mauchly's Test determined that the assumption of sphericity was violated (Nagarsenker and Pillai 1973). Where a significant interaction between a factor and time was indicated by the ANOVA, each of the three time intervals were subsequently analyzed by individual ANOVA for that factor after the procedure described by Park et al. (2009). Note that all *p-values* and subsequent discussion of relevance are based on the Greenhouse-Geisser corrected *p-value.*

2.3.5 ANOVA: nutrient concentration by treatment and time

After both the main effects of treatment and time, as well as the interaction of column and time, were found to be significant in the repeated measures ANOVA, individual ANOVAs were

applied to each time interval (Table 2). Multiple comparisons by means of a Tukey test (HSD.test) from the agricolae package in R (RCD 2012) at a significance level of 0.95 (alpha=0.05) were used to determine which substrate treatments resulted in significantly different nutrient concentrations. The results from this analysis, presented in Table 3, include the mean and standard error for each treatment at each time step for P, NO_3^-, and NH_4^+, as well as division of the treatments means into statistically significantly different groups at each time.

2.3.6 ANOVA: nutrient concentration by presence of biochar and time

Another repeated measures ANOVA was similarly used to determine if the average nutrient concentrations in the biochar treatments differed from the control. The interaction of biochar and time was found to be significant. Subsequent Welch tests (a modification of the t test for data with unequal variances) followed the ANOVAs at each time interval to determine whether biochar consistently resulted in lower nutrient concentrations over the course of the experiment. Results are presented in Table 4.

2.3.7 ANOVA: nutrient concentration by feedstock, particle size, application rate and time

After a significant difference was established between the control and biochar treatments, the biochar treatments were analyzed separately from the control to determine the effect of the specific characteristics of biochar addition on the nutrient concentrations. The combinations of biochar factors comprising each treatment, particle size, application rate, and feedstock, constitute a full factorial experimental design, and a repeated measures ANOVA was used to test for the significance of these characteristics' effects on nutrient concentrations. Where a factor had a significant interaction effect with time, a Welch test was again used to determine the difference in means at each time interval. Results are presented in Table 5.

2.3.8 Gas Sampling and Analysis

Gas samples of 25 μL were collected from the headspace of the columns with a gas tight syringe with a locking valve (SampleLock syringe, Hamilton Company) during the 100 hours after the introduction of the nutrient solution for each of the three trials. Quantification of N_2O concentration was conducted with a Shimadzu QP2010 Ultra gas chromatograph mass spectrometer with a Sigma Aldrich Carboxen 1010 PLOT column (60 m, 0.32 mm i.d.) using ultra pure helium (grade 5.5) as the carrier gas. A 7.8 minute temperature program was developed, beginning at a temperature of 60 °C, holding temperature for 0.5 minutes and then increasing to

180 °C at a rate of 20 °C per minute, followed by a one minute hold at 180 °C. The mass spectrometer was used in selective ion monitoring (SIM) mode to increase sensitivity. Splitless injections were made to maximize the mass that reaches the detector to increase sensitivity, but the split ratio was set to 50 to increase the flow through the column and decrease the run time. A flow control program maintaining the linear velocity of the carrier gas while automatically adjusted the total flow as the column temperature changed; initial settings were 198.8 kPA inlet pressure, 155.9 mL/min total flow, and 3.04 mL/min column flow. The temperature of the injector, interface, and ion source were 110 °C, 150 °C, and 200 °C respectively. An external calibration curve (R^2=0.9876) was prepared using a standard mixture of N_2O in helium. The linear range of quantification was 0.2-925 ppm.

2.4 Results and Discussion

The different treatments were found to have a significant effect on P and NO_3^- concentrations, but not on NH_4+ (Table 2). As hypothesized, the addition of biochar to the traditional woodchip media in the laboratory scale DNBRs significantly enhanced P and NO_3^- removal, resulting in lower concentrations than the control, while having no significant effect on the concentration of NH_4^+ (Table 4). Biochar induced a 65% reduction in P concentration compared to a net increase of 8% in the control (Figure 1). In contrast, all treatments including the control exhibited similar final NO_3^- and NH_4^+ concentrations at the end of the 72 hour trial, decreasing NO_3^- and increasing NH_4^+ relative to the initial concentration (Table 3). However, biochar greatly increased the rate of NO_3^- removal, particularly during the first 18 hours with an average decrease of 94% from the initial concentration compared to a 13% decrease in the control (Table 4 and Figure 2). Biochar factor levels (feedstock, size, and application rate) did not show a statistically significant effect on P or NH_4^+ concentrations, although the pine feedstock resulted in significantly lower NO_3^- concentrations than hardwood during the first 18 hours of the experiment (see Table 5).

2.4.1 Phosphorus

Biochar addition resulted in significantly lower concentrations of DRP than the woodchip-only control (an average of 4.5 mg L^{-1}). We recognize that in quantifying P in filtered water samples, only the DRP was measured. However, adsorption is reported as the removal mechanism of aqueous P by several studies investigating nutrient remediation with biochar (Sarkhot et al.

2013; Streubel et al. 2012; Yao et al. 2011). Biochar also contains significant concentrations of magnesium and calcium with which DRP can form insoluble precipitates. We speculate that the removal mechanism is a combination of adsorption within the matrix and precipitation of the DRP out of solution, although our data do not allow direct quantification of these processes.

The results from the repeated measures ANOVA indicate significant effects of time and the presence of biochar, as well as the interaction between time and biochar on DRP (Table 4). Subsequent Welch tests demonstrate a lower concentration of DRP for the biochar treatments at each of the three time points compared to the control, an average difference of 4.5 mg L^{-1} (Table 4). The DRP removal attributable to the addition of biochar occurred within the first 18 hours, after which there was no detectable change in concentration (Table 3, Figure 1). In contrast, the control treatment resulted in an increase in DRP of 0.6 mg L^{-1} over the course of the experiment (Table 3, Figure 1).

The main effects of the biochar characteristics (particle size, feedstock, and application rate) did not have a significant affect on the P reduction induced by the biochar amendment (at a significance level of α=0.05), although time was found to be significant (Table 5, Figure 1). Note the *p-value* of the size:time interaction after applying the Greenhouse-Geisser correction was 0.058, which is marginally significant, and may be environmentally relevant. Figure 1 shows this relationship, and although the confidence intervals overlap there does appear to be a slight difference induced by biochar size fractionation, the larger 3 mm particles resulting in slightly lower DRP concentrations (on the order of 1 mg L^{-1}). Although this result may seem unexpected based on the relationship between decreasing particle size and increasing surface area, we postulate that the contribution to surface area of biochar's microporosity may overwhelm the effect of particle size. Biochar feedstock may also have a marginal effect of DRP removal given a *p-value* of 0.083, indicating the potential for hardwood to remove more DRP than the pine feedstock (Table 5, Figure 1).

To utilize P adsorption in DNBRs as a means of removal, characterization of the finite uptake capacity and expected lifespan is required. Replenishment of biochar in DNBRs, although not a practice necessitated by traditional woodchip substrate, may constitute acceptable additional maintenance for the added benefits of P mitigation. Given that surface water concentrations of P as low as 0.1 mg L^{-1} are associated with accelerated eutrophication and degradation of stream health (Mainstone and Parr 2002), and that P export from agricultural systems are significant

contributors to surface water P loading (Reid et al. 2012), the evidence provided by this experiment for enhanced P removal in DNBRs augmented with biochar shows promise.

2.4.2 Nitrate

Given that biochar did not have a significant effect on NH_4^+, (all treatments exhibited similar reductions in NH_4^+ concentrations, Table 3) the data do not indicate any effect of biochar on the conversion of NO_3^- to NH_4^+ (e.g., Dissimilarity Nitrate Reduction to Ammonium—DNRA). Consequently, any additional NO_3^- removal attributable to biochar addition can be considered an enhancement of DNBR performance, increased permanent removal of reactive nitrogen via denitrification, and not a result of altered biochemical N processing. These observations corroborate the body of biochar literature that indicates enhanced microbial activity and nutrient cycling can result in reduced leaching of NO_3^- (Beck et al. 2011; Coumaravel et al. 2011; Laird et al. 2010; Lehmann et al. 2011). Work by Anderson et al. (2011) demonstrating an increase in denitrifying bacteria abundance supports our results that denitrification is the mechanism of increased NO_3^- removal. Biochar may provide additional habitat for microbial colonization with its high specific surface, or provide more favorable microsites where its polar sites retain ions, water, and organic compounds (Kookana et al 2011; Laird et al. 2010).

Biochar significantly increased NO_3^- removal compared to the control at each sampling interval (Tables 3 and 4, Figure 2). The majority of NO_3^- removal induced by biochar addition occurred during the first 18 hours, 94% reduction compared to 13% in the control, resulting in the largest difference between the control and biochar treatments of 27.1 mg L^{-1} (see Welsh test in Table 4, Figure 2). The difference between biochar addition and the control decreased to 14.6 and 8.0 mg L^{-1} after 48 and 72 hours, respectively. These results show the effect of biochar not only on the total reduction in NO_3^- achieved after the 72-hour monitoring period but also on the rate at which NO_3^- is removed, which is significant. Examining the effect of biochar addition over shorter residence times may provide further opportunity for DNBR optimization, given the greatest NO_3^- removal occurred during the first sampling interval. The results presented in Figure 2 demonstrate that the largest benefit of biochar to DNBR performance may be enabling the reduction of the residence time required to adequately treat NO_3^- enriched influent. The benefits of biochar addition are relevant to highly enriched sources exceeding the 10 mg L^{-1} maximum contaminant level of NO_3^- for drinking water set by the EPA (2009), not an uncommon concentration in agricultural drainage (Goswami et al. 2009).

For NO_3^-, biochar feedstock, time, and the interaction of feedstock over time were found to have significant effects (Table 5). At 18 hours, the pine feedstock biochar was found to induce significantly lower NO_3^- concentrations than the hardwood feedstock, approximately 2.8 mg L^{-1} additional removal (see Welch test in Table 5). Here the hardwood feedstock outperformed the pine. Particle size and application rate did not have a significant interaction over time, so they were not analyzed by individual ANOVAs (Park et al. 2009). By 48 hours, no difference could be detected between the means of the nutrient concentrations for any of the biochar factor levels. This analysis of the biochar data alone confirms what was observed in the comparison between biochar treatments and the control; the most significant effect of the biochar treatment is observed at the earlier stages of the experiment, which is environmentally relevant, particularly with respect to influent residence times. These results indicate that biochar addition may enable field-scale DNBRs to be designed with shorter residence times, allowing larger volumes of water to be treated more effectively.

Additionally, the maximum level of P removal appears to be achieved at residence times comparable to those required for adequate NO_3^- removal, with the caveat that only one specific influent nutrient solution was tested in this study. However, we believe that these concentrations are a sufficiently high to encompass the maximum levels of nutrient enrichment likely to be encountered in a field scale DNBR receiving agricultural drainage**.**

2.4.3 Nitrous Oxide

The control treatment produced significantly more N_2O than any of the biochar treatments over the observation period (Figure 3). The biochar treatments show overlapping 95% confidence intervals, that is, they are not statistically different, whereas the control treatment produces significantly more N_2O after approximately 36 hours. Note that two of the N2O samples from the control treatment, collected at time 66 and time 72 of the second trial, exceeded the maximum limit of quantification by saturating the MS detector and resulting in an inaccurate quantification. Consequently, these two values were set to 930 ppm for use in the local regression, because the rising limbs of the chromatographic peaks produced before the detector shut off were similar to the largest concentration quantified, 925 ppm. Given the large difference in N2O concentration between the control and biochar treatments by 66-72 hours, assigning a value of 925 to these two data points did not affect statistical analysis. Interestingly, the control exhibited a continued increase in N_2O concentrations over the study duration (Figure 3). However, these results must be

interpreted with acknowledgement that the gas tightness of the laboratory column and the open gas exchange with the atmosphere of field-scale DNBRs would produce different results. The curve representing the change N_2O concentration over time expresses the balance of N_2O production and N_2O consumption during denitrification; the slope is positive when N_2O production dominates and negative slope when N_2O consumption occurs at a greater rate (Figure 3). The observed decease in concentration might be the result of N_2O diffusion from the headspace back into the aqueous phase, where it subsequently becomes available for continued reduction to N_2 by denitrifiers. In contrast, in an open system once N_2O escapes the aqueous phase it is not subject to subsequent reduction. Thus, these results might actually under estimate N_2O from field DNBRs.

2.4.4 Relevance in Application

Many years of research have established the ability of simple woodchip DNBRs to contribute to measureable improvements in water quality through the permanent removal of reactive N from impacted ecosystems, particularly agricultural watersheds. The main factors controlling the rate of denitrification in DNBRs have been identified at the field scale and include influent NO_3^- concentration, source of available carbon, substrate particle size, temperature, and dissolved oxygen concentration (Warneke et al. 2011). Christianson et al. (2010) highlights the importance of characterizing the hydraulic properties of DNBR media, critical to DNBR design. Indeed porosity and hydraulic conductivity dictate the tradeoff between design volume, proportion of flow treated, and residence time. As demonstrated in this experiment, biochar addition significantly reduces the residence time required to achieve a given reduction in NO_3^- and P concentrations, which has not been shown before, as well as reduces N_2O emission during denitrification. Although changes in hydraulic conductivity and porosity were not measured in response to biochar addition, which would affect the residence time and treatment volume respectively, the indistinguishable effect of the 10% and 30% biochar additions indicate the possibility to minimize undesirable changes to the hydraulic properties of the substrate while maintaining the benefits with respect to nutrient removal and N_2O mitigation. Determining the minimum rate of biochar application for enhanced performance would reduce or eliminate negative effects on hydraulic properties and reduce the cost of materials.

As continued research investigates the optimization of NO_3^- removal in DNBRs, the opportunity to leverage P attenuation is warranted. In contrast to the biological conversion of NO_3^- to N_2, enhanced removal of P with biochar addition is a physiochemical process that can be limited

by the saturation of sorption sites for adsorption or consumption of reactants in the precipitation reaction. Unfortunately our data do not allow us to explicitly quantify which mechanism (adsorption or precipitation) is primarily responsible for the observed reductions. Consideration of their relative contributions of precipitation and adsorption to P removal constitutes important future work, because the specific mechanisms of P removal may affect the rate as well as total amount of P that is removed. The longevity of enhanced P removal in biochar amended DNBRs must be adequately described to ensure a practical benefit in the field. Although the long-term performance of biochar in DNBRs is uncertain, future investigation is certainly merited.

Pilot scale DNBR studies are needed to examine the effect of biochar on performance under conditions of fluctuating inlet concentrations, temperatures, and other variable environmental factors. It is important to consider that additional variables in field-scale implementation such as temperature, soil, and pH differences can affect DNBR performance and optimal biochar characteristics and application rates through interactions not addressed in this study. The properties of biochar associated with improved soil function include increased CEC, soil water-holding capacity, surface sorption capacity, base saturation, and increasing pH (Coumaravel et al. 2011). Consequently, the incorporation of biochar into field-scale DNBR experiments may result in more complex responses than laboratory analysis as there are many factors that will affect the long term in response: degradation of the woodchips and biochar, which can alter carbon to N ratios and thus the rate of denitrification; changes in hydraulic properties affecting the residence time and treatment volumes; competition for sorption sites between various polar molecules present, and; ultimately saturation of sorption sites.

2.4.5 Conclusions

This experiment highlights the potential to expand DNBR functionality to include P and N_2O mitigation through the incorporation of biochar and emphasizes the importance of characterizing biochar, which is, in practice, a diverse category of materials with respect to how the physiochemical properties affect specific applications. Having demonstrated the ability of biochar to increase the NO_3^- and P removal in DNBRs while reducing N_2O emissions, future studies to explore more variations of the material could be undertaken to further enhanced nutrient removal, or address other contaminants of agricultural tile drainage such as bacteria, pesticides or pharmaceuticals. Additionally, shorter sampling time intervals could further refine needed residence times for adequate treatment.

2.5 Acknowledgements

This work was supported by a grant from the Institute of Critical Science and Technology at Virginia Tech, funds from the Virginia Department of Environmental Quality and funds from USDA.

2.6 Tables and Figures

Treatment	Feedstock	Particle Size	Application Rate (v/v)
HW_L_10	hardwood	large (3 mm)	10%
HW_S_10	hardwood	small (0.6 mm)	10%
HW_L_30	hardwood	Large	30%
HW_S_30	hardwood	Small	30%
P_L_10	pine	Large	10%
P_S_10	pine	Small	10%
P_L_30	pine	Large	30%
P_S_30	pine	Small	30%
WC	-	-	-

Table 2.1 Nine experimental treatments and description of the characteristics of the biochar amendment.

a) Phosphorus

ANOVA	Effect	DFn	DFd	F	p	Mauchly's W	W *p*-value	p[GG]
repeated measures	column	8	18	3.309	0.002*	-	-	
	time	3	54	49.831	<0.001*	0.5473	0.073	<0.001*
	column:time	24	54	2.408	<0.001*	0.5473	0.073	<0.001*

b) Nitrate

ANOVA	Effect	DFn	DFd	F	p	Mauchly's W	W *p*-value	p[GG]
repeated measures	column	8	18	5.591	0.001*	-	-	-
	time	3	54	95.552	<0.001*	0.0826	<0.001*	<0.001*
	column:time	24	54	1.678	0.058	0.0615	<0.001	0.126

c) Ammonium

ANOVA	Effect	DFn	DFd	F	p	Mauchly's W	W *p*-value	p[GG]
repeated measures	column	8	18	0.850	0.573	-	-	-
	time	3	54	27.121	<0.001*	0.0780	<0.001*	<0.001*
	column:time	24	54	0.970	0.517	0.0780	<0.001*	0.495

Table 2.2 (a-c) Results from repeated measures ANOVA testing the effect of column, time, and their interaction on the concentration of dissolved phosphorus, nitrate, and ammonium. Abbreviations defined from left to right: DFn is the degrees of freedom of the numerator, DFd is the degrees of freedom of the denominator, F statistic, p is the probability of the data given the null hypothesis that the effect of a factor is not significant where * indicates a significance level of $\alpha < 0.05$, Mauchly's W statistic, W p-value where the null hypothesis is sphericity of the data, and p[GG] is the *p*-value for the significance of the effect after the Greenhouse-Geisser correction has been applied.

	Nutrient Concentration								
	PO_4^{2-}			NO_3^-			NH_4^+		
Column	**18**	**48**	**72**	**18**	**48**	**72**	**18**	**48**	**72**
	----------mg L^{-1}----------								
HW_L_10	1.15(0.45)a	1.87(2.35)a	2.17(2.36)a	2.93(2.89)	0.08(0.02)	0.06(0.04)	4.77(1.30)	3.89(3.15)	3.44(2.47)
HW_S_10	1.67(0.14)ab	1.53(0.82)a	2.07(2.11)a	5.38(4.92)	0.05(0.01)	0.05(0.03)	2.19(2.19)	2.14(3.71)	2.46(3.94)
HW_L_30	1.43(0.44)a	0.93(0.46)a	1.76(2.26)a	1.46(1.23)	0.07(0.03)	0.06(0.02)	3.27(0.37)	2.67(1.25)	2.45(0.62)
HW_S_30	3.25(0.23)ab	3.83(2.08)ab	4.36(0.68)ab	4.44(2.85)	0.06(0.06)	0.06(0.05)	6.30(2.57)	6.59(3.54)	4.75(4.37)
P_L_10	3.35(1.04)ab	2.17(2.73)a	4.02(2.00)ab	0.04(0.02)	0.07(0.07)	0.04(0.04)	2.82(1.56)	2.95(2.76)	2.25(3.42)
P_S_10	1.57(0.13)a	1.43(0.74)a	2.42(0.63)a	0.06(0.03)	0.06(0.06)	0.03(0.02)	3.13(0.94)	2.69(2.30)	1.51(1.89)
P_L_30	4.19(1.43)ab	3.70(1.27)ab	2.47(0.76)a	0.05(0.02)	0.08(0.08)	0.04(0.04)	3.86(0.45)	3.06(0.08)	1.26(0.44)
P_S_30	3.43(0.44)a	3.40(1.01)ab	3.40(1.48)ab	3.06(3.00)	0.05(0.05)	0.04(0.03)	4.98(2.89)	4.17(4.77)	3.78(4.19)
WC	6.53(0.82)b	7.15(2.31)b	7.43(1.02)b	29.28(1.94)b	14.68(12.33)b	8.415(14.16)	3.82(0.72)	2.51(1.27)	2.62(1.00)

Table 2.3 Mean and (SE) of nutrient concentrations, dissolved phosphorus, nitrate, and ammonium, observed in aqueous samples from the DNBR columns 18, 48, and 72 hours after introduction of a nutrient solution. Means within each column are significantly different if followed by a different letter, as determined by a Tukey HSD test (=0.05) for each time interval for each nutrient. Where no letter is given the membership in group a is implied.

a) Phosphorus

ANOVA	Effect	DFn	DFd	F	p	Mauchly's W	*W p*-value	p[GG]
repeated measures	biochar			8.823	0.006*	-	-	-
	time			5.027	0.003*	0.6888	0.116	0.006*
	biochar:time			5.135	0.003*	0.6888	0.116	0.005*

Welch tests	t	Df	p	difference woodchips-biochar	95% CI
18 hours	-4.623	2.592	0.026*	4.02	1.00 - 7.06
48 hours	-3.475	2.292	0.061	4.80	0.47 - 10.07
72 hours	-6.754	3.562	0.004*	4.60	2.61 - 6.59

b) Nitrate

ANOVA	Effect	DFn	DFd	F	p	Mauchly's W	*W p*-value	p[GG]
repeated measures	biochar			39.960	<0.001*	-	-	-
	time			21.030	<0.001*	0.0615	<0.001	<0.001*
	biochar:time			6.481	<0.001*	0.0615	<0.001	0.008*

Welch tests	t	Df	p	difference woodchips-biochar	95% C
18 hours	-12.765	2.823	0.001*	27.10	20.11 - 34.09
48 hours	-2.0525	2	0.177	14.62	0 - 45.25
72 hours	-1.0238	2	0.414	8.02	0 - 43.53

c) Ammonium

ANOVA	Effect	DFn	DFd	F	p	Mauchly's W	*W p*-value	p[GG]
repeated measures	biochar			0.015	0.903	-	-	-
	time			9.403	<0.001*	0.0841	<0.001	0.002*
	biochar:time			0.137	0.937	0.0841	<0.001	0.782

Table 2.4 (a-c) Results from a repeated measures ANOVAs testing the effect of biochar, time and their interaction on phosphorus, nitrate, and ammonium concentrations. Individual ANOVAs were conducted at each time interval for phosphorus and nitrate since the interaction of biochar and time was found to be significant. Abbreviations for the ANOVA described in table 2. Abbreviations defined from left to right are t statistic, degrees of freedom, *p*-value, and 95% confidence interval for the mean difference.

a) Phosphorus

ANOVA	Effect	DFn	DFd	F	p	Mauchly's W	W *p*-value	p[GG]
repeated measures	Feedstock	1	16	3.295	0.083	-	-	-
	Size	1	16	2.991	0.103	-	-	-
	Rate	1	16	1.445	0.246	-	-	-
	Time	3	48	51.517	<0.001*	0.5200	0.0871	<0.001*
	size:time	3	48	2.928	0.004*	0.5200	0.0871	0.058

b) Nitrate

ANOVA	Effect	DFn	DFd	F	p	Mauchly's W	W *p*-value	p[GG]
repeated measures	Feedstock	1	16	4.772	0.004*	-	-	-
	Size	1	16	0.588	0.455	-	-	-
	Rate	1	16	0.356	0.559	-	-	-
	Time	3	48	96.280	<0.001*	0.0296	<0.001*	0.046*
	feedstock:time	3	48	3.999	0.001*	0.0296	<0.001*	0.043*

Welch Tests	Effect	t	DF	p	difference hardwood - pine	95% CI
18 hours	Feedstock	1.679	16.439	0.112	2.75	-0.715 – 6.22
48 hours	Feedstock	0.077	21.893	0.939	0	-0.02 – 0.02
72 hours	Feedstock	1.4652	21.708	0.157	0.02	-0.01 – 0.04

c) Ammonium

ANOVA	Effect	DFn	DFd	F	p	Mauchly's W	W *p*-value	p[GG]
repeated measures	Feedstock	1	16	1.014	0.329	-	-	-
	Size	1	16	0.161	0.694	-	-	-
	Rate	1	16	1.000	0.333	-	-	-
	Time	3	48	22.748	<0.001*	0.0501	<0.001*	<0.001*
	size:rate:time	3	48	3.149	0.003*	0.0501	<0.001*	0.084

Table 2.5 (a-c) Results from a repeated measures ANOVA testing the effect of biochar feedstock, size, application rate, time, as well as their interaction on dissolved phosphorus, nitrate, and ammonium. Welch tests following ANOVAS for each time interval for the effect of feedstock on nitrate concentration given the significant interaction of feedstock and time. Abbreviations defined in tables 2 and 4.

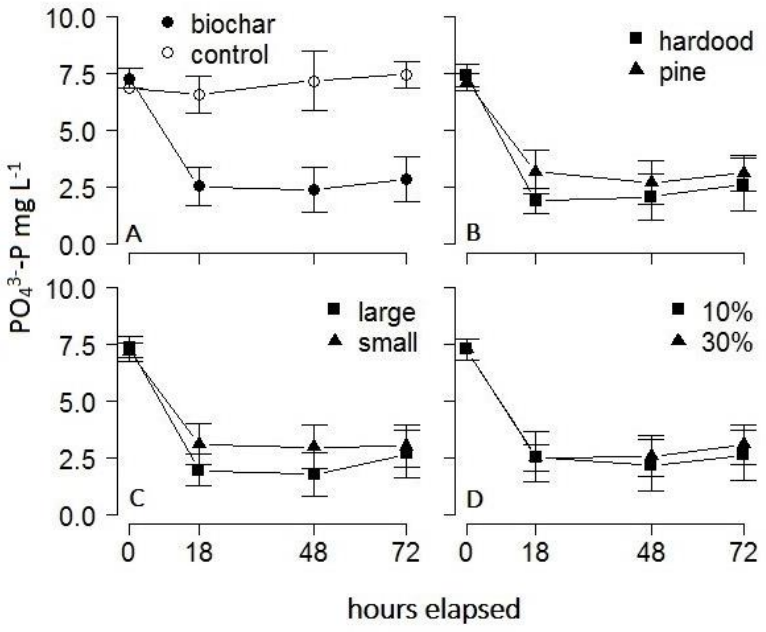

Figure 2.1 Changes in mean phosphorus concentrations and standard errors over time and the difference between the biochar amended treatments and the woodchip control (A) and the levels of biochar characteristics feedstock (B), particle size (C), and volumetric application rate (D).

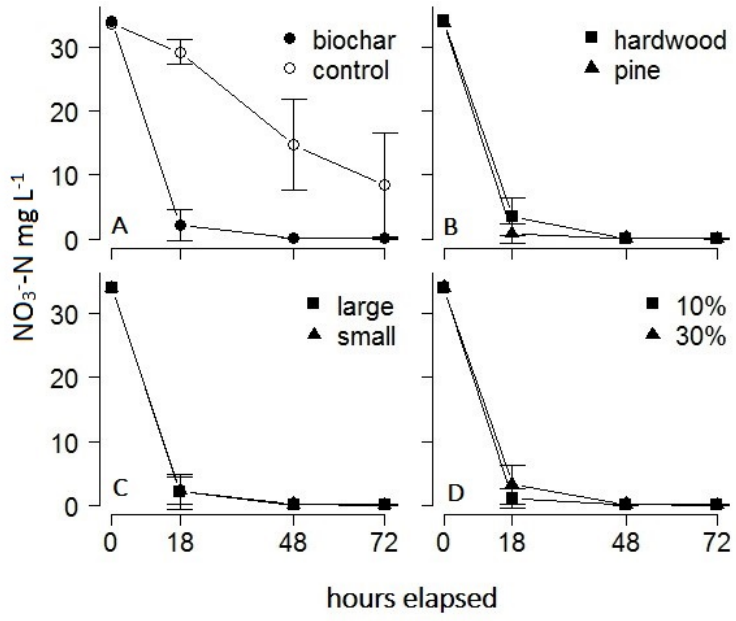

Figure 2.2 Changes in mean nitrate concentrations and standard errors over time and the difference between the biochar amended treatments and the woodchip control (A) and the levels of biochar characteristics feedstock (B), particle size (C), and volumetric application rate (D).

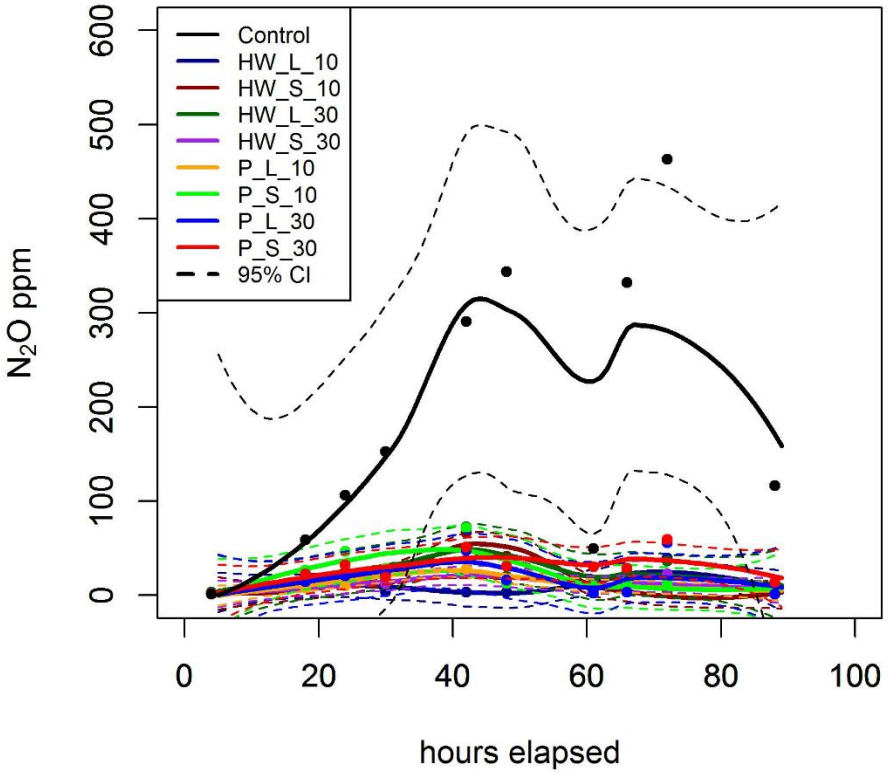

Figure 2.3 Loess fit of mean N_2O concentrations in the column headspace (solid lines) and 95% confidence interval (dashed lines). Points represent the means of measured concentrations. Confidence intervals that do not overlap indicate significant differences.

References

Agudelo, S.C., W. Yuan, and J. Gan. 2011. Nitrogen and Phosphorus Availability in Biochar Amended Soils. Soil Sci. 176:1–226.

Anderson, C.R., L.M. Condron, T.J. Clough, M. Fiers, A. Stewart,. R.A. Hill and R.R. Sherlock. 2011. Biochar induced soil microbial community change: Implications for biogeochemical cycling of carbon, nitrogen and phosphorus. Pedobiologia. 54:309-320.

Averill, B.A. and J.M. Tiedje. 1982. The chemical mechanism of microbioal denitrification. FEBS Lett. 138:8–12.

Ayres, R. 1997. Integrated assessment of the grand nutrient cycles. Environ. Model Assess. 2:107–128.

Beck, D.A., G.R. Johnson and G.A. Spelok. 2011. Amending greenroof soil with biochar to affect runoff water quantity and quality. Environ Pollut. 15:2111-2118.

Blowes, D.W., W.D. Robertson, C.J. Ptacek and C. Merkley. 1994. Removal of agricultural nitrate from tile-drainage effluent water using in-line bioreactors. J. Contam. Hydrol. 15:207–221.

Cayuela, M.L., M.A. Sanchez-Monedero, A. Roig, K. Hanley, A. Enders, and J. Lehmann. 2013. Biochar and denitrificaiton in soils: when, how much and why does biochar reduce N_2O emissions? Sci. Rep. 3:1732–1739.

Chesapeake Bay Commission. 2004. Cost-effective strategies for the Bay: six smart investments for nutrient and sediment reductin. Available: http://www.chesbay.state.va.us/Publications/ cost%20effective.pdf. Accessed: November 9, 2011.

Christianson, L., A. Castello, R. Christianson, M. Helmers and A. Bhandari. 2010. Technical note: hydraulic property determination of denitrifying bioreactor fill media. Trans. ASABE. 26:849–854.

Clough, T. J. and L.M. Condron. 2010. Biochar and the nitrogen cycle: introduction. J. Environ. Qual. 39:1218–1223.

Coumaravel, K., R. Santhi, V.S. Kumar and M.M. Mansour. 2011. Biochar—a promising soil additive. Agric. Rev. 32:134–139.

Dils, R.M. and A.L. Heathwaite. 1999. The controversial role of tile drainage in phosphorus export from agricultural land. Water Sci. Technol. 39:55–61.

Duarte, C.M. 2009. Coastal eutrophication research: a new awareness. Hydrobiologia. 629:263–269.

Elgood, Z., W.D. Robertson, S.L. Schiff and R. Elgood. 2010. Nitrate removal and greenhouse gas production in a stream-bed denitrifying bioreactor. Ecol. Eng. 36:1575–1580.

Erisman, J.W. 2004. The Nanjing Declaration on Management of Reactive Nitrogen. BioScience 54:286–287.

Galloway, J., J. Aber, J. Erisman. S. Seitzinger, R. Howarth, E. Cowling and B. Cosby. 2003. The nitrogen cascade. BioScience. 5:341–356.

Goswami, D., P.K. Kalita, R.A.C. Cooke and G.F. McIsaac. 2009. Nitrate-N loadings through subsurface environment to agricultural drainage ditches in two flat Midwestern (USA) watersheds. Agric. Water Manage. 96:1021–1030.

Ilhan, Z.E., S.K. Ong and T.B. Moorman. 2011. Dissipation of Atrazine, Enrofloxacin, and Sulfamethazine in Wood Chip Bioreactors and Impact on Denitrification. J. Environ. Qual. 40:1816–1823.

Jaynes, D.B., T.S. Colvin, D.L. Karlen, C.A. Cambardella and D.W. Meek. 2001. Nitrate loss in subsurface drainage as affected by nitrogen fertilizer rate. J. Environ. Qual. 30:1305–1314.

Jacoby, W.G. 2000. Loess: a nonparametric, graphical tool for depicting relationships between variables. Elect. Stud. 19:577–613.

Jickells, T. 2005. External inputs as a contributor to eutrophication problems. J. Sea Res. 54:58–69.

Kleinman, P.J.A., A.N. Sharpley, R.W. McDowell, D.N. Flaten, A.R. Buda, L. Tao, L. Bergstrom and Q. Zhu. 2011. Managing agricultural phosphorus for water quality protection: principles for progress. Plant Soil. 349:169–182.

Kolb, S.E., K.J. Fermanich and M.E. Dornbrush. 2009. Effect of charcoal quantity on microbial biomass and activity in temperate soils. Soil Sci. 73:1173–1181.

Kookana, R.S., A.K. Sarmah, L. Van Zwieten, E. Drull and B. Singh. 2011. Chapter three Biochar application to soil: agronomic and environmental benefits and unintended consequences. Adv. in Agron. 112:103–143.

Laird, D., P. Fleming, B. Wang, R. Horton and D. Karlen. 2010. Biochar impact on nutrient leachingfrom a Midwestern agricultural soil. Geoderma. 158:436–442.

Lehmann, J. 2007. Bio-energy in the black. Front. Ecol. Environ. 5:381–387.

Lehmann, J., M.C., Rillig, J. Thies, C.A. Masiello, W.C., Hockaday and D. Crowley. 2011. Biochar effects on soil biota – A review. Soil Biol. Biochem. 43:1812–1836.

Long, L.M., L.A. Schipper and D.A. Bruesewitz. 2011. Long-term nitrate removal in a denitrification wall. Argic. Ecosyst. Environ. 140:514–520.

Macrae, M.L., M.C. English, S.L. Schiff and M. Stone. 2007. Intra-annual variability in the contribution of tile drains to basin discharge and phosphorus export in a first-order agricultural catchment. Agric. Water Manage. 92:171–182.

Mainstone, C.P. and W. Parr. 2002. Phosphorus in rivers—ecology and management. Sci. Total Environ. 25:282–283.

McLaughlin, H., P.S. Anderson, F.E. Shields and T.B. Reed. 2009. All biochars are not created equal and how to tell them apart. N. Am. Biochar. 2:1–36.

Melillo, J.M. and E.B. Cowling. 2002. Reactive Nitrogen and Public Policies for Environmental Protection. AMBIO. 31:150–158.

Moorman, T.B., T.B. Parkin, T.C. Kaspar and D.B. Jaynes. 2010. Denitrification activity, wood loss, and N_2O emissions over 9 years from a wood chip bioreactor. Ecol. Eng. 36:1567–1574.

Nagarsenker, B.N. and K.C.S. Pillai. 1973. The distribution of the sphericity test criterion. J. Multivariate Anal. 3:226–235.

Nelson, N.O., S. Agudelo, W. Yuan and Gan, J. 2011. Nitrogen and phosphorus availability in biochar amended soils. Soil Sci. 176:218–226.

Park, E., M. Cho and C.S. Ki. 2009. Correct use of repeated measures analysis of variance. Korean J. Lab Med. 29:1–9.

Reid, K.D., B. Ball and T.Q. Zhang. 2012. Accounting for the risks of phosphorus losses through the tile drains in a phosphorus index. J. Environ.Qual. 41:720–1729.

RCD Team. 2012. R: A Language and Environment for Statistical Computing. Available: http://www.R-project.org. Accessed: 02/12/2014.

Robertson, W.D. and J.A. Cherry. 1995. In Situ Denitrification of Septic-System Nitrate Using Reactive Porous Media Barriers: Field Trials. Ground Water. 33:99–111.

Robertson, W.D., J.L. Vogan and P.S. Lombardo. 2008. Nitrate Removal Rates in a 15-Year-Old Permeable Reactive Barrier Treating Septic System Nitrate. Ground Water Monit. Rev.

28:65–72.

Rogers, M.E., E.M. Lassiter, M. Eick and Z.M. Easton. 2014. Mitigation of sulfate reduction and nitrous oxide emission in denitrifying bioreactors with amorphous iron oxide and biochar. Ecol. Eng. (In Review).

Saarnio, S., K. Heimonen and R. Kettunen. 2013. Biochar addition indirectly affects N_2O emissions via soil moisture and plant N uptake. Soil Biol. Biochem. 58:99–106

Sarkhot, D.V., T.A. Ghezzehei and A.A. Berhe. 2013. Effectiveness of biochar for sorption of ammonium and phosphate from dairy effluent. J. Environ. Qual. 42:1545–1554.

Schipper, L.A. and M. Vojvodić-Vukovi. 2000. Nitrate removal from groundwater and denitrification rates in a porous treatment wall amended with sawdust. Ecol. Eng. 14:269–278.

Shipper, L.A., W.D. Robertson, A.J. Gold, D.B. Jaynes and S.C. Stewart. 2010. Denitrifying bioreactors - An approach for reducing nitrate loads to receiving waters. Ecol. Eng. 36:1532–1543.

Streubel, J.D., H.P. Collins, J.M. Tarar and R.L. Cochran. 2012. Biochar produced from anaerobically digested fiber reduces phosphorus in dairy lagoons. J. Environ. Qual. 41:1166–1174.

United States Environmental Protection Agency. 2009. An urgent call to action report of the State EPA nutrient innovations task group. USEPA.

Verheijen, F., S. Jeffery, A.C. Bastos, M. van der Velde and I. Diafas. 2010. Biochar application to soils: a critical scientific review of effects on soil properties, processes and functions. European Commission Joint Research Centre, Institute for Environment and Sustainability.

Warneke, S., L.A. Schipper, D.A. Bruesewitz, I. McDonald and S. Cameron. 2011. Rates, controls, and potential adverse effects of nitrate removal in a denitrification bed. Ecol. Eng. 37:511–522.

Woli, K.P., M.B. David, R.A. Cooke, G.G. McIsaac and C.A. Mitchell. 2010. Nitrogen balance in and export from agricultural fields associated with controlled drainage systems and denitrifying bioreactors. Ecol. Eng. 36:1558–1566.

Yao, Y., B. Gao, M. Inyang, A.R. Zimmerman, X. Cao, P. Pullammanappallil and L. Yang. 2011. Removal of phosphate from aqueous solution by biochar derived from anaerobically digested sugar beet tailings. J. Hazard. Mater. 190:501–50

3.0 Examining Denitrification with Dissolved Gas Analysis

The development an analytical method of gaseous standard addition for static headspace analysis of dissolved gases with gas chromatography mass spectrometry (GSMS) presented in this section conveys the objectives of ongoing work that will result in a manuscript prepared for publication. Analysis of Greenhouse Gasses by GCMS will be presented at the National Environmental Monitoring Conference August 2014 as a result of an ongoing collaboration with Shimadzu analytical chemist Paul Macek. This following work also represents a portion of the effort on synergistic project to address contamination in trace gas analysis.

3.1 Abstract

Denitrifying bioreactors (DNBRs) represent an opportunity to engineer these systems to promote hyper-functional denitrification while minimizing nitrous oxide (N_2O) emissions from incomplete denitrification. Indirect N_2O emissions resulting from downstream transformations of exported excess nitrate (NO_3^-) have been identified as a significant portion of greenhouse gas production from agriculture. An investigation of the potential to utilize DNBRs to mitigate agricultural N_2O emissions examined isotopic enrichment of ^{15}N and ^{18}O in N_2 and N_2O in a field-scale DNBR and provided qualitative evidence of denitrification as the mechanism of NO_3^- removal and the accumulation of a dissolved N_2O pool. The need for closer examination of the ratio of N_2 to N_2O and to directly quantify denitrification with dissolved gas analysis to elucidate the controlling factors relevant to DNBR design and management incited the development of an improved analytical method to analyze dissolved gases in environmental samples using the established static headspace analysis technique with the added component of a gaseous standard addition to produce an internal calibration. Sources of error in resulting from headspace preparation, sample removal and injection were identified and minimized. A proof of concept of the gaseous standard addition was expressed by the strong linear trend observed in a three point curve of the initial headspace concentration after equilibrium and two standard additions. The data also showed that introduction of excess air into the sample vial, likely during the introduction of the helium headspace, contributed to variable and inaccurate calculations of the original dissolved gas concentration. Our findings also supported the conclusion of Jahangir et al. (2012a) that the ratio of headspace to liquid sample ratio affects the calculated value of dissolved concentration. However, the gaseous standard addition method shows potential to be developed into a robust analytical method for quantifying dissolved gas concentration in samples that may improve upon the traditional external calibration curve because matrix effects that may affect gas portioning are incorporated into the calculation.

3.2 Introduction

The accumulation of the denitrification intermediate product N_2O has been identified as a concern and potential drawback of widespread DNBR implementation and the presence of N_2O is observed here in both laboratory and field scale DNBRs (Bock et al. 2014; Moorman et al. 2010; Warneke et al. 2011). Although previous observation has failed to establish significant

N_2O emissions from DNBRs, a growing body of research characterizes the factors that control N_2O production during denitrification enabling the pursuit of managing denitrification at the level of product ratios (e.g. Blagodatsky and Smith 2011; Bohlke et al. 2007; Liu et al. 2010). Given that 75% of N_2O emissions in the United States result from agriculture and soil management (EPA 2006), engineering DNBRs to minimize N_2O emission represents an opportunity for mitigation of indirect emissions (Jahangir et al. 2012b; Jahangir et al. 2013; Mosier et al. 1998; Weymann et al. 2008). Indeed, a laboratory scale experiment revealed that biochar addition to traditional woodchip DNBR media resulted in lower accumulation of N_2O during removal of NO_3^- (Bock et al. 2014).

To examine the composition of denitrification products at the field-scale, isotope analysis of the N^{15} and O^{18} content in dissolved N_2O and N_2 in a field-scale DNBR was undertaken. A passive diffusion gas sampler was constructed and used to collect samples of dissolved gases in a woodchip DNBR located at the Eastern Shore Agricultural Research and Experiment Station in fall 2012. The results provide qualitative evidence for denitrification as the mechanism of NO_3^- removal by the N^{15} enrichment in N_2 as well as indicate the accumulation of N_2O in a pool, which provides an opportunity for emission to occur. At each step in the process of denitrification isotope partitioning occurs because there is a higher probably of each successive reducing reaction utilizing an isotopically lighter substrate, as utilizing light nitrogen is thermodynamically favored (Zumft 1997). Additionally, the correlation between ^{15}N and ^{18}O enrichment in NO_3^- is associated with denitrification, and a linear correlation was found here in dissolved N_2O. However, the passive diffusion gas samplers were inadequate for quantitative analysis of the dissolved gas component. Regardless, natural abundance isotope data alone do not form a sound basis for quantifying denitrification due to a lack of correlation between enrichment factors and denitrification rates (Groffman et al. 2006).

Dissolved gas analysis provides a simple and minimally invasive snap shot of excess N_2 attributable to denitrification and the ratio of products N_2:N_2O. The simplicity of direct measurement of dissolved gases and the minimal disturbance caused lends well to quantification of denitrification in DNBRs, especially in comparison to more complex methods that alter the system in ways that influence denitrification such as adding NO_3^- in the push-pull method. Argon is used as a conservative tracer, because it is unaffected by the process of denitrification for

incorporation of atmospheric gases into water, and can be used to determine the fraction of total dissolved N_2 assumed to be the product of denitrification (e.g. Blicher-Mathiesen et al. 1998).

Static headspace analysis, also known as equilibrium headspace analysis, is the most common method to analyze dissolved gases in water (Liotta and Martelli 2012). This method consists of adding a gaseous headspace to an airtight vial containing a water sample and allowing the dissolved gases to reach equilibrium between the aqueous and gaseous phases, subsequently measuring the concentration of analyte in an aliquot of the headspace (Kolb and Etra 1997). See Figure 3.1. Subsequently the original dissolved concentration is calculated using Henry's law, which states that gases dissolve in liquid in proportion to their partial pressure and a constant that is a function of the physical properties of both the specific liquid and gas as well as temperature and salinity. However, Liotta and Martelli (2012) who point out that "while this method is widely used, we are not aware of any studies that have elucidated both practically and theoretically how to collect and manage a water sample, analyze the dissolved gas phase, and obtain the concentration of dissolved gases using equations containing appropriate solubility coefficients" indicating that although this analytical technique is common, it is not standardized. Jahangir et al. (2012a) found that different procedures used to reach equilibrium between the two phases, namely shaking time, standing time, and the ratio between headspace and liquid sample in the vial, significantly affected the calculated dissolved gas concentrations for greenhouse gases N_2O, CH_4, CO_2. Additional concerns about the validity of static headspace analysis calculations arise when matrix effects of environmental samples are considered. Given that salinity affect the Henry's law constant, it is not unreasonable to suspect that other constituents of environmental water samples such as organic acids or particulates may impact gas partitioning, and consequently the calculated value of dissolved gas concentration.

As a potential solution to both established and theoretical impediments to SHA-DGA, adaptation of the fundamental technique to address sample matrix effects, the standard addition method, was explored. Standard addition consists of sequentially adding known amounts of analyte to a matrix, relying on a linear or characterized response to be detected. (See Figure 3.1) Although the standard addition method is often applied in analysis of volatile organic compounds (Kolb and Ettra 1997), the known mass of analyte is added as liquid solution, not as a gas. Since standard solutions of known concentration of dissolved gases are not readily available, the use of a gaseous standard addition was investigated. Using a gas addition is an

uncommon practice, not employed in dissolved gas analysis in environmental research. This research provides a proof of concept for the method of gaseous standard addition as a potential solution to the lack of comparability due to different sample processing indicated by Jahangir et al. (2012a).

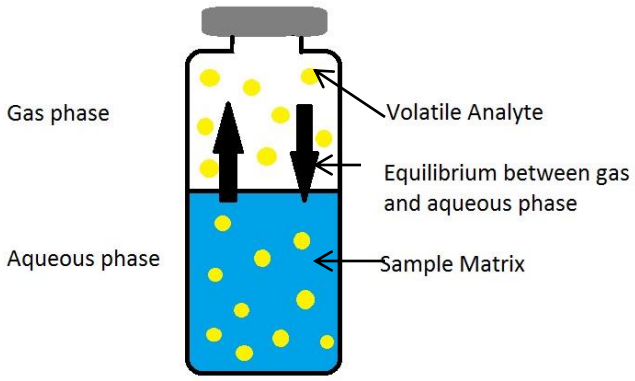

Figure 3.1 Sample vial prepared for static headspace analysis showing equilibrium of the analyte between the gaseous headspace and liquid sample.

3.3 Materials and Methods

3.3.1 Isotopic Analysis—Proof of Concept Data

N isotopes were used to determine sources of NO_3^- on the basis of characteristic signatures and identify the occurrence of denitrification (Avrill and Tiedje 1981; Germon et al. 1981). Observed ^{15}N enrichment in NO_3^- has been used to identify and confirm denitrification, often employed is studies of enriched aquifers where other techniques to assess denitrification are not practical (e.g. Bottcher et al. 1990; Mariotti et al. 1988). This fractionation effect occurs because of the preferential use of lighter stable isotopes by denitrifiers, ^{14}N and also ^{16}O. Previous studies have established that a linear relationship between the enrichment of ^{15}N and ^{18}N in NO_3^- indicates isotope discrimination accompanying denitrification (Chen and MacQuarrie 2006). In an examination of the isotopic signature of dissolved N_2 and N_2O in a DNBR we cite the depletion of ^{15}N in product N_2 relative to atmospheric ^{15}N abundance as qualitative evidence of denitrification. Additionally the ^{15}N and ^{18}O content in dissolved N_2O was quantified to determine if isotopic enrichment of N_2O resulted in the same pattern as NO_3^- in aquifers in which denitrification occurs.

Dissolved gas samples were collected with a simply-constructed passive diffusion gas sampler in a woodchip DNBR with 10% biochar addition by volume receiving tile drainage enriched in NO_3^- in which the capacity for NO_3 removal had been established. Each sampler consisted of a length of silicone tubing, which is permeable to gases but impermeable to water, attached to a length of PTFE tubing, which is impermeable to both air and water, sealed with silicone adhesive at the end of the silicone tube and affixed with a butyl rubber septa at the end of the PTFE tubing. To minimize the time until equilibrium between the dissolved gases in the DNBR and within the chamber of the sampler, the surface area to volume ratio was maximized and the thickness of the silicone tubing was minimized. The internal volume was 5 mL and the surface area of the silicone was approximately 320 cm^2, using tubing with a 3.2 mm inner diameter and 1.6 mm wall thickness. The internal diameter of the PTFE tubing was 1.6 mm, so it added minimal volume to the chamber while having sufficient length to connect the submerged PTFE tubing to the surface where the septum could be accessed for sampling. Samples were collected by lowering the samplers into piezometers until the silicone portion was completely submerged and allowing the contents to come to equilibrium for a minimum of 12 hours. Samples were collected with a 5 mL gastight syringe with luer lock (sample lock syringe, Hamilton Company) and stored in 3.7 mL evacuated exetainers (Labco Ltd, UK). Samples were collected during two precipitation events resulting in saturation of the DNBR in September and October 2012. Samples were promptly shipped to the U.C. Davis Stable Isotope Facility for analysis by isotope ratio mass spectrometry (IRMS).

3.3.2 Determination of Dissolved Gas Component in Environmental Samples: Gaseous Standard Addition Method Static Headspace Analysis

Adapting the method of standard static headspace analysis of dissolved gases for specific application to environmental samples to quantify denitrification and the ratio of its products is described. The ability to quantify major dissolved gas species (N_2, O_2, Ar) and trace greenhouse gases (CO_2, CH_4, and N_2O) is a unique application of GCMS, as GC is most commonly used. However, to analyze the complete suite of dissolved gases either multiple GCs, each with a different detector, or complex multi-column multi-detector setups within a single instrument are employed. Conducting DGA with a single GCMS, therefore provides a significant advantage, in reduced cost and increased simplicity. Additionally, this method development incorporated the use of a gaseous standard addition to create an analysis more robust to matrix effects in

environmental samples that may affect gas partitioning as well as the differences in sample preparation techniques that can alter dissolved concentration calculations (Jahangir et al. 2012a).

The fundamental reference on static headspace gas chromatography by Kolb and Ettra (1997) states that the gas phase concentration of an analyte in the headspace vial (Figure 3.1) can be calculated as:

$$C_g = C_o / (K + B) \quad (3.1)$$

where C_g is the concentration of analyte in the headspace, C_o is the concentration of analyte in the dissolved phase, K is the dimensionless form of the Henry's Law constant, and B is the ratio of the headspace volume to the liquid volume. Indeed, Kolb and Ettra (1997) suggest that a standard addition, otherwise known as an internal calibration, is the ideal method to determine the original concentration. Standard addition consists of the sequential introduction of a known amount of analyte to a sample and recording the response to build a regression (Figure 3.2). The total amount of mass of the analyte in the sample is represented by the x intercept of the curve (Figure 3.2). Employing a standard addition eliminates the use of Henry's Law constant and circumvents the assumptions inherent in Henry's Law (Equation 3.2), dilute solutions and the absence of matrix effects on gas partitioning, which may be violated by environmental condition.

Henry's Law: $P_X = K_H * C$

Where P_X is the partial pressure of the solute X in the gas above the solution, C is the concentration of the analyte X in solution, and K_H is the Henry's law constant, unique to the specific solute-solvent interaction and a function of temperature and salinity, having the dimensions of pressure divided by concentration. The dimensionless Henry's Law constant as utilized in Equation 3.1 is expressed as:

$$K_H = C_{aq}/C_{gas} \quad (3.1)$$

where C_{aq} is the aqueous concentration of analyte and C_{gas} is the concentration in the gas above the liquid. By using a standard addition the gas partition coefficient can easily be calculated for each sample and compared to published values to determine if a deviation has occurred. The following describes the progress made in method development as a proof of concept for the application of a gaseous standard addition to static headspace analysis.

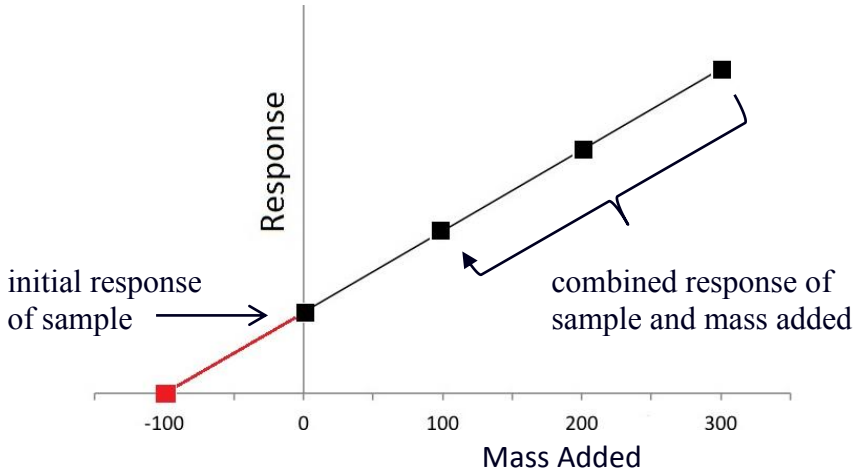

Figure 3.2 Idealized standard addition curve.

3.3.2.1 GCMS Configuration and Programs

Quantification of N_2, O_2, Ar, and N_2O in gaseous headspace samples was conducted with a Shimadzu QP2010 Ultra gas chromatograph mass spectrometer with a Sigma Aldrich Carboxen 1010 PLOT column (60 m, 0.32 mm i.d.) using ultra pure helium (He grade 5.5, 99.9995% purity) as the carrier gas. This carbon molecular sieve column is claimed by Sigma Aldrich to be "ideal for the separation of all major components in permanent gas (He, H_2, O_2, N_2, CO, CH_4, and CO_2) and light hydrocarbons (C_2-C_3) in the same analysis. It is the only column commercially available that is able to separate all major components in permanent gas." Consequently, this analysis could be expanded to include more constituents of interest such as greenhouse gases CO_2 and CH_4. A temperature program was developed to separate N_2, O_2, Ar, CO_2, and N_2O with the use of a custom gas standard containing 5.02% O_2, 1.00% Ar, 40.0% CO_2, 5.09% N_2O, and 48.9 N_2. It consisted of a 4 minute hold at 35 °C followed by an increase to 180 °C at a rate of 25 °C/min. The mass spectrometer was used in scan mode, scanning from mass 15 to mass 100 at a rate of 588 times per minute. A flow control program maintaining the linear velocity of the carrier gas while automatically adjusted the total flow as the column temperature changed; initial settings were 128.1 kPa inlet pressure, 786.6 mL/min total flow, 3.13 mL/min column flow, 45.0 cm/sec linear velocity, 1.0 mL purge flow, and a split ratio of 250. The temperature of the injector, interface, and ion source were 110 °C, 150 °C, and 200 °C respectively. The high split ratio was required because the MS is such a sensitive detector to reduce the amount of mass reaching the detector while maintaining a reasonable injection volume that could be measured accurately (10-50 µL). A chromatogram of the standard mixture is presented in Figure 3.3. Note that this method does not

allow for simultaneous quantification of atmospheric levels of N_2, O_2, Ar, and N_2O due to the high split ratio required to quantify atmospheric levels of N_2 and the low background concentration of N_2O, approximately 400 ppb (EPA 2006). Henceforth, this method will be referred to as the N_2/ O_2/Ar (NOA) method.

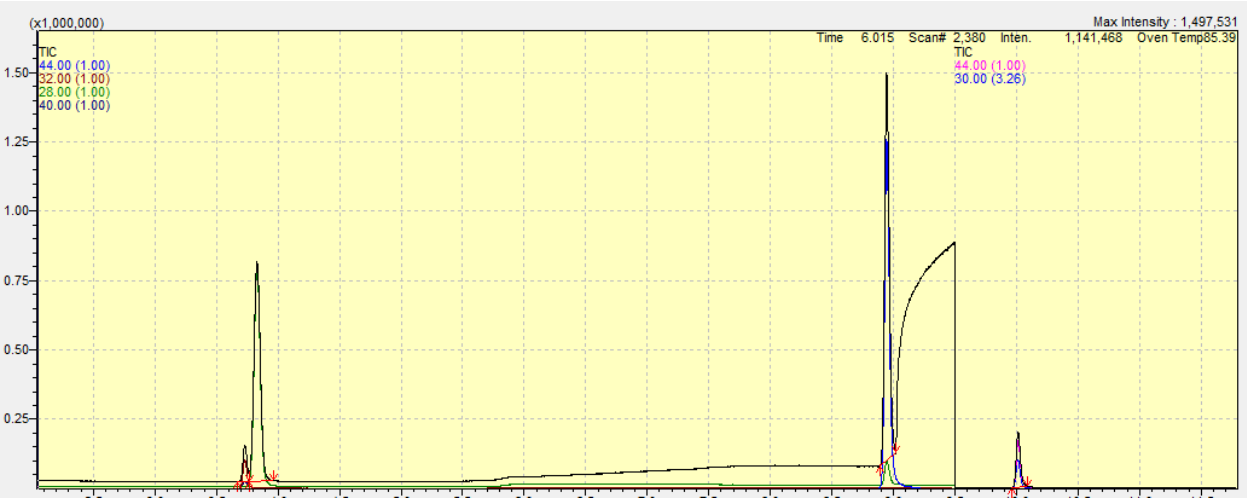

Figure 3.3 Chromatogram showing peaks for O_2 and Ar (overlaid), N_2, CO_2, and N_2O present in a custom gas mixture consisting of 5.02% O_2, 1.00% Ar, 40.0% CO_2, 5.09% N_2O, and 48.9 N_2.

In addition, 7.8 minute temperature program was developed to separate CH_4, CO_2, and N_2O with maximum sensitivity. Due to the fact that trace levels of greenhouse gases can occur at concentrations orders of magnitude smaller than the primary atmospheric gases, the previous method could not provide sufficient sensitivity. The greenhouse gas temperature program began at a temperature of 60 °C, holding temperature for 0.5 minutes and then increasing to 180 °C at a rate of 20 °C per minute, followed by a one minute hold at 180 °C. The mass spectrometer was used in selective ion monitoring (SIM) mode to increase sensitivity. Splitless injections were made to maximize the mass that reaches the detector to increase sensitivity, but the split ratio was set to 50 to increase the flow through the column and decrease the run time. Injection volumes were typically 50 to 100 µL. A linear velocity flow control program was used and the initial settings were 198.8 kPA inlet pressure, 155.9 mL/min total flow, and 3.04 mL/min column flow. The temperature of the injector, interface, and ion source were 110 °C, 150 °C, and 200 °C respectively. This method will henceforth be referred to as the GHG method.

3.3.2.2 Isolation of Error

In measuring sub-ambient concentrations of atmospheric gases it is essential for the sample vial to remain gas tight and minimize contamination with air for accurate quantification of the dissolved components. Air can be introduced into the sample vial during sample storage, headspace introduction, headspace aliquot extraction, and during addition of the gaseous standard to the headspace vial. Additionally, contamination can be introduced during the transfer of the gaseous sample to the GCMS by leakage of the syringe, carryover of analytes in the syringe barrel, or as injection of the dead volume of non-sample (air) in the needle. The following details specific tests conducted to identify and minimize these sources of contamination that result in error in the calculation of the original dissolved gas concentration.

Manual Injection Reproducibility

To establish baseline reproducibility of the concentrations detected in sequential injections of identical samples at a given volume, then injections of air were analyzed with both the NOA and GHG method. Variability in the response to repeated injections of a sample arises from the measurement of sample volume in the syringe as well as from the inherent variation in injection technique, such as the speed at which the plunger is depressed. Figure 3.4 displays the total ion chromatogram (TIC) that contains the peaks of N_2, O_2, and Ar from 7 injections of 100 µL of air, which resulted in a percent residual standard error (%RSD) of 5.06, 4.31, and 4.01, respectively. Note that Figure 3.5 shows how the Ar and O_2, which are not chromatographically separated and coelute, are distinguished by the MS based on their mass to charge ratio (m/z). Likewise, 7 injections of 100 µL of air were analyzed for N_2O with the GHG method, and resulted in a %RSD of 4.48 (Figure 3.6). It was surprising to find such low variability of trace levels of N_2O, noting the prominence of the baseline fluctuations relative to peak size having a signal to noise ration of approximately 5. Assessing the %RSD of N_2O compared to N_2, O_2 and Ar, and noting the similarity, it seems likely that the variability in the latter could be reduced. A high split ratio contributes to variability because small differences in injection speed have an effect on the percentage of mass in a sample that reaches the detector. Analysis of a sample with lower concentrations of these analytes allowing for a lower split ratio may increase the reproducibility and minimize this source of error.

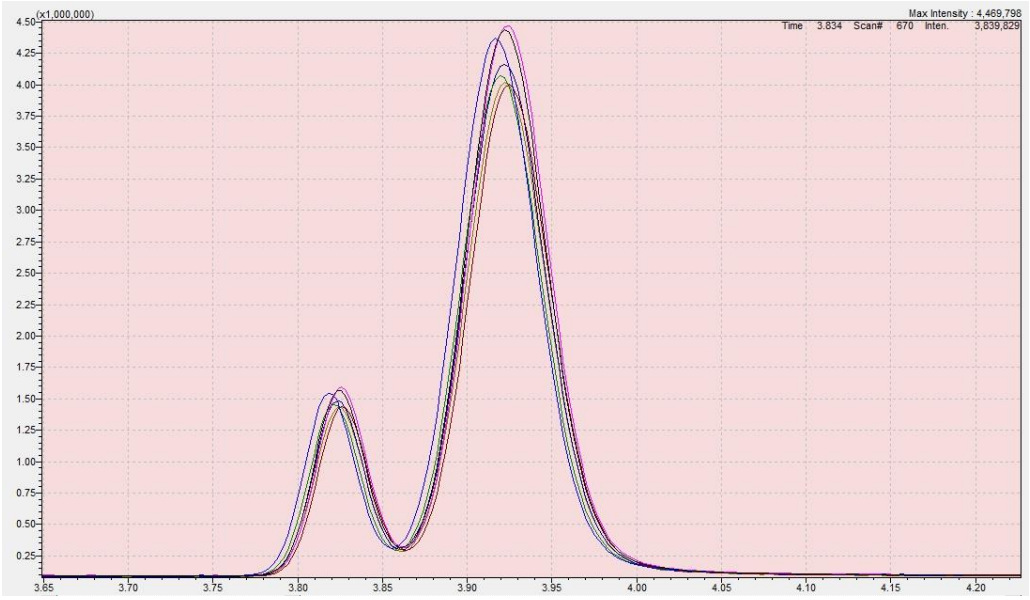

Figure 3.4 Seven 100 µL injections of air analyzed with the NOA method. %RSD of N_2, O_2, and Ar of 5.06, 4.31, and 4.01, respectively.

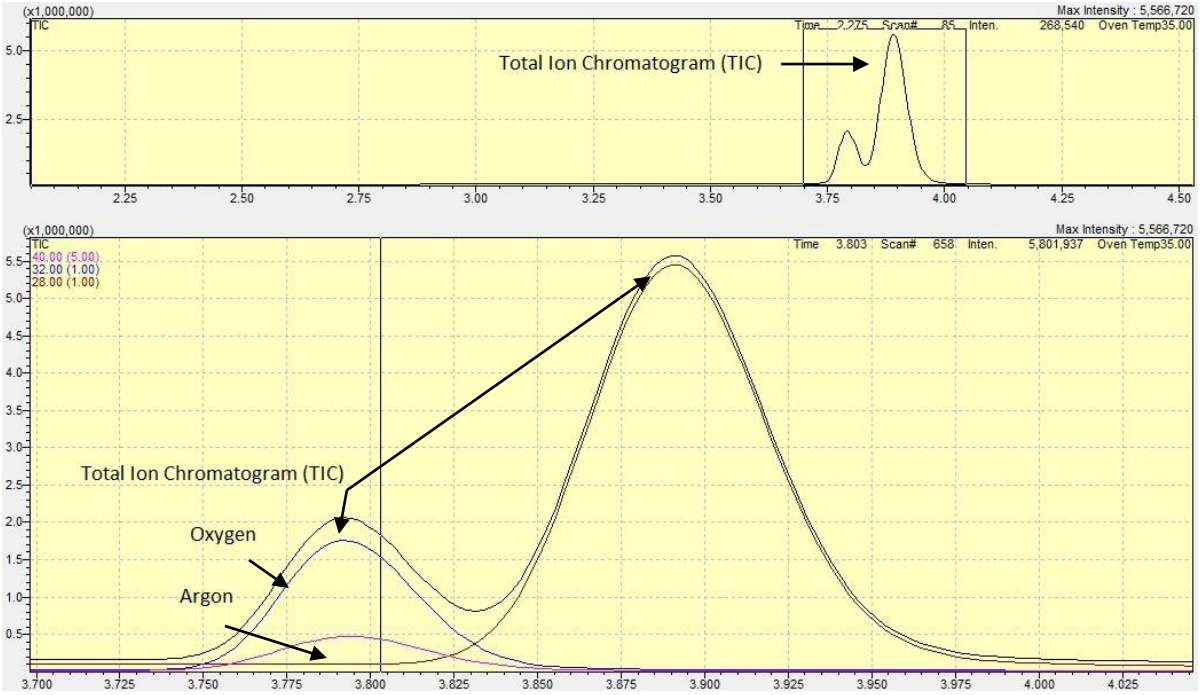

Figure 3.5 Total ion chromatogram (top) with coelution of Ar and O_2 from poor chromatographic separation due to similar solubilities revealed by the mass chromatogram output of the MS which distinguishes the Ar and O_2 peaks by their mass to charge ratio, demonstrating the necessity of the MS as detector for this application.

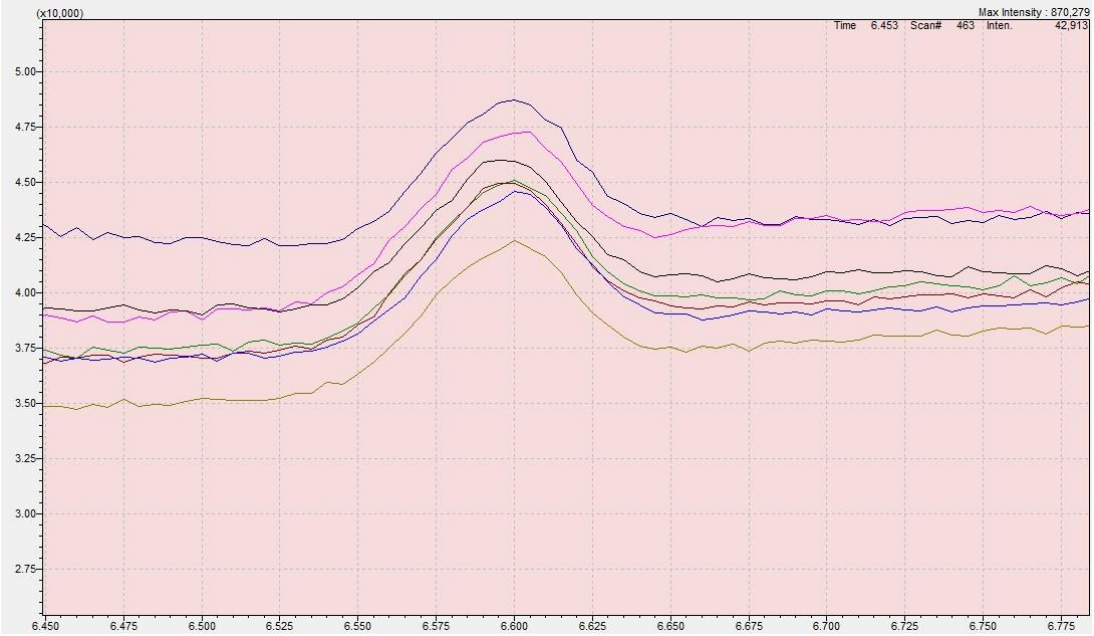

Figure 3.6 Seven 100 µL injections of air analyzed with the GHG method with %RSD of 4.48.

Carryover Study and Purging Protocol

Contamination of the gas syringe itself becomes a concern when working with trace gas concentrations. A series of tests were conducted to establish a purging procedure to prevent sample carryover due to syringe contamination. The effects of carryover contamination are best displayed by alternating injections of air with approximately 400 ppb N_2O and a 10 ppm standard of N_2O, having 40 times the concentration. Figure 3.7 shows that the N_2O from the higher concentration standard contaminates the subsequent three air injections, and only by the fourth air injection does the response accurately reflect the background concentration of N_2O. Consequently, a purging protocol was established. As He is used as the carrier gas because the other common carrier gases N_2 and Ar are analytes of interest, it was also used as the purge gas. He is far from an ideal purge gas because of its low mass; N_2 and Ar are more commonly employed as purge gases because the larger molecules are better at displacing matter interacting with the syringe barrel. Although hydrogen can also be used as a carrier gas, it is also a poor purge gas and safety concerns precluded its use in the lab. Purging was conducted by placing the syringe needle in a stream of ultra pure carrier He flowing from a two stage pressure regulator and pumping the plunger from the maximum capacity of the syringe to complete evacuation several times. Figure 3.8 shows that the amount of N_2O detected in injections of air alternated with injections of 10 ppm standard remained at a constant level, indicating that the carryover had

been eliminated. Figure 3.9 shows that this purging technique was also successful for minimizing the air component present in a He sample. Minimizing the amount of air contained in an aliquot of He transferred by syringe is critical to the preparation of a headspace vial. Injections of helium 1 and 2 show the background minimum levels of air contamination achieved by sequential purging of the syringe quantified with a split ratio of 10, equivalent to 0.238% N_2, 0.071% O_2, and 0.0029% Ar. Note that the air injections were made at a split ratio of 200, so the peaks would be 20 times larger if shown at the same scale as the helium. Peaks 4 and 6 show the lowest levels of air contamination in a helium injection achieved by the pumping purge technique, approximately 0.298% N_2, 0.078% O_2, and 0.022% Ar. The increases in N_2 and Ar concentration after air injections were acceptable, as carry over was still minimal.

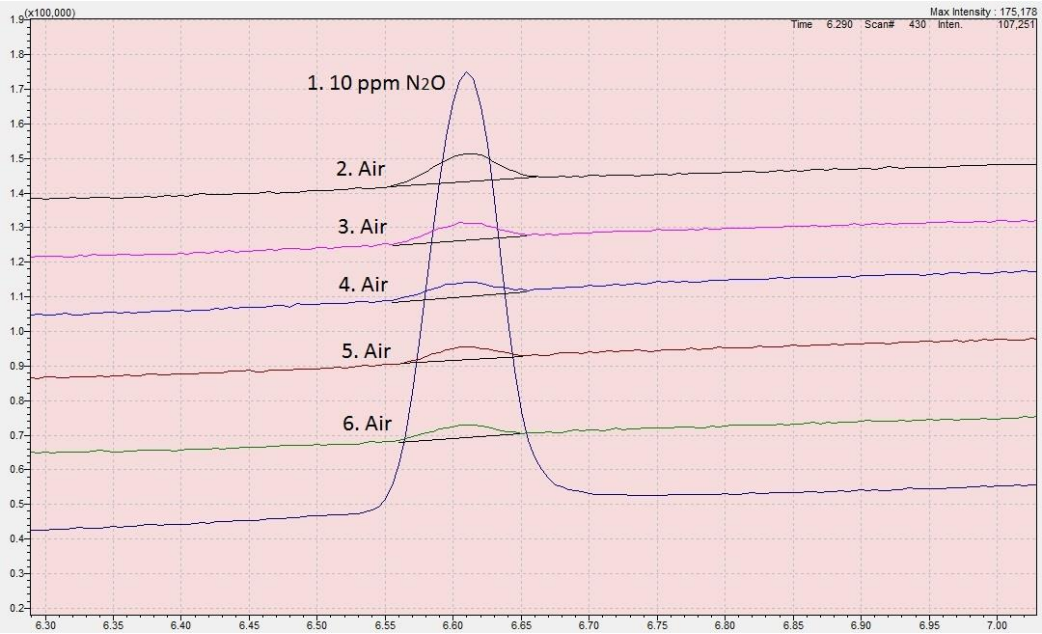

Figure 3.7 Demonstration of the carryover of N_2O present in air injections following an injection of 10 ppm standard at approximately 40 times more N_2O than air.

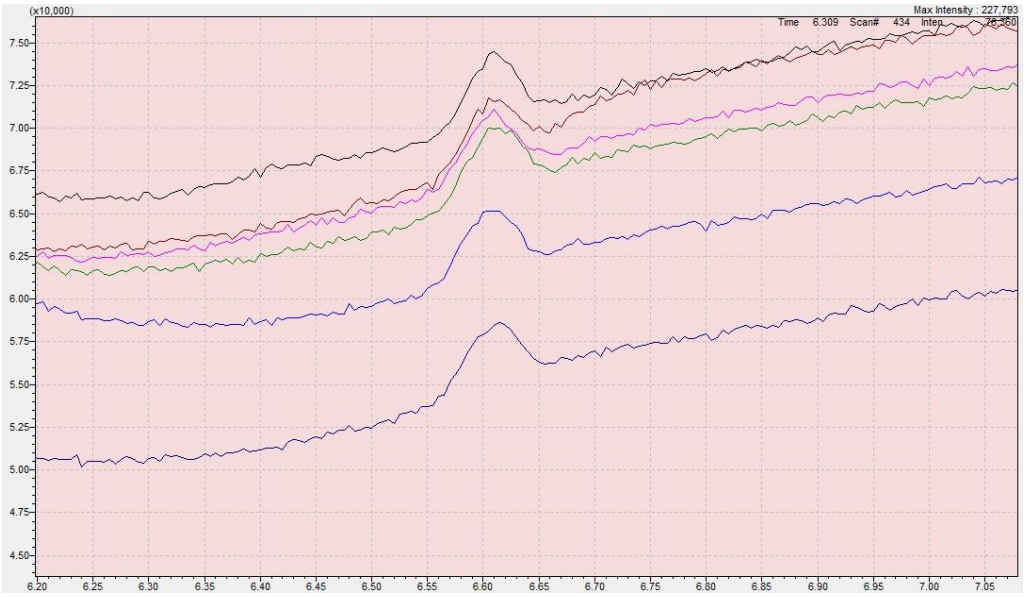

Figure 3.8 N_2O peaks for injections of air before and after injection of 10 ppm standard, showing no carry over effect because the syringe was purged with He prior to each injection. Note that the view of increased noise in the baseline relative to Figure 3.7 is a feature of scale.

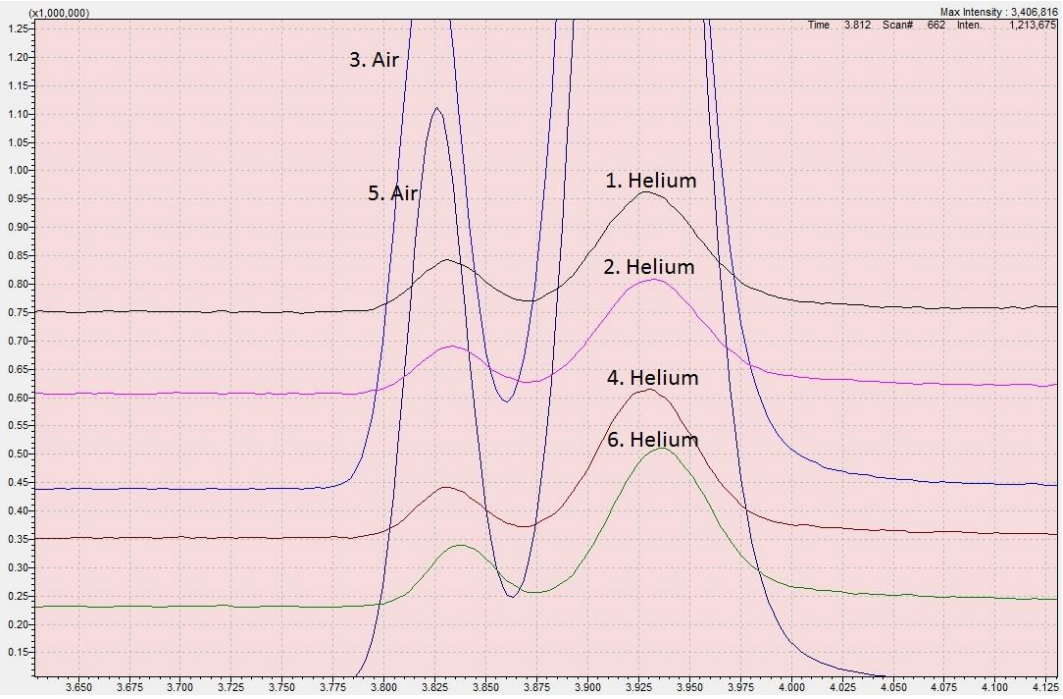

Figure 3.9 Purge technique developed to prevent air contamination within the helium introduced as headspace consisted of pumping the syringe in a stream of He. Numbers indicate the order in which injections were made.

Headspace Preparation

Serum vials with aluminum crimp caps with PTFE-coated silicone septa were used to collect environmental samples (Sigma Aldrich). Although the advertised volume of the vials was 20 mL, the internal volume turned out to average just over 16 mL. An automatic crimper was used to ensure consistent and gastight sealing of the crimp caps (Sigma Aldrich). Headspace introduction was conducted as a modification of the procedure described by Liotta and Martelli (2012). It was suspected that each time the septum was pierced with a needle, either to introduce headspace or gas standard or to extract a sample, this provided an opportunity for air to enter the vial. Therefore, an apparatus that will be referred to as a water guard was constructed to prevent contact between air and the septum. A 50 mL Falcon tube was fitted with styrofoam and a plastic collar to hold the sample vial in place, and a hole was cut in the screw on cap which was fit with a butyl rubber septum (Figure 3.10). Once the sample vial was positioned in the Falcon tube and held in place approximately 2 cm from the cap fitted with septum, the apparatus was filled with water and inverted. This created a barrier filled with water between the septum of the Falcon tube cap and the septum of the sample vial, and thus the sample vial was protected against air intrusion each time it was punctured.

The headspace was introduced into the sealed sample by with a 5 mL gastight syringe with a luer lock (sample lock syringe, Hamilton Company) inserted through the septum of the water guard and the septum of the sample vial while the bottle is inverted. A few tenths of a milliliter were injected to create excess pressure, and then a second needle was inserted to allow the displacement of sample water as the desired volume of He was introduced. After the removal of the needle and syringe, it is assumed that the vial is a closed system with an internal pressure equivalent to barometric pressure. Next, the bottle was manually shaken vigorously for 1 minute to allow the dissolved gases to equilibrate between the liquid and headspace phase, followed by a five minute standing time prior to injection. The resulting headspace pressure is no longer the barometric pressure, but is equal to the sum of the partial pressure of the gases; this difference is negligible relative to the other sources of error in the analysis.

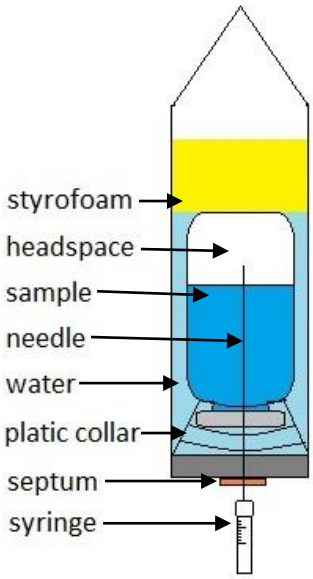

Figure 3.10 Water guard constructed from Falcon tube to prevent contact between sample vial septum and air to minimize air intrusion during septum puncture and reduce vial leakage.

Headspace Contamination

To estimate the amount of air actually introduced into the headspace with the He, the 5 mL syringe was specifically tested as such a large volume might respond differently to the purging protocol. Since the total 5 mL volume cannot be analyzed by GCMS, a 200 µL aliquot was analyzed. Air contamination levels were found to average 0.112% N_2, 0.040% O_2, and 0.0014% Ar, they demonstrated high variability and ranged 0.018-0.257% N_2, 0.007-0.078% O_2, and 0.0001-0.0030% Ar, with %RSD of 69.3, 58.6, and 65.5, respectively (Figure 3.11). Introduction of the He headspace with this 5 mL syringe was the greatest potential source of error identified. The high variability raises doubt to the consistency of the level of the contamination.

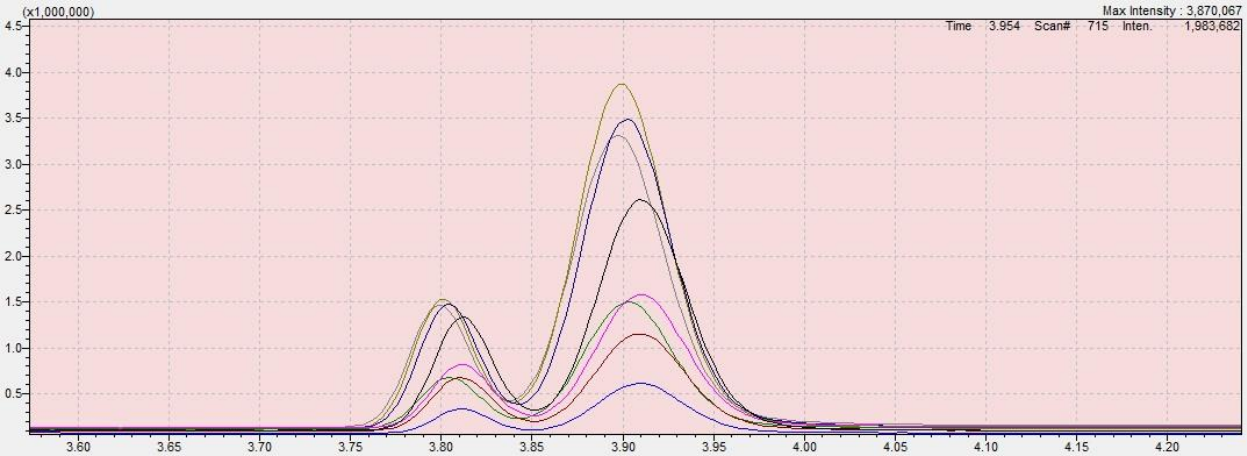

Figure 3.11 Shows the large variability in 200 uL injections of He with the 5 mL syringe used to introduce the He headspace. The %RSD for N_2, O_2, and Ar were 69.3, 58.6, and 65.5, respectively.

Headspace Aliquot Reproducibility

The variability of repeated headspace injections was expected to be greater than that of repeated air injections because not only can the measurement of sample volume and injection technique create variability, but so can the intrusion of air into or leakage of sample out of the syringe, the dead volume of air in the syringe needle, and the technique used to extract an aliquot of the headspace from the vial. After several pumps to purge the syringe, it was filled with He and the luer lock between the syringe barrel and needle was closed. Right before inserting the needle into the sample vial via the water guard, the luer lock was opened and the He was expelled to displace any air in the dead volume. Then, with the plunger completely depressed, the needle is inserted into the vial until it contacts the headspace. To obtain a 10 µL a 50 µL syringe was used and the plunger was slowly pulled to 30-40 µL and then slowly depressed back to 20 µL. The luer lock was closed and the needle was removed from the sample vial and water guard. The plunger was then adjusted to 10 µL, creating overpressure. Before injection, the luer lock was opened to allow the excess mass to be released, thereby again displacing the air in the dead volume and ensuring that 10 µL at atmospheric pressure is injected. Figure 3.12 shows the reproducibility of seven sequential 10 µL injections from a vial with a 4.2626 mL headspace. The %RSD for N_2, O_2, Ar were 6.46, 5.66, and 5.98, respectively, which is only slightly poorer than that achieved with air (Figure 3.4). Figure 3.13 shows the reproducibility of seven sequential 10 µL injections from a vial with a 8.17 mL headspace (B = 1.0126) to which 30 µL of air has been added. The %RSD for N_2, O_2, Ar were 9.09, 7.99, and 8.28, respectively. Notice that a higher concentration of analytes

results in greater reproducibility and lower %RSD. Therefore, reducing the headspace volume to concentrate the analytes may be beneficial to reducing the error in the analysis. However, reducing the headspace volume to concentrate the analytes must be weighed against increasing the percentage of headspace extracted during sampling. Although the volumes of the headspace in these two tests of reproducibility differ, only 2-3% of the total headspace volume was extracted over the seven removals of 20 µL aliquots. Future examination of the limiting percentage of headspace that can be extracted before affecting the sample reproducibility might useful to optimizing the headspace to liquid sample ratio. This variability observed in removing multiple aliquots from the headspace indicates an opportunity to improve the analytical technique that may improve the precision of the ultimate calculation of dissolved gas concentration. The reproducibility of the N_2O recovered from the headspace could not be measured because the background concentrations of atmospheric origin in environmental samples are too low to be detected in a headspace. Establishing the variability of N_2O would require samples taken under conditions supporting high rates of denitrification. Selection of sample bottle size and the headspace to liquid ratio becomes increasingly important and the concentration of analyte in the sample decreases. Establishing the detection limit of N_2O in environmental samples will be a necessary step in method development.

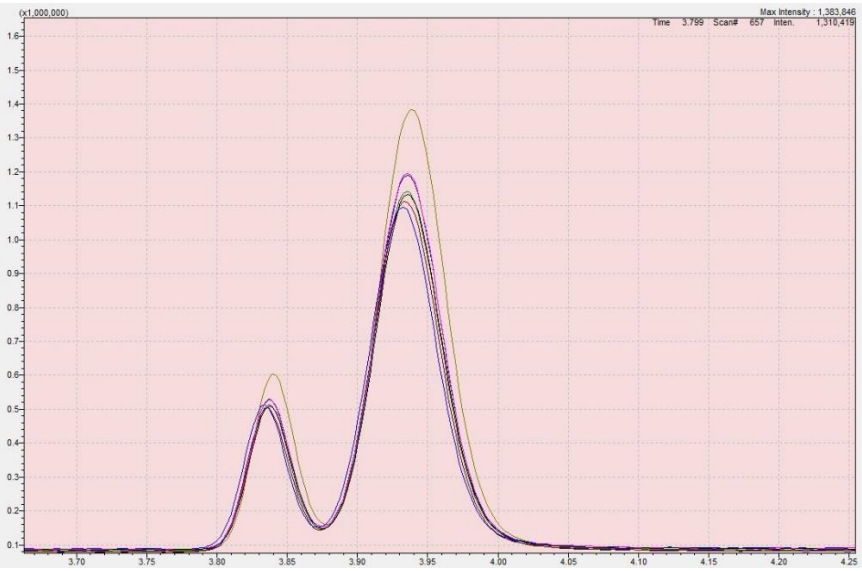

Figure 3.12 Seven repeated 10 µL injections of headspace from a vial with a 4.2626 mL headspace (B = 0.3558). Note that a single injection seems to be responsible for the higher %RSD. The %RSD for N_2, O_2, Ar are 9.09, 7.99, and 8.28, respectively.

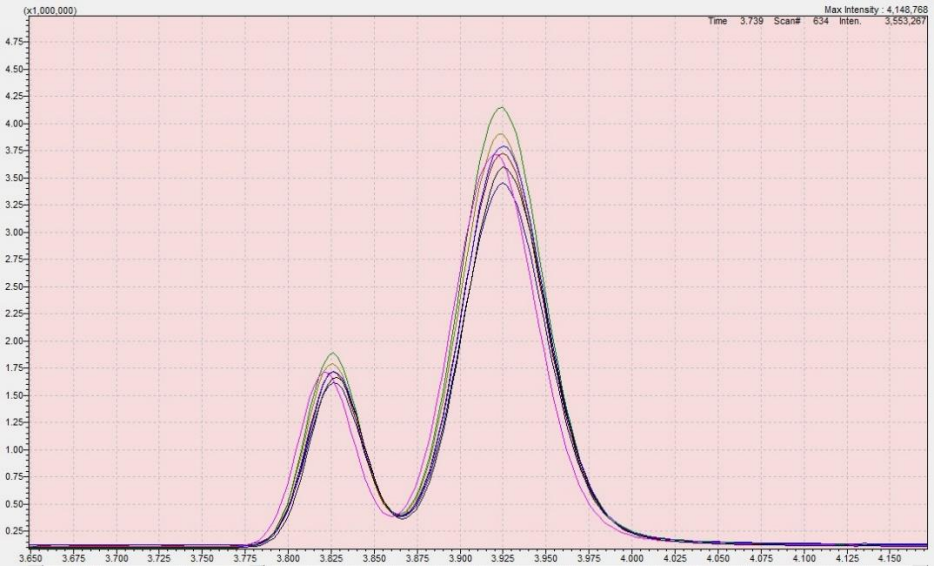

Figure 3.13 Seven repeated 10 µL injections of headspace from a vial with a 8.1700 mL headspace (B = 1.0126) to which 30 µL of air has been added. Note the greater intensity indicated on the y axis relative to Figure 3.12, indicating a higher concentration in the samples in Figure 3.13. The %RSD for N_2, O_2, Ar are 6.46, 5.66, and 5.98, respectively.

Leak Testing

A sample vial was prepared with the addition of the headspace and equilibrium procedure described above. A 10 µL aliquot of the headspace was analyzed with the NOA method made every hour beginning immediately after the headspace had been created and the vial equilibrated, until hours had passed. These five injections resulted in poorer reproducibility than the headspace reproducibility test with a mass addition (Figures 3.13), but show a similar if slightly poorer reproducibility than the 7 injections of headspace without an addition having a lower concentrations of analytes (Figure 3.12). Since the order of injections does not show a trend of increasing or decreasing concentration, indicating the absence of a significant source of contamination via air leakage over four hours—a reasonable time frame to include conducting a standard addition. The total volume withdrawn relative to the headspace, the gauge and point style of the needle, and the type of septum of the serum vial are also likely to influence the opportunity for a leak to occur during the multiple punctures and volume extractions involved in standard addition.

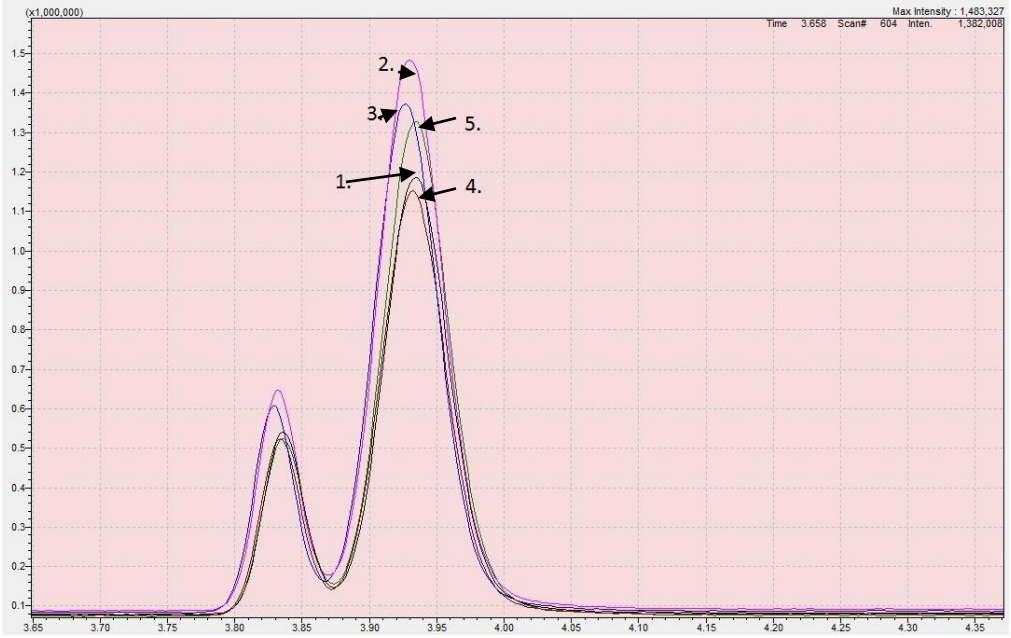

Figure 3.14 A leak test of a prepared sample vial consisting of five injections of headspace made every hour beginning at time zero after the headspace had been created and the vial equilibrated, until hour 4. The %RSD for N_2, O_2, Ar are 10.74, 9.81, and 10.22, respectively.

Mass Transfer Reproducibility

This study was critical for determining how accurately a mass of analyte can be added to the sample vial. Gas standards were extracted through compressed gas cylinders through a syringe adaptor that consists of a metal nozzle holding a butyl rubber septum in place attached to the two stage pressure regulator connected to the gas cylinder. Before a volume of standard is extracted, the syringe was purged by pumping with He, filled and locked, then the He was expelled right before the needle was inserted into the syringe adaptor. Next, the syringe was filled with sample, removed from the adaptor, its contents expelled, and quickly inserted back into the adaptor. This procedure was repeated several times to essentially flush the syringe with the standard. Similarly to transferring the headspace sample, a larger volume than would be injected into the GCMS was extracted by slowly pulling the plunger past the mark and then adjusting back down to it, after which the luer lock was closed and the syringe was removed from the adaptor. The plunger was then depressed to the desired volume, usually half of what was extracted, and the luer lock opened and allowed to remain open for about half a second before the sample was introduced into the injection port of the GCMS. This procedure was repeated 7 times for both the NOA and GHG

methods, resulting in %RSD of 4.75, 3.27, 4.79, and 5.88 for N_2, O_2, Ar, and N_2O respectively (see Figure 3.15 and 3.16).

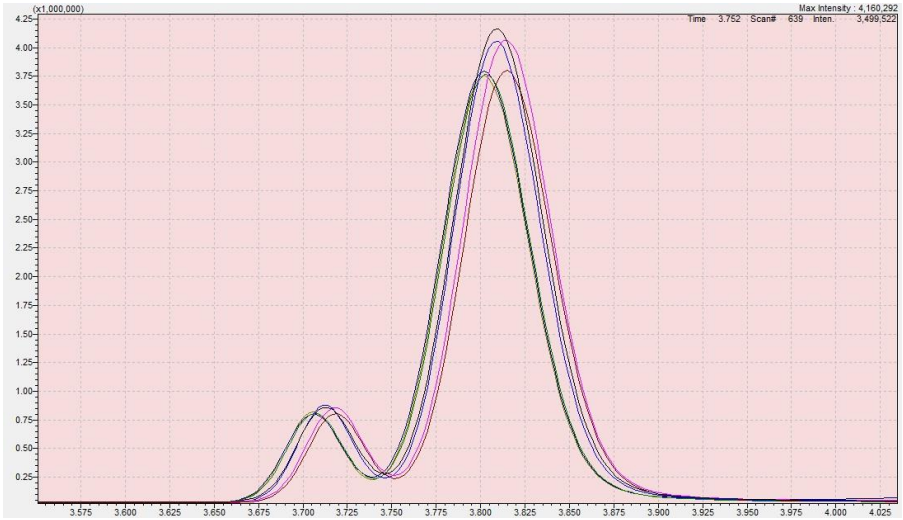

Figure 3.15 Reproducibility from seven injections of a standard mixture consisting of consisting of 5.02% O_2, 1.00% Ar, 40.0% CO_2, 5.09% N_2O, and 48.9 N_2 are extracted from gas cylinder and transferred to GC/MS by gas tight syringe. The %RSD for N_2, O_2, Ar are 4.75, 3.27, and 4.79 respectively.

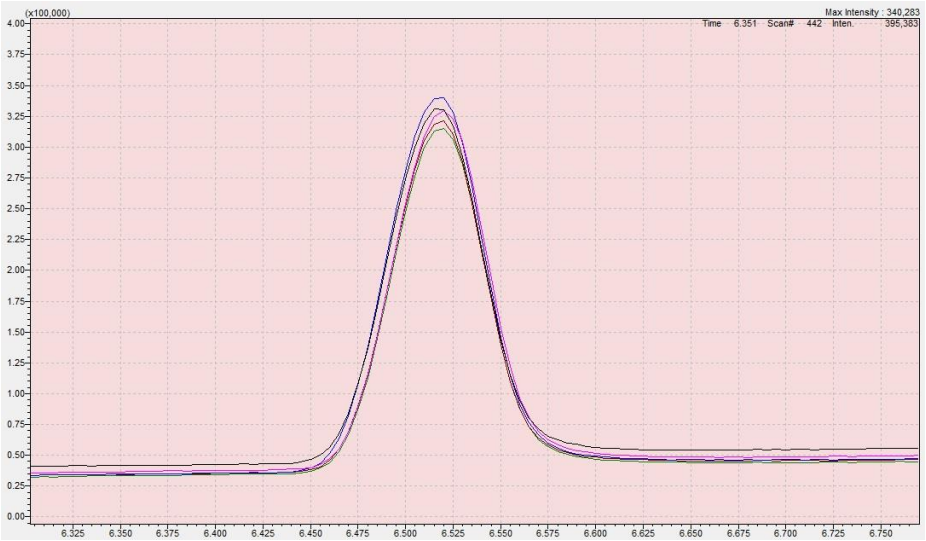

Figure 3.16 Reproducibility from seven injections of a 10 ppm N_2O extracted from gas cylinder and transferred to GC/MS by gas tight syringe. The %RSD for N_2O was 5.88.

3.4 Results and Discussion

3.4.1 Analysis of Isotope Data

Although the enrichment of ^{15}N in NO_3^- can be the result of processes other than denitrification, if it is assumed that a simple Rayleigh fractionation process governs denitrification, a linear relationship between ^{15}N enrichment in NO_3^- and the natural logarithm of the NO_3^- concentration is predicted (Kendall 1998). Indeed, this relationship has been cited as evidence of the occurrence of denitrification (Bottcher et al. 1990), where isotopic enrichment of ^{15}N is presented as part per thousand (δ) relative to the natural abundance of ^{15}N - N_2 and ^{15}N - N_2O in the atmosphere, while^{18}O is relative to Vienna Standard Mean Ocean Water (VSMOW). Rayleigh fractionation models the multistep process of denitrification by a single fractionation factor, and predicts that the concentration isotopic composition becomes lighter as the concentration of N_2 increases. However, our data showed the opposite trend, that the concentration of N_2 is proportional to ^{15}N (Figure 3.17 A). Although these results at first seem unexpected, the same relationship between N_2 and ^{15}N was observed in an aquifer by Wilson et al. (1989). We observed that although the N_2 was isotopically lighter than atmospheric N_2, as more N_2 was produced via denitrification, it became heavier. This is a result of heavy NO_3^- building up in a pool, so as denitrification proceeds, the proportion of $^{15}NO_3^-$ increases and consequently the percentage of $^{15}N_2$ produced also increase, which would explain the trend observed by Wilson et al. (1989) and confirm our observations. The reproduction of the relationship correlation between $\delta^{15}N$ and N_2 observed in an aquifer where denitrification was known to occur may provide qualitative evidence that denitrification is occurring the DNBR.

At each step in denitrification, isotope partitioning occurs because there is a higher probably of each successive reducing reaction utilizing an isotopically lighter substrate, and it is probable that each step has a unique fractionation factor. Consequently, although the pattern of ^{15}N enrichment in NO_3- fits the Rayleigh equation and this relationship is reproduced by many independent studies (e.g. compilation of four aquifer studies by Bottcher et al. 1990), it holds because the reduction of NO_3^- is the initial step in denitrification. Chen and MacQuarrie (2005) obtained a theoretical fractionation ratio of 0.51 between $d^{15}N$ and $d^{18}O$ based on first-order or Monod kinetics, which was corroborated by their review of field data which yielded an average ratio of 0.55 (sd=0.08, n=6). Chen and MacQuarrie (2005) concluded that "A linear relationship between $\delta^{15}N$ and $\delta^{18}O$ values, with a slope (b) close to 0.51, provides additional, unambiguous

evidence that denitrification is responsible for the nitrate concentration decline and enrichment of nitrogen isotope values in shallow groundwater." This correlation between isotopic enrichment of N and O was not observed in dissolved N_2O; however, almost half of the samples were contained levels of N_2O below the limit of quantification, which may have contributed to the inability to detect a relationship. Alternatively, because N_2O is both a reactant and a product in the stepwise process of denitrification, a clear relationship between $\delta^{15}N$ and $\delta^{18}O$ may not emerge because the kinetics of multiple enzymes affected by various rate limiting factors is in play.

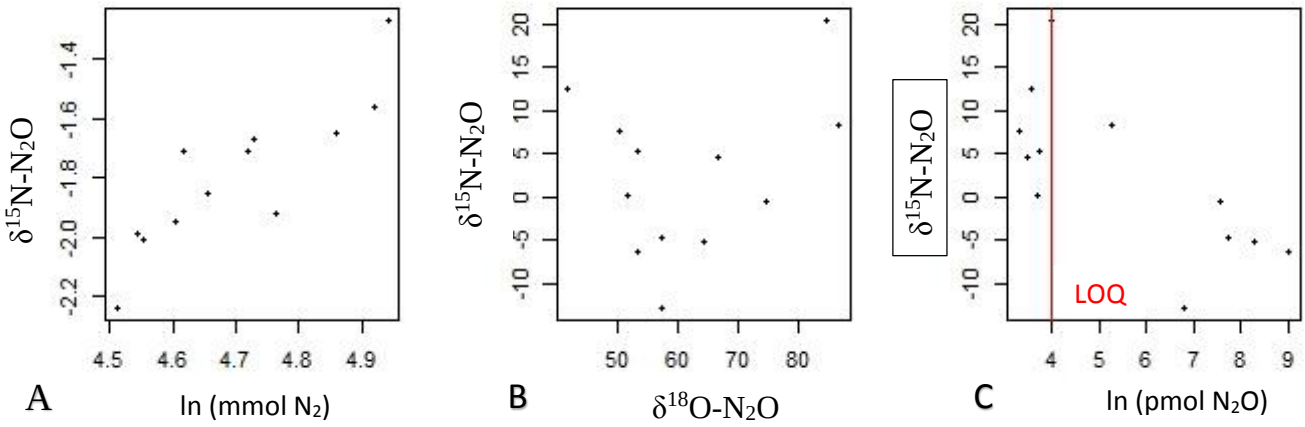

Figure 3.17 (a-c) A) Linear relationship between $\delta^{15}N$ and the natural logarithm of the dissolved concentration of N_2. B) Non-significant correlation between $\delta^{15}N$ and $\delta^{18}O$ in N_2O. C) Moderate correlation between $\delta^{15}N$ and the natural logarithm of the dissolved concentration of N_2O. The red line represents the limit of quantification.

An interesting relationship emerged between $\delta^{15}N$ and the natural logarithm of the dissolved N_2O: $\delta^{15}N$ increases as the concentration of N_2O decreases, indicating that the heavy isotopes build up in the residual pool of N_2O as it is reduced. This implies that some N_2O is accumulating during denitrification. However, the production of N_2O during both nitrification and denitrification makes N_2O lighter, so enrichment with decreasing concentration shows that it is subsequently reduced. This pattern is explained if N_2O residual gets enriched, implying that N_2O does accumulate, at least temporarily, while denitrification occurring, and as denitrification

continues it has to use heavier N_2O, so the isotopic enrichment of N_2 subsequently increases. Qualitative evidence that after N_2O is produced it is subsequently reduced to N_2. However, N_2O turnover cannot be quantified by isotope data alone (Well et al. 2012), which necessitates the employment of other tools to quantify the amount of N_2O produced during denitrification.

3.4.2 Gaseous Standard Addition Method

Assessment of the significance of N_2O production in DNBRs requires an accurate quantification, as does investigation of opportunities for mitigation. Likewise, the quantification of the ratio of N_2O:N_2 attributable to denitrification is necessary for identifying and optimizing the factors in DNBR design and management to maximize complete denitrification. Although the factors controlling the rate and ratio of products produced via denitrification have been studied in natural ecosystems (e.g. Liu et al. 2010), constructed wetlands (Inamori et al. 2008), as well as in controlled systems such as wastewater treatment plants (Kampscheur et al. 2009), the specific application of managed denitrification in DNBRs merits further investigation to maximize the rate of denitrification while avoiding the accumulation of deleterious intermediates. The ratio of N_2O:N_2 in the context of the denitrification rate as quantified by the N_2/Ar method previously discussed can be compared to the IPCC emission factor of 0.0025 to determine the potential role of DNBRs in mitigating indirect N_2O emissions from agriculture. The viability of the gaseous standard addition method as an improved analytical technique for static headspace analysis of dissolved gases, as well as a tool to study denitrification and the ratio of its products in DNBRs, was investigated.

As the first step in method development the sources of error than could contribute to reducing the overall precision of the gaseous standard addition method were identified and minimized, as described above. The largest opportunity for error reduction was to refine the procedure for headspace introduction given the wide variation in concentrations observed with repeated injections (Figure 3.11). However, the highest levels of contamination detected in the samples from the He tank taken with the syringe used for headspace introduction were 0.257% N_2, 0.078% O_2, and 0.003% Ar. The ratio between the headspace and liquid sample volume in the vial, B, could be selected so that the contribution of this contamination to the expected headspace concentration of analytes following the equilibrium procedure would be acceptable. For example, with B less than or equal to 0.45, the contamination from the helium headspace

will contribute only about 9.5% of the expected headspace concentration for N_2 if the sample is water in equilibrium with the atmosphere at 17 ˚C, 5.5% O_2 and 4.4% Ar.

Six headspace vials were prepared with the same sample water and a range of headspace volumes to quantify the concentrations of dissolved N_2, O_2 and Ar and determine if B had an effect on the concentration of analyte in the headspace, three samples with $B < 0.45$ and three with $B > 0.45$. Table 3.1 summarizes the linear fits achieved with two standard additions to each vial creating a three point standard addition curve, the slopes of each regression, and the calculated values for the analytes. The goodness of linear fit of the curve is indicated by the R^2 values demonstrates the potential for using the gaseous standard addition method as an alternative calculating the dissolved concentrations in environmental samples as predicted by Henry's law constant as described in Equation 3.1. However, the lack of agreement between the calculated values in these six similar samples that were expected to produce the same calculated result of original dissolved gas concentration is concerning, with a %RSD for the dissolved concentrations for N_2, O_2, and Ar of 86.4, 107.7, and 104.4 respectively. The quantification of excess N_2 to estimate denitrification depends upon the ratio of N_2 to Ar. This ratio ranged from 39.2-77.3 with a %RSD of 27, considerably lower than any that of any of the analytes individually. This evidence supports the conclusion that some of the error resulted from the incorporation of excess air, as does the correlation between the concentrations of the three analytes, a linear model of N_2 with Ar and O_2 as predictor variables having an R^2 of 0.9996. Interestingly, the vial with $B = 0.5667$ yielded dissolved gas concentrations very similar to the predicted value, but greater than what would be expected even with the highest level of He contamination observed extrapolated to contamination of the headspace.

However, the variability in the slopes produced by the regression of the response and the volume of analyte added is perhaps more concerning. Regardless of the potential for incorporation of excess air into the sample vial, the slopes produced from the regression for each analyte are expected to be the same because the concentration of analyte in the headspace and consequently the mass of analyte that reaches the detector are assumed to be linearly related to the GCMS response over the range of expected concentrations. The variability in B between the vials could contribute to the variability in the calculated dissolved concentrations, and potentially also the variability in the slopes, indicating that the standard addition method may not compensate for the dependence of the dissolved concentration on the ratio of headspace to liquid

sample in the vial, as pointed out by Jahangir et al. (2012a). Although standing and shaking time were also identified by Jahangir et al. (2012a) as affecting the calculated dissolved concentration, and confounding the comparability of data between independent studies employing DGA by static headspace analysis, these factors were kept constant in this experiment. Notably, there was a significant correlation between the calculated original dissolved concentration and B, as well as between the related total dissolved mass in the vial and B for both O_2 and Ar, but unexpectedly B was not shown to have a significant effect on the initial headspace concentration (Table 3.2). This lack of correlation, contrary to the basis of static headspace analysis, the original dissolved gas concentration is not controlling the concentration of analyte in the headspace (Table 3.2), which corroborates the unexpected variation in the calculated dissolved concentrations (Table 3.1).

3.5 Conclusions and Future Work

Analysis of the isotopic enrichment of ^{15}N and ^{18}O in N_2 and N_2O supported the dominance of denitrification as the mechanism of NO_3^- removal in DNBRs and confirmed the accumulation of N_2O during denitrification, meriting further investigation into the dynamics of denitrification in DNBRs. Direct measurement of denitrification through analysis of the dissolved gas component was identified as the most promising technique to both quantify the rate of denitrification and the ratio of its products in the investigation of the controlling factors specific to DNBR design and management. Development of a novel analytical method for DGA-SHA incorporating a gaseous standard addition was undertaken with the aim to increase the comparability of studies using this technique in response to the findings of Jahangir et al. (2012a) that variation in B affects the calculated value of the dissolved gas. However, the use of an internal calibration curve to calculate dissolved concentrations of analytes did not circumvent the impact of B, and rather our results corroborated the findings of Jahangir et al. (2012a). Although six replications of three point internal calibration curves produced with two sequential gaseous standard additions to the headspace vial produced good linear fits and supported the viability of the gaseous standard addition, there was wide variability in the calculated dissolved concentrations and the slopes of the regressions. The largest source of error identified was in the contamination of the He headspace introduced by syringe. Future development of this analytical method will incorporate an alternative method to introduce the headspace, such as a line

plumbed directly into the tank of ultra pure carrier He fitted with a valve and needle on the end so that the volume added can be easily controlled. Although continued investigation into sources of contamination and error in the method are required, this work serves as a proof of concept for utilizing a gaseous standard addition to quantify dissolved gases by static headspace analysis. Utilizing DGA in DNBRs will further study of how to increase the rates of complete denitrification and make these systems hyper-functional while simultaneously mitigating the impact of indirect N_2O emission associated with NO_3^- export from agroecosystems.

	R^2			**Slope**			**sample mg/L**		
B	**N_2**	**O_2**	**Ar**	**N_2**	**O_2**	**Ar**	**N_2**	**O_2**	**A_r**
0.1310	-	0.9934	0.994	-	673,002	1,175,951	-	0.42	0.01
0.3610	0.9798	0.9927	0.9964	22,848	26,566	42,235	42.83	12.23	0.55
0.4408	0.9807	0.9407	0.9748	190,304	434,684	245,351	5.37	0.78	0.11
0.5667	0.9537	0.9122	0.9281	75,587	44,094	82,558	**14.63**	**8.33**	**0.37**
0.7427	0.9942	0.9912	0.9993	11,547	9,861	17,950	107.17	41.78	1.91
0.8922	0.9989	0.9999	1.0000	17,710	12,859	24,485	76.57	35.04	1.54
						predicted:	**12.61**	**6.77**	**0.33**
						predicted with maximum He contamination:	**13.80**	**7.1**	**0.34**

Table 3.1 Shows the goodness of fit of six standard additions for each of the three analytes N_2, O_2, and Ar as well as the values of the original dissolved concentration present in the sample calculated from the respective standard addition curves as the x intercept divided by the volume of liquid sample in the vial. B refers to the volume of headspace to liquid sample. The values for N2 from the first vial are missing because the concentration observed in the headspace saturated the detector and prevented quantification.

Regressions	N_2		O_2		Ar	
	R^2	**p**	**R^2**	**p**	**R^2**	**p**
Original dissolved concentration ~ B	0.4885	0.1891	0.7493	0.0259*	0.7399	0.0280*
Total dissolved mass ~ B	0.3471	0.2959	0.6705	0.0463*	0.6608	0.0492*
Initial headspace response ~ B	0.2238	0.4210	0.0371	0.7145	0.0314	0.7371
SAM slope ~ B	0.2337	0.4095	0.4188	0.1650	0.3568	0.2108

Table 3.2 Summarizes the goodness of fit and p-values from four linear regressions of the headspace to liquid sample ratio (B) as the independent variable and the dependent variables 1) original dissolved gas concentration calculated as the x intercept of the standard addition curve divided by the volume of liquid sample in the vial 2) the total dissolved mass taken to be the x intercept of the standard addition curve 3) the initial headspace response form the GCMS, which is proportional to the mass detected and also the headspace concentration of analyte, and 4) the slope of the standard addition curves.

References

Averill, B.A., and J.M. Tiedje. 1982. The chemical mechanism of microbioal denitrification. FEBS Lett. 138:8–12.

Blagodatsky, S., and P. Smith. 2012. Soil physics meets soil biology: towards better mechanistic prediction of greenhouse gas emissions from soil. Soil Bio. Biochem. 47:78–92.

Blicher-Mathiesen, G., G.W. McCarty and L.P. Nielsen. 1998. Denitrification and degassing in groundwater estimated from dissolved dinitrogen and argon. J. Hydro. 208:16–24.

Bock, E., N. Smith, M. Rogers, B. Coleman, M. Reiter, B. Benham, and Z. Easton. 2014. Enhanced nitrate and phosphate removal with a denitrifying bioreactor with biochar. J. Environ. Qual. In press.

Böhlke, J.K., R.L. Smith and J.E. Hannon. 2007. Isotopic analysis of N and O in nitrite and nitrate by sequential selective bacterial reduction to N_2O. Anal. Chem. 79:5888–95.

Bottcher, J., O. Strebel, S. Voerkelius and H.L. Schmidt. 1990. Using isotope fractionation of nitrate-nitrogen and nitrate-oxygen for evaluation of microbial denitrification in a sandy aquifer. J. Hydro. 114:413–24.

Chen, D.J.Z., and K.T.B. MacQuarrie. 2005. Correlation of δ15N and δ18O in NO3- during denitrification in groundwater. J. Environ. Eng. Sci. 4:221–26.

EPA. 2006. Global Mitigation of non-CO_2 Greenhouse Gases. < http://www.epa.gov/ climatechange/EPAactivities/economics/nonco2projections.html >

Germon, J.C., P. Kaiser, A. Mariotti, P. Hubert, P. Tardieux, A. Tardieux, and R. Letolle. 1981. Experimental determination of nitrogen kinetic isotope fractionation: some principles; illustration for the denitrification and nitrification processes. Plant Soil 62:413.

Groffman, P.M., M.A. Altabet, J.K. Böhlke, K. Butterbach-Bahl, M.B. David, M. Firestone, A.E. Giblin, T.M. Kana, L.P. Nielsen and M.A. Voytek. 2006. Methods for measuring denitrification: diverse approaches to a difficult problem. Ecol. App. 16:2091-2122.

Inamori, R., Y. Wang, T. Yamamoto, J. Zhang, H. Kong, H., K. Xu and Y. Inamori. 2008. Seasonal effect on N_2O formation in nitrification in constructed wetlands. Chemosphere 73:1071–1077.

Jahangir, M.M.R., P. Johnston, M.I. Khalil, J. Grant, C. Somers, K.G. Richards. 2012a. Evaluation of headspace equilibration methods for quantifying greenhouse gases in

groundwater. J. Environ. Manage. 11:208–212

Jahangir, M.M.R., P. Johnston, M.I. Khalil, D. Hennessy, J. Humphreys, O. Fenton, and K.G. Richards. 2012b. Groundwater: a pathway for terrestrial C and N losses and indirect greenhouse gas emissions. Agric. Ecosys. Environ. 159: 40–48.

Jahangir, M.M.R., P. Johnston, M. Barrett, M.I. Khalil, P.M. Groffman, P. Boeckx, P., O. Fenton, J. Murphy and K.G. Richards. 2013. Denitrification and indirect N_2O emissions in groundwater: Hydrologic and biochemical influences. J. Contam. Hydro. 152:70–81.

Kampschreur, M. J., H. Temmink, R. Kleerebezem, M.S.M. Jetten, and M.C.M. van Loosdrecht 2009. Nitrous oxide emission during wastewater treatment. Water res. 43:4093–103.

Kendall, C. 1998. Tracing nitrogen sources and cycling in catchments. Istope Tracers in Catchment Hydrology. Elsevier, Amsterdam, 519–576.

Kolb, B., and L.S. Ettra. 1997. Static Headspace-Gas Chromatography: Theory and Practice. John Wiley & Sons.

Liotta, M., and M. Martelli. 2012. Dissolved gases in brackish thermal waters: an improved analytical method. Geofluids 12:236-244..

Liu, B., P.T. Mørkved, Å. Frostegård and L.R. Bakken. 2010. Denitrification gene pools, transcription and kinetics of NO, N_2O and N_2 production as affected by soil pH. FEMS Microb. Ecol. 72:407–417.

Liu, Y., Y. Min, Y. Wu and H. Wang. 2011. Reducing CH_4 and CO_2 emissions from waterlogged paddy soil with biochar. J. Soils Sediment 1: 930–39.

Mariotti, A. J.C. Germon, P. Hubert, P. Kaiser, R. Letolle, A. Tardieux and P. Tardieux. 1981. Experimental determination of nitrogen kinetic isotope fractionation– some principles– illustration for the denitrification and nitrification processes. Plant Soil. 62:413-430.

Moorman, T.B., T.B. Parkin, T.C. Kaspar and D.B. Jaynes. 2010. Denitrification activity, wood loss, and N_2O emissions over 9 years from a wood chip bioreactor. Ecol. Eng. 36:1567–1574.

Mosier, A, C. Kroeze, C. Nevison, O. Oenema, S. Seitzinger and O. van Cleemput. 1998. Closing the global N_2O budget: nitrous oxide emissions through the agricultural nitrogen cycle - OECD/IPCC/IEA phase II development of IPCC guidelines for national greenhouse gas inventory methodology. Nutr. Cycl. Agroecos. 52:225–48.

Warneke, S., L.A. Schipper, G.M. Matiasek, K.M. Scow, S. Cameron, D.A. Bruesewitz and I.R. McDonald. 2011. Nitrate removal, communities of denitrifiers and adverse effects in different carbon substrates for use in denitrification beds. Water Res. 45:5463–75.

Well, R., W. Eschenbach, H. Flessa, C. von der Heide and D. Weymann. 2012. Are dual isotope and isotopomer ratios of N_2O useful indicators for N_2O turnover during denitrification in nitrate-contaminated aquifers? Geochimica et Cosmochimica Acta 90:265–82.

Weymann, D., R. Well, H. Flessa, C. von der Heide, M. Deurer, K. Meyer, C. Konrad and W. Walther. 2008. Groundwater N_2O emission factors of nitrate-contaminated aquifers as derived from Denitrification Progress and N_2O accumulation. Biogeosciences 5:1215–26.

Wilson, G.B., J.N. Andrews and A.H. Bath. 1989. Dissolved gas evidence for denitrification in the Lincolnshire Limestone groundwaters, eastern England. J. Hydro. 113:51–60.

Zumft, W.G. 1997. Cell biology and molecular basis of denitrification. Micro.Molec. Bio. Rev. 61:533–550.

4.0 Conclusions

4.1 Summary and Future Work

This work contributes to the overarching objective of mitigating the environmental impacts of anthropogenic reactive nitrogen (N). Management of the global N cycle has been identified as a central environmental issue and engineering challenge in the 21st century by the national academy of engineering (Galloway et al. 2008; Seitzinger et al. 2006). This priority is reflected internationally by pollution control goals focused on reactive N in both the United States and Europe, as well as regionally in the nutrient load reductions called for the Chesapeake Bay Total Maximum Daily Load, the most extensive and complex TMDL created under the Clean Water Act (Melilo and Cowling 2002). Indeed, Executive Order 13508 calls for renewed efforts to restore the Chesapeake Bay to its unimpaired condition by reducing nutrient and sediment inputs, and innovated strategies for nutrient management have been an exciting frontier of these efforts (Chesapeake Bay Commission 2004). Managing the natural process of microbial denitrification and harnessing the ability to remove excess reactive N from impacted ecosystems is the subject of much ongoing research (Schipper et al. 2010). Research on denitrifying bioreactors has established the ability to construct systems specifically and successfully for the purpose of promoting denitrification. DNBRs are continuing to remove nitrogen in the field after better than a decade of use and the DNBR design and management factors are elucidated, DNBR research moves forward with establishing design guidelines for incorporation of these systems as agricultural best management practices, such as the cost-share opportunity with Maryland Natural Resource Conservation Service (NRCS), with much ongoing work focusing on establishing the optimal residence time (Christainson, personal communication).

I have described additional opportunities to leverage DNBR deployment to mitigate the excess phosphorus (P) also present in agricultural drainage as well as minimize the indirect emissions from agriculture as a result of the export of excess N. Addressing diffuse nutrient pollution from agriculture at the source possible minimizes its negative consequences has driven the development of edge-of-field technology, for example the interception and capture of P with gypsum curtains (Bryant 2012). Additionally a systems approach to controlled drainage management in farms utilizing irrigation and tile drains is the subject of ongoing research to control the export of N and P, as evidenced by a recent disbursement of a Conservation

Innovation Grants by the United States Department of Agriculture awarded to Virginia Tech to support research on this subject. I believe that expanding the functionality of DNBRs to address other pollutants, namely P export from agriculture and nitrous oxide (N_2O) emissions from agriculture represents a linear advancement of DNBR technology.

In this document I have presented evidence that N and P removal can be increased while N_2O production can be decreased in traditional woodchip DNBRs with the addition of biochar based on the results of a laboratory scale study. These results also raise a series of questions that may form the basis for future research on the effect of biochar in DNBRs. Was the enhanced nitrate removal a result of increased rates of denitrification or some other process? Was N_2O production reduced by an increase in complete denitrification converting NO_3^- to N_2 rather than build of the intermediate N_2O? How does biochar alter the ratio of denitrification products? What was the dominant mechanism of phosphorus removal, adsorption or precipitation? What is the lifespan of DNBRs with respect to phosphorus removal, and how is this affected by the mechanism of removal? Although all of these questions are significant to understanding the role biochar can play in DNBRs, the central question is how might the results of this work transfer to the field scale.

Techniques of dissolved gas analysis for the purpose of quantifying denitrification and the ratio of its products were explored. Analysis of stable isotope abundance in denitrification products provided quantitative evidence of the occurrence of denitrification and the accumulation of the intermediate N_2O, but was not sufficient to quantitatively assess the impact of biochar on the rate of denitrification and ratio of its products. Static headspace analysis of dissolved gases was identified as a method to examine the dynamics of denitrification, allowing for the examination of the spatial and temporal variability in the quantities of denitrification products within a DNBR. Although measuring the dissolved gas component of an aqueous sample is analytically challenging, it is hoped that using this tool may lead to better understanding of the denitrification process and DNBRs and enable refined control over this microbial process.

Future work building upon these findings and attempting to answer the questions raised by this research will optimize DNBR performance not only with respect to N but also P and potentially N_2O. It is our hope that we continue to examine the potential of biochar to improve DNBR function. Incorporating DNBRs into a broader scheme of nutrient and drainage

management in an agricultural setting will be essential moving forward. Finally, assessing the watershed scale impact of DNBR deployment will be necessary to conduct a cost benefit analysis and establish the potential for widespread impact of DNBR implementation.

References

Bryant, R.B., A.R. Buda, P.J. Kleinman, C.D. Curch, L.S. Saporito, G.J. Folmar, S. Bose and A.L. Allen. 2012. Using flue gas desulfurization gypsum to remove dissolved phosphorus from agricultural drainage waters. J. Environ. Qual. 41:664-671.

Chesapeake Bay Commission. 2004. Cost-effective strategies for the Bay: six smart Investments for nutrient and sediment reduction. <http://www.chesbay.us/ Publications/cost%20 effective.pdf >

Galloway, J.N., A.R. Townsend, J.W. Erisman, J. W., M. Bekunda, Z. Cai, Z., J.R. Freney, L.A. Martinelli, S.P. Seitzinger and M.A. Sutton. 2008. Transformation of the nitrogen cycle: recent trends, questions, and potential solutions. Science 320:889–892.

Melillo, J.M. and E.B. Cowling. 2002. Reactive nitrogen and public policies for environmental protection. AMBIO 31:150–158.

Schipper, L.A., A.J. Gold and E.A. Davidson. 2010. Managing denitrification in human dominated landscapes. Ecol. Eng. 36:1503–1506.

Seitzinger, S., J.A. Harrison, J.K. Böhlke, A.F. Bouwman, R. Lowrance, B. Peterson, C. Tobias and G.V. Drecht. 2006. Denitrification across landscapes and waterscapes: A synthesis. Ecol. App. 6:2064–2090.

Appendix

A. Comparison of selected laboratory and field DNBR studies. Abbreviations: NR refers to not reported, NS refers to not significant, DEA refers to a denitrifying enzyme activity assay, NM refers to not measured, and GW refers to ground water. DNBR size listed as multi refers to studies where multiple sized reactors were used, but removal rates presented as an average over all systems. Note that some of these studies examine the same DNBR: Robertson and Cherry 1995 and Robertson et al. 2008; Long et al. 2011 and Schipper and V-V 2001; Moorman et al. 2010 and Jaynes et al. 2008; as well as Schipper and Vojvodic-Vukovic 2000 and Schipper et al. 2010.

Study	Location	Age	Size (m^3)	Water source	Inlet [NO3] mg/L	Outlet [NO3] mg/L	NO_3 Removal	Denitrific-ation	GHG Emission	Carbon Media
Blowes et al. 1994	Ontario, Canada	1 yr	0.2	crop tile drainage	2-6	< 0.02	nearly 100%	NM	NM	leaf bark compost and woodchips
Cameron and Schipper 2001	New Zealand	15 mo	3.5	municipal wastewater	50-100	<0.1	21.8 +/- 8.3 g N/m^3 mo 5-15	NM	NM	maize cobs
Chun et al. 2009	laboratory	new	0.4	prepared solution	8-33.7	NR	10-40%	NM	NM	woodchips
Elgood et al. 2010	Ontario, Canada	3 yr	40	crop tile drainage	0.3-5.8	<0.1-3.9	18-100%	NM	N_2O 0.6% removal CH_4 974 ug C/L	woodchips
Gibert et al. 2008	laboratory	New	0.006	GW with added NO_3^-	50	NR	66-96%	regression NO_3^- vs time, 0.001-0.217 mg/L-d-g	NM	many types tested
Greenan et al. 2006	laboratory	New to day 180	*180 mL	prepared solution	10-100	NR	96-98%	Isotope, 0.066 g/kg-d to 0.427 g/kg-d	NM	cornstalk, cardboard, woodchips and woodchips with oil
Hunter 2001	laboratory	New	0.085	prepared solution	20	NR	39%	NM	NM	sand coated with oil

Study	Location	Age	Size (m^3)	Water source	Inlet [NO3] mg/L	Outlet [NO3] mg/L	NO_3 Removal	Denitrific-ation	GHG Emission	Carbon Media
Jaynes et al. 2008	Iowa, USA	5 yr	47	crop tile drainage	<0.3-35	NR	55%	NM	NM	woodchips
Long et al. 2011	New Zealand	14 yr	40	dairy farm drainage	2.2-3.7	0.2	92%	DEA similar to year 1	NM	sawdust
Moorman et al. 2010	Iowa, USA	9 yr	47	crop tile drainage	20-25	NR	avg in-out 24.5 kg/ha	Acetylene block 8.2-34 ng/kg last 5 years; push-pull 23.6 kg/ha	0.0062 N_2O per kg NO_3 is < control plot	woodchips
Robertson and Cherry 1995	Ontario, Canada	1 yr	1.1	septic system GW plume	57-62	2-25	60-100%	NM	NM	sawdust
Robertson et al. 2000	Ontario, Canada	6-7 yr	multi	septic and crop drainage	4-400	NR	58-91%	NM	NM	wood mulch sawdust leaf compost
Robertson et al. 2005	Ontario, Canada	3-5 yr	multi	septic system	14.3-37.7	0.7-1.9	87-98%	calculated form nitrate	NM	woodchips
Robetson et al. 2008	Ontario, Canada	15 yr	1.1	9.7 +/- 0.2	5.9 +/- 2.2	NR	0.22-1.1 mg/L/d 6 ˚C 3.5-6 mg/L/d 22 ˚C	NM	NM	woodchips and sawdust
Robertson and Merkley 2008	Ontario, Canada	1.5	40	crop drainage	4.8	1.04	79%	NM	NM	woodchips
Saliling et al. 2007	laboratory	new	0.004	synthetic wastewater	50,120 200	1.7-5.1, 1.7-12, 0.14-4.4	240, 810, and 1380 mg/L/d	NM	NM	wheat straw, plastic media, and woodships
Schipper and McGill 2008	New Zealand	19 mo	30	dairy drainage	NR	NR	NS	DEA as indicator	NM	garden mulch
Schipper and Vojvodic-Vukovic 2000	New Zealand	4 yr	78.8	GW	8.1-13.3	0.3-8.1	0.8-12.8 mg/L	0.6-18.1 $ng/cm^3/h$ acetylene block on soil cores in lab	NM	sawdust

Study	Location	Age	Size (m^3)	Influent Type	Inlet [NO3] mg/L	Outlet [NO3] mg/L	NO_3 Removal	Denitrific-ation	GHG Emission	Carbon Media
Schipper and Vojvodic-Vukovic 2001	New Zealand	5 yr	78.8	GW	5-15	NR	95%	DEA as indicator	NM	sawdust
Schipper et al. 2005	New Zealand	8 yr	78.8	dairy drainage	50	NR	1.4 $g/m^3/d$	DEA as indicator	NM	sawdust
Schipper et al. 2010	New Zealand	2-4	83 294 1320	dairy domestic green -house	NR	NR	1.4 $g/m^3/d$ 0-11 $g/m^3/d$ 5-10 $g/m^3/d$	NM	NM	sawdust and woodchips
van Driel et al. 2006	Ontario, Canada	20 & 4 mo	0.73 0.21	leached crop GW	11.5, 23.7-35.1	NR	33% 41-63%	NM	NM	woodchips
Warneke et al. 2011	New Zealand	1 yr	1320	green -house	NR	NR	7.6 $g/m^3/d$	DEA method in lab 43.1 $g/m^3/d$	N_20 1% of NO_3^- removal CH_4 0.02+/- 0.08 ug/m_2 min CO_2 4.9 kg/bed day	woodchips
Warneke et al. 2011	New Zealand							acetylene block Push-pull Direct N_2/N_20 measurement	yes	
Woli et al. 2010	Illinois, USA	1-2 yr	41.6 76.9	crop tile drainage	2.8-18.9	0.1-14.6	12-99.5%	acetylene block cores in lab highly variable 0-3110 $g/m^3/d$	gas flux in lab N^20 0.01–0.13mg-$N/m^2/h$ CO_2 0.2-7.5 $g\text{-}C/m^2/h$	woodchips
Warneke et al. 2011	New Zealand	1 yr	1320	greenhouse	NR	NR	7.6 $g/m^3/d$	DEA method in lab 43.1 $g/m^3/d$	N_20 1% removal CH_4 0.02+/- 0.08 ug/m_2 min CO_2 4.9 kg/bed day	woodchips